UNIVERSITY OF CALIFORNIA,
IRVINE

Bioinformatic Analysis of Circadian Reprogramming Events

DISSERTATION

submitted in partial satisfaction of the requirements
for the degree of

DOCTOR OF PHILOSOPHY

in Computer Science

by

Nicholas Joseph Ceglia

Dissertation Committee:
Professor Pierre Baldi, Chair
Professor Paolo Sassone-Corsi
Assistant Professor Marco Levorato

2018

DEDICATION

To my mom and dad.

TABLE OF CONTENTS

LIST OF FIGURES

ACKNOWLEDGMENTS

I would like to sincerely thank my advisor, Pierre Baldi, who has shown tremendous support and understanding, I am extremely grateful.

I would like to thank my labmates Yu Liu, Vishal Patel, and Mike Zeller for support and friendship.

I would like to thank collaborators Kristin Eckel-Mahan, Selma Masri, Paola Tognini, Ken Kenichiro, and Paolo Sassone-Corsi.

I would like to thank Camilla Favaretti for pretty much everything else.

I thank the editors and publishers of Nature Methods, Cell, Journal of Biological Chemistry, Bioinformatics, Cell Reports, Nature Communications, and Nucleic Acid Research for publishing parts of this work.

Section 2.1 adapted from Agostinelli et al. (2016).
Section 2.2 adapted from Ceglia et al. (2018).
Section 3.1 adapted from Eckel-Mahan et al. (2013).
Section 3.2 adapted from Abbondante et al. (2015).
Section 4.1 adapted from Masri et al. (2014).
Section 4.2 adapted from Sahar et al. (2014).
Section 4.3 adapted from Kenichiro et al. (2014).
Section 5.1 adapted from Mazziotti et al. (2017).
Section 5.2 adapted from Liu et al. (2018).
Section 6.1 & 6.2 adapted from Patel et al. (2015).

CURRICULUM VITAE

Nicholas Joseph Ceglia

EDUCATION

Doctor of Philosophy in Computer Science — **2018**
University of California, Irvine — *Irvine, California*

Master of Science in Computer Science — **2018**
University of California, Irvine — *Irvine, California*

Bachelor of Science in Computer Science — **2011**
University of Nevada, Reno — *Reno, Nevada*

RESEARCH EXPERIENCE

Graduate Research Assistant — **2013–2018**
University of California, Irvine — *Irvine, California*

TEACHING EXPERIENCE

Teaching Assistant — **Fall 2017 – Winter 2018**
ICS 33 - University of California, Irvine — *Irvine, California*

Reader — **Spring 2017**
ICS 99 - University of California, Irvine — *Irvine, California*

INTERNSHIPS

Data Science Intern — **Summer 2014 – Spring 2015**
The Retail Equation — *Irvine, California*

Product Development Intern — **Spring 2017**
MSC Software — *Santa Ana, California*

REFEREED JOURNAL PUBLICATIONS

Reprogramming of the circadian clock by nutritional challenge. **2012**
Nature Methods

Partitioning circadian transcription by SIRT6 leads to segregated control of cellular metabolism. **2014**
Cell

Circadian Control of Fatty Acid Elongation by SIRT1 Protein-mediated Deacetylation of Acetyl-coenzyme A Synthetase 1. **2014**
Journal of Biological Chemistry

The pervasiveness and plasticity of circadian oscillations: the coupled circadian-oscillators framework. **2015**
Bioinformatics

Comparative circadian metabolomics reveal differential effects of nutritional challenge in the serum and liver. **2016**
Journal of Biological Chemistry

What time is it? Deep learning approaches for circadian rhythms. **2016**
Bioinformatics

SIRT6 suppresses cancer stem-like capacity in tumors with PI3K activation independently of its deacetylase activity. **2017**
Cell Reports

Mir-132/212 is required for maturation of binocular matching of orientation preference and depth perception. **2017**
Nature Communication

CircadiOmics: circadian omic web portal. **2018**
Nucleic Acid Research

ABSTRACT OF THE DISSERTATION

Bioinformatic Analysis of Circadian Reprogramming Events

By

Nicholas Joseph Ceglia

Doctor of Philosophy in Computer Science

University of California, Irvine, 2018

Professor Pierre Baldi, Chair

Circadian oscillations play a fundamental role in many biological processes including cell metabolism and cell cycle. As such, interest in understanding these molecular oscillations has generated an increasingly large collection of circadian omic data. These studies have demonstrated the remarkable plasticity with which the set of oscillating molecular species within a cell are selected. These large shifts in oscillating species are known as circadian reprogramming events. These events have been observed across experimental condition, tissue, and species. While many of these studies have made tissue or condition specific conclusions, a consolidated framework of software tools and a central repository of data has become necessary to answer questions about the orchestration of these reprogramming events.

By combining the largest repository for circadian omic data with improved methods for the detection of circadian oscillation and regulation in omic studies, a model for the transcriptomic organization of circadian rhythms can be identified. Results are presented from a collection of specific reprogramming studies utilizing these new methods, as well as a high through-put analysis of a large collection of comparable transcriptomic datasets from mouse tissue. The identified model can be viewed as a deep hierarchical network of circadian regulation that originates from the core circadian clock to over 95% of oscillating transcripts.

Chapter 1

Data Analysis of Circadian Rhythms

1.1 Introduction

Circadian oscillations in the concentrations of molecular species play a fundamental role in many biological processes from metabolism, to cell cycle, and to neuronal function [18, 57, 87, 193]. To study the role of these oscillations, an increasing amount of high through-put circadian omic data is being generated under diverse genetic, epigenetic, and environmental conditions. In any single circadian transcriptomic experiment, roughly 10% of measured transcripts are found to oscillate in a circadian manner [68, 67, 183, 182, 204]. However, the intersection of oscillating transcripts between any two experiments is typically small, only about 2% [224]. This small overlap between experiments suggests that the union of all oscillating transcripts across all experiments is large. Remarkably, we calculate that over 95% of all of protein coding transcripts in mouse are found to oscillate in at least one condition [34]. Previous studies have demonstrated specific mechanisms by which a cell can select different oscillating subsets of transcripts, an event known as circadian reprogramming [167, 168, 319, 204]. However, the question of how almost every transcript is capable of

oscillating in a circadian manner remains unanswered. The body of this research is devoted to the development of informatic tools and the analysis of specific reprogramming events to generate an understanding of the mechanisms behind these events. Finally, this research aims to identify a model for the transcriptomic organization of circadian rhythms.

To address this problem, it must be noted first that the concentration of any molecular species cannot oscillate in isolation [20]. The fundamental unit of any such oscillation is a feedback loop of molecular interactions, such as transcriptional regulation, post-trascriptional modification, and protein-protein interactions [183, 245, 224], causing all species in the loop to oscillate at the same frequency. A very large number of such regulatory loops have been identified using informatics methods and large omic repositories [224, 48, 315, 281, 126, 248]. The empirically observed pervasiveness of circadian oscillations implies that a significant fraction of these loops is capable of oscillating with a 24 hour period. This 24 hour common period is most likely due to evolution given the importances of the differences between night and day for all biological life, the $\sim$ 2 trillion night-day transitions that have occurred since the origin of life 3.5 billion years ago, and the inherently circadian nature of the molecular circuitry of early photosynthetic life (cyanobacteria) [217]. Thus, in short, modern cells contain entire networks of circadian coupled oscillators. The question again is how specific subsets of oscillators are selected under specific genetic, epigenetic, and environmental conditions.

A key element of the answer to this question is the circadian core clock. The circadian core clock is genetically implemented by a relatively small set of genes whose transcripts are consistently found to oscillate in most circadian experiments [140, 145, 283]. The core clock regulates an extensive number of transcripts through a set of transcription factors (TF) including CLOCK-BMAL [243]. CLOCK-BMAL binds to E-box motifs that are found abundantly throughout the genome [211, 327]. A possible centralized model of organization is that the core clock directly orchestrates the selection of oscillators in the coupled network.

While the importance of the core clock is undeniable [297, 243, 147, 249], additional findings have shown that knocking out elements of the core clock (including CLOCK-BMAL) does not lead to a complete loss of circadian oscillations [148, 171, 7, 320, 54]. Thus, at the other extreme, a completely decentralized model of circadian oscillations is also conceivable where oscillators compete and self organize. Here we seek to find where in this spectrum, from centrally orchestrated to completely decentralized, the cellular network of coupled-oscillators operates.

1.2 Tools and Methods

A main component of the informatic tools within this manuscript is the collection of data on CircadiOmics (www.circadiomics.ics.uci.edu). We have aggregated the largest repository of high through-put circadian omic data on this webserver and built a suite of software tools for its analysis. Among others, CircadiOmics contains 161 transcriptomic datasets from 8 species and over 23 broad tissue categories. The most important component of this suite of informatic tools is BIO_CYCLE, a deep learning based software available on CircadiOmics. BIO_CYCLE is used to identify oscillating transcripts with statistical significance [3]. MotifMap and MotifMap-RNA are used to study transcription factors (TF) and RNA binding proteins (RBP) and their binding sites [315, 48, 174]. These binding sites can provide evidence for transcriptional and post-transcriptional regulation.

1.3 Experimental Results

Several studies observing large reprogramming events are examined. These studies fall into three broad categories: nutritional challenge by high fat diet and fasting, metabolism, and developmental processes including cell fate determination. Experiments are focused on both

transcriptome and metabolomic reprogramming. The findings illustrate the pervasiveness of circadian oscillation across tissue and condition. Additionally, these results provide conclusions for specific reprogramming mechanisms that will be explained through large scale analysis over many such diverse conditions.

1.4 Large Scale Analysis

With the goal of identifying a model for the organization of circadian reprogramming, we performed a series of analyses on 87 mouse transcriptomic datasets and 64 baboon transcriptomic datasets. We formulate the Circadian Regulatory Control (CRC) method for the identification of regulatory edges in a circadian feedback loop. Finally, we construct large CRC graphs based on this method to demonstrate the hierarchical transcriptomic organization on which circadian reprogramming events can take place.

Chapter 2

Software

2.1 BIO_CYCLE

2.1.1 Motivation

The importance of circadian rhythms cannot be overstated: circadian oscillation have been observed in animals, plants, fungi and cyanobacteria and date back to the very origins of life on Earth. Indeed, some of the most ancient forms of life, such as cyanobacteria, use photosynthesis as their energy source and thus are highly circadian almost by definition. These oscillations play a fundamental role in coordinating the homeostasis and behavior of biological systems, from the metabolic [65, 80, 283, 324] to the cognitive levels [65, 87]. Disruption of circadian rhythms has been directly linked to health problems [138, 156, 283] ranging from cancer, to insulin resistance, to diabetes, to obesity and to premature ageing [9, 80]. At their most fundamental level, these oscillations are molecular in nature, whereby the concentrations of specific molecular species such as transcripts, metabolites and proteins oscillate in the cell with a 24 h periodicity. Modern high-throughput technologies allow

large-scale measurements of these concentrations along the circadian cycle thus creating new datasets and new computational challenges and opportunities. To mine these new datasets, here we develop and apply machine learning methods to address two questions: (i) which molecular species are periodic? and (ii) what time or phase is associated with high-throughput transcriptomic measurements made at a single timepoint?

At the molecular level, circadian rhythms are in part driven by a genetically encoded, highly conserved, core clock found in nearly every cell based on negative transcription/translation feedback loops, whereby transcription factors drive the expression of their own negative regulators [219, 257], and involving only a dozen genes [219]. In the mammalian core clock, two bHLH transcription factors, CLOCK and BMAL1 heterodimerize and bind to conserved E-box sequences in target gene promoters, thus driving the rhythmic expression of mammalian Period (Per1, Per2 and Per3) and Cryptochrome (Cry1 and Cry2) genes. PER and CRY proteins form a complex that inhibits subsequent CLOCK-BMAL1-mediated gene expression. The master core clock located in the suprachiasmatic nucleus (SCN) [200] of the hypothalamus interacts with the peripheral core clocks throughout the body.

In contrast to the small size of the core clock, high-throughput transcriptomic (DNA microarrays, RNA-seq) or metabolomic (mass spectrometry) experiments [68, 117, 182, 217], have revealed that a much larger fraction, typically on the order of 10%, of all transcripts or metabolites in the cell are oscillating in a circadian manner. Furthermore, the oscillating transcripts and metabolites differ by cell, tissue type, or condition [217]. Genetic, epigenetic and environmental perturbationssuch as a change in dietcan lead to cellular reprogramming and profoundly influence which species are oscillating in a given cell or tissue [21, 67, 182]. When results are aggregated across tissues and conditions, a very large fraction, often exceeding 50% and possibly approaching 100%, of all transcripts is capable of circadian oscillations under at least one set of conditions, as shown in plants, cyanobacteria and algae, and mouse [224, 328].

In a typical circadian experiment, high-throughput omic measurements are taken at multiple timepoints along the circadian cycle under both control and treated conditions. Thus the first fundamental problem that arises in the analysis of such data is the problem of detecting periodicity, in particular circadian periodicity, in these time series. The problem of detecting periodic patterns in time series is of course not new. However, in the cases considered here the problem is particularly challenging for several reasons, including: (i) the sparsity of the measurements (the experiments are costly and thus data may be collected for instance only every 4hours); (ii) the noise in the measurements and the well known biological variability; (iii) the related issue of small sample sizes (e.g. n=3); (iv) the issue of missing data; (v) the issue of uneven sampling in time; and (vi) the large number of measurements (e.g. 20,000 transcripts) and the associated multiple-hypothesis testing problem. Here we develop and apply deep learning methods for robustly assessing periodicity in high-throughput circadian experiments, and systematically compare the deep learning approach to the previous, non-machine learning, approaches [117]. While this is useful for circadian experiments, the vast majority of all high-throughput expression experiments have been carried, and continue to be carried, at single timepoints. This can be problematic for many applications, including applications to precision medicine, precisely because circadian variations are ignored creating possible confounding factors. This raises the second problem of developing methods that can robustly infer the approximate time at which a single-time high-throughput expression measurement was taken. Such methods could be used to retrospectively infer a time stamp for any expression dataset, in particular to improve the annotations of all the datasets contained in large gene expression repositories, such as the Gene Expression Omnibus (GEO) [69], and improve the quality of all the downstream inferences that can be made from this wealth of data. There may be other applications of such a method, for instance in forensic sciences, to help infer a time of death. In any case, to address the second problem we also develop and apply deep learning methods to robustly infer time or phase for single-time high-throughput gene expression measurements. 2.1 illustrates the neural network architecture of

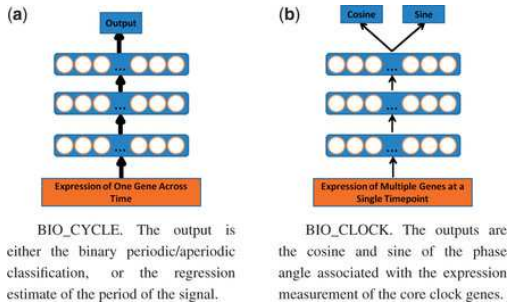

Figure 2.1: Visualizations of the deep neural networks (DNNs)

BIO_CYCLE.

2.1.2 Dataset Curation

To train and evaluate the deep learning methods, we curate BioCycle, the largest dataset including both synthetic and real-world biological time series, and both periodic and aperiodic signals. While the main goal here is to create methods to analyze real-world biological data, relying only on biological data to determine the effectiveness of a method is not sufficient because there are not many biological samples which have been definitively labeled as being periodic or aperiodic. Even when one can be confident that a signal is periodic, it can be difficult to determine the true period, phase and amplitude of that signal. Therefore, we rely also on synthetic data to provide us with signals that we can say are definitely periodic or aperiodic, and whose attributessuch as period, amplitude, and phasecan be controlled and are known. Furthermore, previous approaches were developed using synthetic data and thus the same synthetic data must be used to make fair comparisons.

Synthetic Data

We first curate a comprehensive synthetic dataset *BioCycleSynth*, which includes all previously defined synthetic signals found in JTK_CYCLE [117] and ARSER [322], but also

contains new signals. *BioCycleSynth* is in turn a collection of two different types of datasets: a dataset in which signals are constructed using mathematical formulas (*BioCycleForm*), and a dataset in which signals are generated from a Gaussian process [240] (*BioCycleGauss*). In previous work, synthetic data was generated with carefully constructed formulas to try to mimic periodic signals found in real-world data. While this gives one a lot of control over the data, it can create signals that are too contrived and therefore not representative of real-world biological variations. In addition, the noise added at each timepoint is independent of the other timepoints, which may not be the case in real-world data. The *BioCycleGauss* dataset uses Gaussian processes to generate the data and address these problems. Samples of synthetic signals are shown in 2.2.

The datasets used in JTK_CYCLE contain the following types of formulas or signals: cosine, cosine with outlier timepoints and white noise. The ARSER dataset contains cosine, damped cosine with an exponential trend, white noise and an auto-regressive process of order AR(1). In addition to all the aforementioned signals, *BioCycleForm* contains also 9 additional kinds of signals: combined cosines (cosine2), cosine peaked, square wave, triangle wave, cosine with a linear trend, cosine with an exponential trend, cosine multiplied by an exponential, flat and linear signals (many of which can be found in [53]). For clarity, the periodic signals are shown without noise. Signals in the *BioCycleForm* dataset have an additional random offset chosen uniformly between 200 and 200, random amplitudes chosen uniformly between 1 and 100, signal to noise ratios (SNRs) of 15, random phases chosen uniformly between 0 and 2π, and periods between 20 and 28. At each timepoint sample, zero mean Gaussian noise is added with the proper SNR variance.

The BioCycleGauss dataset is obtained from a Gaussian process. The value of the covariance matrix corresponding to the timepoints x and x' is determined by a kernel function $k(x,x)$. Equation 2.1 is the kernel function used to generate the periodic signals, and Equation 2.2 is the kernel function used to generate the aperiodic signals in *BioCycleGauss*. Sample signals

from *BioCycleGauss* are shown in 2.3

$$k_p(x, x') = \exp(\frac{-sin^2(\left|\pi\frac{1}{p}(x - x')\right|)}{2t^2}) + \sigma^2\delta(x, x') + \beta xx' \tag{2.1}$$

$$k_a(x, x') = \exp(\frac{-(x - x')^2}{2t^2}) + \sigma^2\delta(x, x') \tag{2.2}$$

The parameter l controls how strong the covariance is between two different timepoints, σ controls how noisy the synthetic data is, and β can add a non-stationary, linear, trend to the signals. The parameter p in equation 1 is the period of the signal. To generate the data in *BioCycleGauss*, the values of l, σ, β, p, as well as the offset and the scale are varied, in a way similar to the data in *BioCycleForm*.

BIO_CYCLE analyzes synthetic signals sampled over 48 hours with a sampling frequency of 1 and 4hours. ARSER analyzes synthetic signals sampled over 44 hours with a sampling frequency of 4h. BioCycle analyzes synthetic signals sampled over 24 and 48hours. Signals sampled over 24 h have a sampling frequency of 4, 6 and an uneven sampling at timepoints 0, 5, 9, 14, 19 and 24. Signals sampled over 48 h have sampling frequencies of 4, 8 and an uneven sampling at timepoints 0, 4, 8, 13, 20, 24, 30, 36, 43. The sampling frequencies in these datasets are intentionally sparse to mimic the sparse temporal sampling of real-world high-throughput data. The number of synthetic signals at each sampling frequency is 1024 for JTK_CYCLE, 20,000 for ARSER and 40,000 for *BioCycleSynth*. Finally, each signal in *BioCycleSynth* has three replicates, obtained by adding random Gaussian noise to the signal, to mimic typical biological experiments.

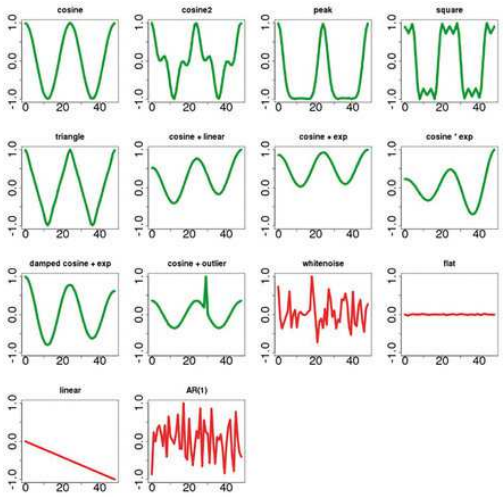

Figure 2.2: Samples of synthetic signals in the *BioCycleForm* dataset. Signals in green are periodic; signals in red are aperiodic

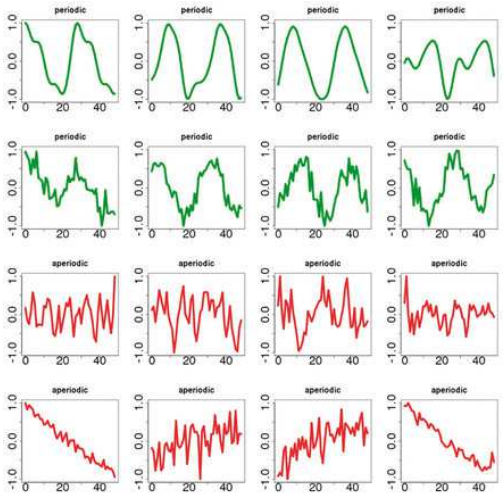

Figure 2.3: Samples of synthetic signals in the *BioCycleGauss* dataset. Signals in green are periodic; signals in red are aperiodic

Biological Data

The performance of any circadian rhythm detection method requires extensive validation on biological datasets. In previous work, due to the aforementioned difficulty of not having ground truth labels, the biological signals detected as being periodic had to be inspected by hand, or loosely assessed by comparison to other methods [323]. In addition to the scaling problems associated with manual inspection, this approach did not allow the computation of precise classification metrics [15], such as the AUC the Area Under the Receive Operating Characteristic (ROC) Curve. The repository of circadian data hosted on CircadiOmics [224] includes over 30 high-throughput circadian transcriptomic studies, as well as several circadian high-throughput metabolomic studies, that provide extensive coverage of different tissues and experimental conditions. From the CircadiOmics data, a high-quality biological dataset BioCycleReal is created with periodic/aperiodic labels.

To curate BioCycleReal, we start from 36 circadian microarray or RNA-seq transcriptome datasets, 32 of which are currently publicly available from the CircadiOmics web portal (28 of these are also available from CircaDB [234]). Five datasets are from ongoing studies and will be added to CircadiOmics upon completion. All included datasets correspond to experiments carried out in mice, with the exception of one dataset corresponding to measurements taken in Arabidopsis Thaliana. *BioCycleReal* comprises experiments carried over a: 24 hour period with a 4 hour sampling rate; 48 hour period with a 2 hour sampling rate; and 48 hour period with a 1 hour sampling rate.

To extract from this set a high-quality subset of periodic time series, we focus on the time series associated with the core clock genes in the control experiments. These gene include Clock, Per1, Per2, Per3, Cyr1, Cry2, Nr1d1, Nr1d2, Bhlhe40, Bhlhe41, Dbp, Npas2 and Tel [101] for mouse, and the corresponding homologs in Arabidopsis [100]. Arabdiposis homologs were obtained from Affymetrix NetAffx probesets and annotations [172]. These core gene

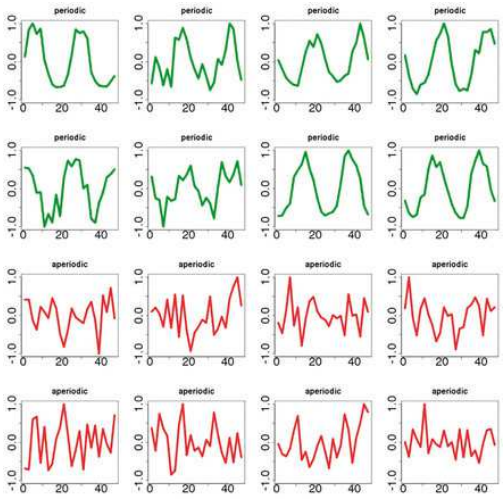

Figure 2.4: Samples of biological signals in the *BioCycleReal* dataset.

time series were further inspected manually to finally yield a set of 739 high-quality periodic signals. To extract a high-quality biological aperiodic dataset, we start from the same body of data. To identify transcripts unlikely to be periodic, we select the transcripts classified as aperiodic consistently by all three programs JTK_CYCLE, ARSER and Lomb-Scargle with an associated p-value of 0.95. After further manual inspection, this yields a set of 18094 aperiodic signals.

2.1.3 Periodic and Aperiodic Signals

To classify signals as periodic or aperiodic, we train deep neural networks (DNNs) using standard gradient descent with momentum [279]. We train separate networks for data sampled over 24 and 48hours. The input to these networks are the expression time-series levels of the corresponding gene (or metabolite). The output is computed by a single logistic unit trained to be 1 when the signal is periodic and 0 otherwise, with relative entropy error function. We experimented with many hyperparameters and learning schedules. In the results reported, the learning rate starts at 0.01, and decays exponentially. The training set consists of 1 million examples, a size sufficient to avoid overfitting. The DNN uses a mini-batch size of

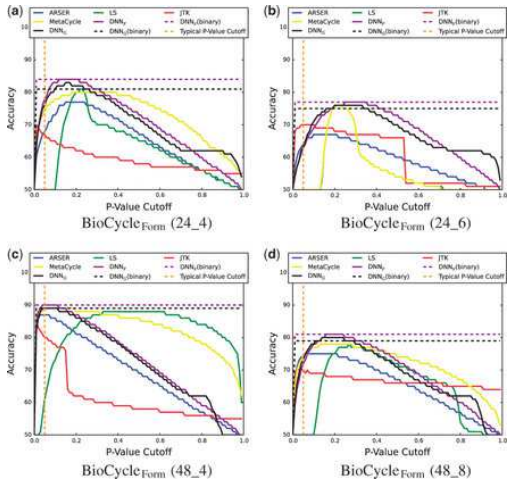

Figure 2.5: Accuracy of periodic/aperiodic classification at different p-value cutoffs on the *BioCycleForm* dataset

100 and is trained for 50,000 iterations. Use of dropout [16], or other forms of regularization, leads to no tangible improvements. The best performing DNN found has 3 hidden layers of size 100. We are able to obtain very good results by training BIO_CYCLE on synthetic data alone and report test results obtained on *BioCycleForm*, *BioCycleGauss* and *BioCycleReal*.

2.1.4 Statistics

In a way similar to how we train DNNs to classify between periodic and aperiodic signals, we can also train DNNs to estimate the period of a signal classified as periodic. During training, only periodic time series are used as input to train these regression DNNs. The output of the DNNs are implemented using a linear unit and produce an estimated value for the period. The error function is the squared error between the output of the network and the true period of the signal, which is known in advance with synthetic data. Except for the difference in the output unit, we use the same DNNs architectures and hyperparameters as for the previous classification problem.

To calculate p-values, the distribution of the null hypothesis must first be obtained. To

do this, N aperiodic signals are generated from one of the two *BioCycleSynth* datasets. Then we calculate the N output values *V(i)* (i=1,,N) of the DNN on these aperiodic signals. The p-value for a new signal s with output value V is now $\frac{1}{N}\sum N_i l(V > V(i))$, where l is the indicator function. This equation provides an empirical frequency estimate for the probability of obtaining an output of size V or greater, assuming that the signal s comes from the null distribution (the distribution of aperiodic signals). Therefore, the smaller the p-value, the more likely it is that s is periodic. The q-values are obtained through the Benjamini and Hochberg procedure. We also compute a posterior probability of periodic expression (PPPE), which models the distribution of p-values as a mixture of beta distributions.

2.2 CircadiOmics

2.2.1 Goals

It is well known that circadian oscillations at the transcriptomic level are pervasive and well coordinated [217, 224]. Oscillation in transcription is strongly regulated by a number of key transcription factors, such as CLOCK, BMAL1, PERs and CRYs that comprise the core clock [140]. These transcript level oscillations form regulatory feedback loops that oscillate throughout the transcriptome [183, 245, 224]. Moreover, a large number of metabolites and proteins in cells exhibit circadian oscillations and may play a key role within the organization of genetic circadian regulation. Strikingly, the circadian landscape in a cell can be drastically different depending on genetic and epigenetic conditions [145, 68, 319, 224]. The process by which these circadian landscapes evolve is understood as circadian reprogramming. Reprogramming can be induced by external perturbations such as inflammation or dietary challenge [103, 168, 14, 204]. The large repository of omic data provided in CircadiOmics, together with several comparative analysis tools, provide a foundational platform

that can be used to analyze these complex mechanisms and their implications.

2.2.2 Web Server Architecture

The CircadiOmics web application is constructed as a three-tier Model View Controller architecture. The web server is implemented with the Flask Python library. The interface is generated dynamically with Twitter Bootstrap and Google Charts. Fast query response times are accomplished by caching JSON serialized datasets on disk as the server is started. The interface loads with an example search of ARNTL (CLOCK-BMAL) in a sample liver control dataset. Dynamic filtering of the available datasets is provided based on tissue and experimental perturbations. Examples of filtering options are provided in the documentation on the main web server in the context of various sample workflows. Downloadable results for each search include high resolution images in PNG or SVG format, and an excel table of BIO_CYCLE reported statistics. Dataset documentation includes a short technical description as well as a link to the corresponding article in PubMed. At last, additional help information on the features of CircadiOmics is provided through a link on the main page of the web server. 2.6 shows a simplified view of the web server architecture.

2.2.3 Data Repository

The omic datasets available on CircadiOmics are compiled from project collaborations, automated discovery and manual curation. Over 6400 individual time points spanning 227 separate circadian experiments are available for search and visualization. In aggregate, these datasets form the largest single repository of circadian data available, including all datasets from other repositories including CircaDB (25). Eight species are currently available on CircadiOmics. The majority are collected from Mus musculus and Papio anibus.

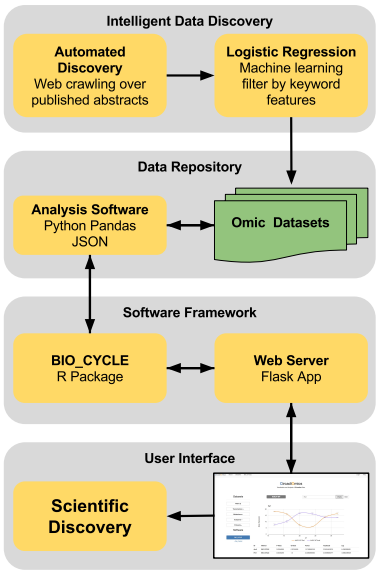

Figure 2.6: Three-tier Model-View-Controller architecture of the CircadiOmics web portal. Intelligent data discovery supplies candidate datasets for inclusion in the repository using a machine learning filter applied to key word features derived from web crawling published abstracts. BIO_CYCLE results are obtained and stored for all datasets. The user interface sends requests and displays results from the web server allowing for interactive hypothesis generation and scientific discovery.

Over 62 tissues grouped into 18 categories are represented in the database. Within these categories, liver and brain experiments comprise the majority. Diverse experimental conditions grouped into nine broad categories are available for comparison. Unique conditions include chronic and acute ethanol consumption, high-fat diet, traumatic brain injury, fibroblast undergoing myogenic reprogramming and several cancer-specific datasets [182, 94]. At last, CircadiOmics is the only tool that includes transcriptome, metabolome, acetylome and proteome experiments. The full table of datasets is available, with a short description and experimental details such as number of replicates, on the CircadiOmics web portal. Figure 2.7 quantifies the number of datasets by category.

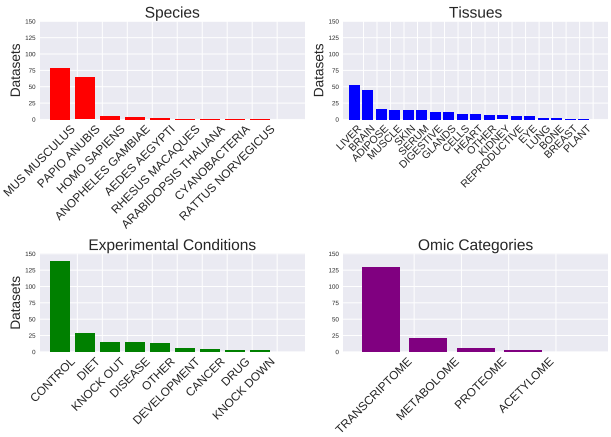

Figure 2.7: Dataset Collection by Species, Tissues, Experimental Conditions, and Omic Categories.

2.2.4 Data Discovery

Increased interest in circadian rhythms is driving a continuous increase in publicly available omic datasets. Automated discovery of datasets has become necessary to maintain the most current and comprehensive repository. A Python framework built with scholarly and geotools Python packages is used to continuously search the literature for new circadian omic studies and datasets. Automated discovery based on keyword searches in published abstracts is filtered using several features including publishing journal, author and provided supplementary materials. A logistic regression step is used to classify datasets that are good candidates for inclusion in CircadiOmics. Results produced by this automated pipeline are then manually inspected for quality, based primarily on the time point resolution of the dataset. The minimum sampling density for any dataset in the repository is every eight hours over a 24-h cycle. Additionally, the CircadiOmics team and collaborating biologists periodically search recent publications for new datasets that qualify for inclusion in CircadiOmics.

2.2.5 Visualization

The main functionality of CircadiOmics is the search, comparison and visualization of oscillation trends. The user can search any molecular species in the omic datasets within the repository and overlay multiple searches together to initiate a comparative study. A typical work flow may consist of comparing a set of specific transcripts, metabolites or proteins among several datasets. Intelligent auto-completion facilitates user queries within the currently selected dataset. Searches can be performed individually or in batch on a selected dataset. When datasets do not have the same time course, results are displayed from the minimum to the maximum time point over all selected datasets. Documentation available on the web server illustrates common query tasks and results. Datasets with large difference in intensity values at each time point can be dynamically scaled for easy visual comparison. Minimum and maximum values are normalized to zero and one, respectively.

A table of statistics is compiled and displayed beneath the main search window after each query. Statistics can be updated dynamically to reflect results obtained with BIO_CYCLE. The table can be downloaded in several formats compatible with Excel. Individual searches can be removed from both the search view and the statistics table. Figure 2.8 highlights an example query and accompanying results.

With a rapidly expanding dataset collection, filtering candidate dataset within the interface has become necessary. The filtering menu allows the user to limit the scope of datasets displayed under drop-down menus for each dataset type. Filtering can be done by species, tissues and experimental conditions. Similar experimental conditions are categorically grouped together in the filtering menu. These include knock-downs, knock-outs, diet changes and drug treatments. The search interface uses an abbreviated dataset identification. Upon selection of a dataset, the user can quickly verify the source of the data through a corresponding literature citation. Additional details for each dataset can be found in tabular form

under the dataset tab. These details include a brief description of the experimental protocol.

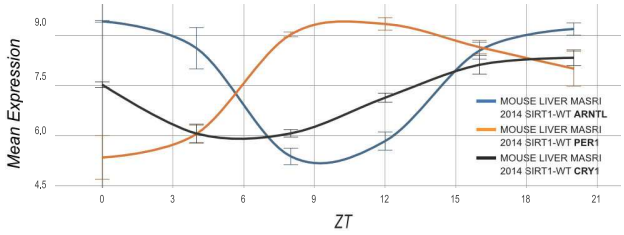

Figure 2.8: Visualization of queries for ARNTL, PER1, and CRY1 in a control mouse dataset. Any number of queries, across any number of datasets, can be displayed simultaneously.

2.2.6 Metabolomic Atlas

The Metabolic Atlas web portal (http://circadiomics.ics.uci.edu/metabolicatlas) is also available under the CircadiOmics umbrella. In addition to metabolite time series, interactive metabolic networks can be generated and visualized. These networks are derived in part from the KEGG database (30) and can be filtered using BIO_CYCLE statistics.

2.2.7 Impact

Central to the study of circadian rhythms are large-scale reprogramming events. Understanding these events at the molecular level critically depends on being able to access and compare significant amounts of high-throughput circadian omic data. CircadiOmics, with its advanced search features and unprecedented amount of high quality circadian data, is a primary enabling tool for such studies. In a circadian reprogramming event, changes in oscillation of one molecular species can often be related to changes in other molecular species [224, 117]. One of the main qualities of CircadiOmics is the flexibility of the comparative analyses it enables. For instance, a user can compare transcripts across species, or relate metabolites to proteins and transcripts and identify underlying oscillatory trends. An im-

portant example can be seen in the loss of oscillation in the metabolite NAD+ as a response to changes in the transcriptomic oscillatory landscape [68]. As a result, CircadiOmics has proven to be highly effective for hypothesis generation in new studies. To date, the web server has contributed to multiple studies that have been published in high impact journals. The server has been accessed more than 250,000 times in total traffic in 2017 alone.

Figure 2.9 details some examples of the impact of CircadiOmics. For instance, Eckel-Mahan et al. utilized CircadiOmics to analyze three related omic datasets in mouse liver [68]. They found that core clock genes regulate the acetylation of the enzyme AceCS1. AceCS1 is responsible for changes in the oscillation of the metabolite acetyl-CoA, a key metabolite involved in fatty acid synthesis (Figure 2.9 A). Similarly, Masri et al. compared liver transcriptomic data with metabolomic data in mice afflicted with cancer using CircadiOmics (Figure 2.9 B). They discovered that a distal tumor-bearing lung can reprogram the liver circadian transcriptome through inflammatory pathways and insulin related metabolic pathways [182]. More recently, CircadiOmics has been used to examine the role of circadian regulation in myogenic reprogramming of fibroblast (https://www.biorxiv.org/content/early/2017/06/18/151555). It was observed that the *core clock* is completely disrupted during this process. However, exogenous MYOD1 gains rhythmicity during transition to muscle cell. As a result, MYOG and a majority of critical transcription factors related to muscle development known to be regulated by MYOD1 synchronize oscillation. This behavior was identified in CircadiOmics through visualization and confirmed by BIO_CYCLE reported phase lag (Figure 2.9 C). Finally, aggregating all mouse transcriptomic datasets confirms and amplifies the notion that circadian oscillations are pervasiveness: 93.5% of all possible protein coding transcripts exhibit circadian oscillations in at least one tissue or experiment (up from about 67% in [224]) (Figure 2.9 D). The large number of datasets in CircadiOmics facilitates these kinds of integrative analyses.

The latest release of CircadiOmics is the largest single repository of circadian omic data avail-

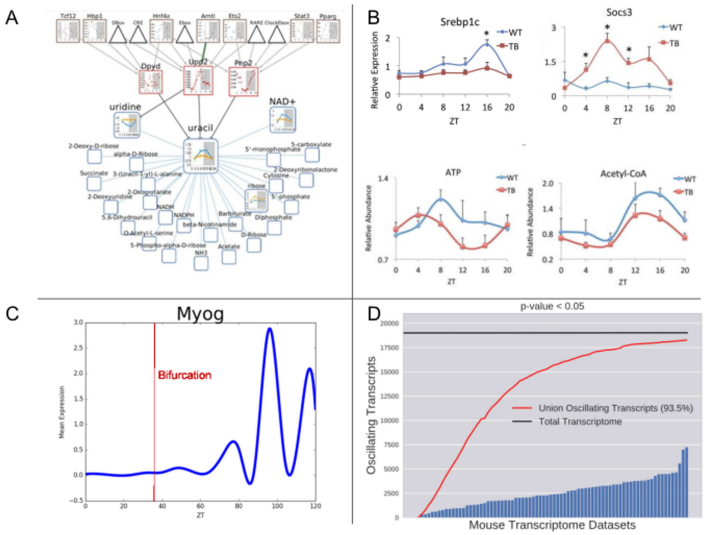

Figure 2.9: Selected Examples of the Impact Of CircadiOmics. **(A)** CircadiOmics was used to link a multitude of circadian metabolites with functionally related circadian transcripts. Figure taken from Figure 5A of [68]. **(B)** CircadiOmics was used to discover reprogrammed circadian transcripts and metabolites related to inflammatory and energy pathways. Figure taken from Figure 2E, 4B and 5D of [182]. **(C)** Exogenous MYOD1, during MEF myogenic reprogramming, entrains oscillation in MYOG and related targets in absence of oscillation of the core clock. **(D)** Bar heights show the ordered number of oscillating protein coding transcripts with a $p \leq 0.05$ in each mouse transcriptomic experiment in the repository. The trend is the cumulative union of oscillating transcripts. Over 93% of possible protein coding transcripts are found to oscillate in at least one tissue or condition across all mouse datasets.

able. Updates in server architecture and data mining ensure that CircadiOmics will continue to maintain and grow as new data is published. Improvement in features for search and visualization expand the possibilities for study of circadian rhythms in omic datasets. These possibilities include generating specific hypothesis for individual experiments and answering larger questions about the organization of oscillation within a cell.

Chapter 3

Circadian Reprogramming by Nutritional Challenge

3.1 High Fat Diet-Induced Reprogramming

Circadian rhythms and cellular metabolism are intimately linked. We revealed that a high-fat diet (HFD) generates a profound reorganization of specific metabolic pathways, leading to widespread remodeling of the liver clock. Strikingly, in addition to disrupting the normal circadian cycle, HFD causes an unexpectedly large-scale genesis of de novo oscillating transcripts, resulting in reorganization of the coordinated oscillations between coherent transcripts and metabolites. The mechanisms underlying this reprogramming involve both the impairment of CLOCK-BMAL1 chromatin recruitment and a pronounced cyclic activation of surrogate pathways through the transcriptional regulator PPARy. Finally, we demonstrate that it is specifically the nutritional challenge, and not the development of obesity, that causes the reprogramming of the clock and that the effects of the diet on the clock are reversible.

Accumulating evidence supports the notion that oscillating metabolites are also important for the maintenance of cellular rhythmicity [68, 206, 214, 49, 239], but the extent to which the circadian metabolome is affected by nutritional stress is not known. Metabolic homeostasis is not maintained when components of the circadian clock are missing or functioning improperly [149, 161, 180, 249, 250, 265, 295, 328], and circadian disruption can result in disorders such as diabetes, obesity, and cardiac disease [9, 61, 63, 76, 81, 138, 156, 264, 280]. Conversely, metabolic disruptions such as the restriction of energy intake to a phase that opposes that of the traditional feeding phase, can reset some peripheral clocks almost entirely, disrupting energy balance [11, 51, 116, 274, 302]. Hepatic circadian rhythmicity, in particular, is highly responsive to cyclic energy intake [106, 229, 302].

The molecular mechanisms by which a high-fat diet (HFD) affects the circadian clock are not known. Using high-throughput profiling of the liver metabolome and transcriptome, we establish that HFD has multifaceted effects on the clock, including a phase advance of metabolite and transcript oscillations that are maintained on the diet, as well as an abolition of otherwise oscillating transcripts and metabolites. In addition to these disruptive effects, we find a surprising, elaborate induction of newly oscillating transcripts and metabolites. Thus, HFD has pleiotropic effects that lead to a reprogramming of the metabolic and transcriptional liver pathways. These are mediated both by interfering with CLOCK-BMAL1 recruitment to chromatin and by inducing the de novo oscillation of PPARy-mediated transcriptional control at otherwise noncyclic genes.

We analyzed the circadian transcriptome using the same liver samples used for the metabolome. In all, 2,828 transcripts oscillated in expression; of these, 49.5% (1,394) were rhythmic only in the normal chow (NC) condition. An additional 778 were rhythmic in both NC and HF conditions, and a surprising 654 were newly oscillating exclusively in HFD. When analyzed for singular enrichment in metabolic pathways, we found that genes oscillating in both NC and HF showed unique annotations, including purine metabolism and circadian rhythm. The

persistence of circadian clock gene oscillation in both NC and HFD validates the notion that circadian oscillation within the core clock genes is highly resistant to perturbation, whereas clock output genes are more sensitive to food as a zeitgeber [51]. Metabolic pathways whose oscillation was uniquely lost in HFD included ubiquitin-mediated proteolysis and insulin signaling.

The disruptive effect of HFD on CLOCK-BMAL1 chromatin recruitment does not explain the de novo rhythmicity gained by a large group of genes in HFD. Notably, with the exception of the group of genes whose oscillation is lost under HFD, the group of newly oscillating genes is the largest, more than doubling the number of genes that showed phase advancement as a result of the HFD.

Transcription factor motif analysis by MotifMap [48, 315] was performed on a region located 10 kb upstream and 3 kb downstream of the transcriptional start sites to determine what transcriptional pathways might be most heavily affected by the HFD. Using a Bayesian branch length score of 1 or greater, E boxes were significantly enriched in genes oscillating only under NC, as well as in genes oscillating under both NC and HFD conditions. On the contrary, no enrichment for E boxes was observed in the group of genes oscillating exclusively in HFD condition. Analysis of the frequency of specific transcription factor binding sites in the promoters of genes whose oscillation was induced by HFD revealed that HFD promotes the use of additional transcriptional pathways to reprogram the hepatic transcriptome. One of the most represented transcription factors in the newly oscillating group of genes was PPAR. Several other transcription factors oscillated in HF only, which included SREBP-1 (Srebf), CREB1, and SRF. PPAR and SREBP1 were identified as having one or more target sites in 322 and 91 genes, respectively. In line with the idea of increased PPAR-mediated gene expression under HFD, metabolomics analysis revealed that PPAR ligands were elevated in livers of HFD-fed animals, specifically 13-HODE, 15-HETE, linolenate, and arachidonate. PPAR is a nuclear receptor involved in glucose and lipid metabolism [71, 230] and has been

described as a nutrient sensor in metabolic tissues [271, 292]. PPAR expression is induced in response to HFD and during the development of diet-induced fatty liver disease [120]. We found that PPAR expression was robustly oscillatory in the liver of HFD-fed animals, with a peak at ZT12. Whereas the levels of total PPAR protein were elevated, but not circadian, in HFD-fed mice, nuclear PPAR showed a significant circadian oscillation, with a robust peak in expression at ZT12. Levels of PPAR in NC-fed mice had no variation. Importantly, chromatin-bound PPAR displayed a robust change at different zeitgebers only in HFD-fed mice. Expression of nocturnin (NOC), which has been implicated in PPAR nuclear translocation in adipocytes [133], was phase advanced under HFD but showed similar amplitude under both diets.

We next analyzed the expression of several known PPAR target genes. Cell-death-inducing DFFA-like effector C (Cidec, also known as fat-specific protein 27-Fsp27) is substantially elevated in the livers of the obese ob/ob mice [186]. Cidec expression is not considered to be circadian under normal conditions but became robustly oscillatory under HFD, corresponding with a circadian change in H3K4me3 at its promoter. We validated the role of PPAR by injecting GW9662, a specific PPAR antagonist, into HFD-fed animals. GW9662 blocks PPAR activity while not affecting its binding to DNA [163]. While the circadian fluctuation in PPAR in the chromatin fraction was unaltered, GW9662 produced a decrease in PPAR-induced Cidec expression at the peak. Furthermore, we found that PPAR occupied the Cidec promoter in a circadian manner only in HFD-fed animals. We analyzed another known PPAR target, pyruvate carboxylase (Pcx), an enzyme that converts pyruvate to oxaloacetate and is an important regulator of hepatic gluconeogenesis [124]. Liver- and adipose-specific inhibition of Pcx produces a reduction in plasma glucose, adiposity, plasma lipid concentrations, and hepatic steatosis in HFD-fed animals [154]. Pcx expression was significantly elevated and rhythmic in livers of HFD-fed mice, and PPAR occupied the Pcx promoter in a circadian manner only in HFD conditions. Thus, the transcriptional reprogramming induced by HFD relies on changes in the presence and pattern of oscillation and

chromatin recruitment of PPAR.

3.1.1 Reorganization of the Circadian Metabolome

To understand how altered nutrients affect circadian metabolism, we explored the effect of HFD in mice by studying the hepatic metabolome, where a large number of metabolites are circadian or clock controlled [50, 68, 129]. After 10 weeks on a HFD, mice displayed expected metabolic features. Importantly, the timing and quantity of energy intake was similar between feeding groups. Metabolome profiles were obtained by tandem mass spectrometry (MS/MS) and gas chromatography-mass spectrometry (GC/MS) from livers isolated every 4 hr throughout the circadian cycle [5]. A large number of metabolites across several metabolic pathways displayed changes in HFD-fed animals. Of 306 identifiable metabolites, 77% showed a diet effect, and 45% showed a time effect. When analyzed for circadian oscillations, 141 metabolites cycled in abundance. Of these, 61 metabolites (43%) oscillated in both feeding conditions (both), whereas 42 metabolites (30%) oscillated only in normal chow-fed animals (NC). Importantly, 38 metabolites oscillated only in HFD-fed animals (HF). Many of the metabolite changes were present at ZT12 and ZT16, and included numerous nucleotide, amino acid, and xenobiotic metabolites. The metabolite peak profiles differed across several of the metabolic pathways throughout the circadian cycle. Interestingly, the phase and amplitude of remaining oscillatory metabolites also differed. Specifically, metabolites that oscillated in both feeding conditions generally showed a shift in phase when in HFD. Of the phase-shifted metabolites, 28% were delayed in phase, whereas 72% were phase-advanced in HFD. Considering the phase of metabolites that oscillated only in NC or only in HFD, metabolites that oscillated only in HFD tended to peak earlier.

A majority of metabolite oscillations previously shown to be CLOCK dependent [68] are affected by HFD. As seen in our previous experiments, specific metabolic subpathways are

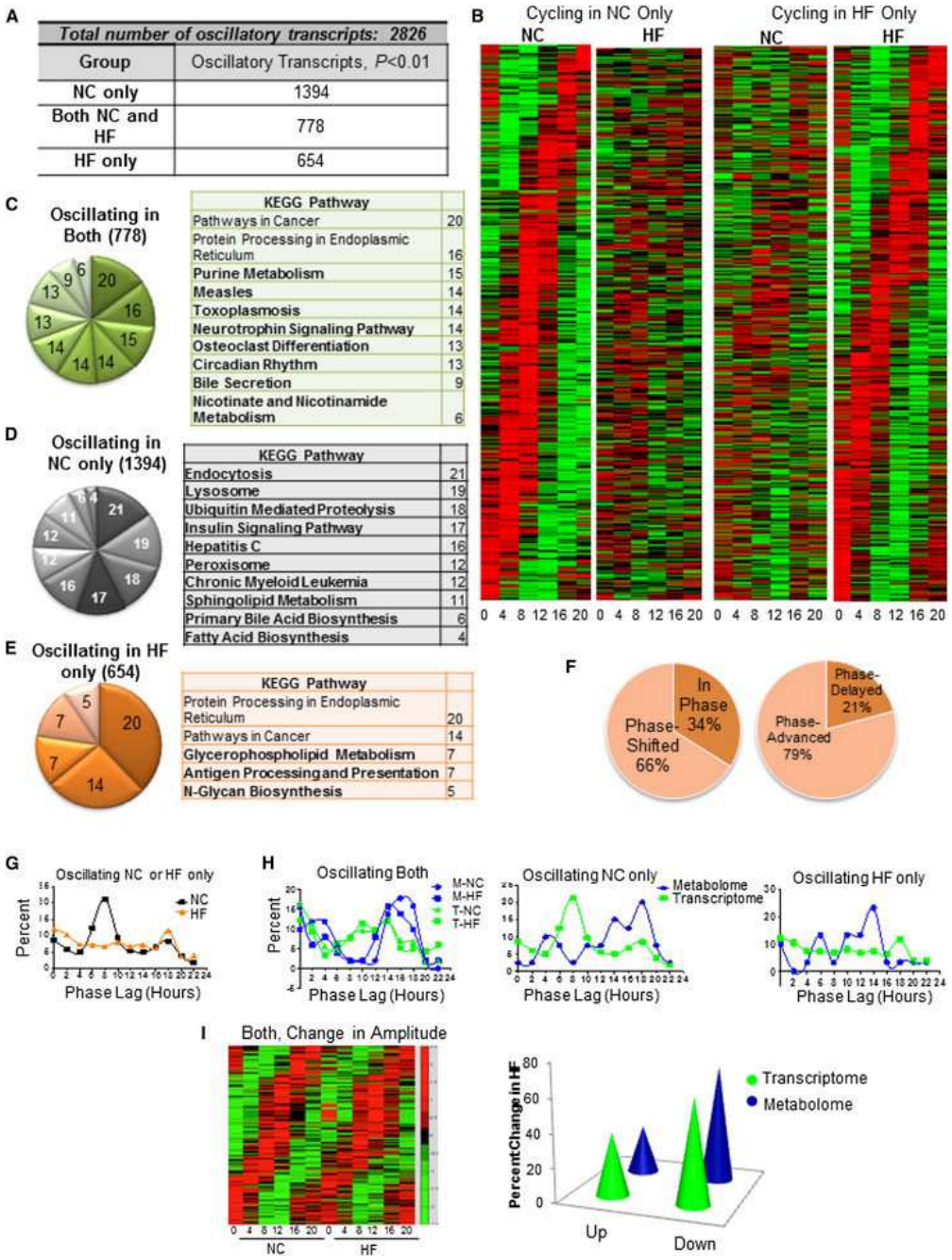

Figure 3.1: The Circadian Transcriptome Is Reprogrammed by a HFD. **(A)** The number of oscillatory transcripts only in NC, only in HF, or in both NC and HF groups (p-value = 0.01, JTK_CYCLE). **(B)** Heat maps for NC- and HF-only oscillating transcripts (p-value = 0.05). **(C)** Gene annotation on oscillating genes with a p-value = 0.01 reveals pathways that are oscillatory in both NC and HF livers (unique pathways in bold font). (D) Pathways in which oscillatory expression is lost by the HF diet. **(E)** KEGG pathways represented by genes oscillatory only in the HF liver. **(F)** Proportion of the oscillatory transcriptome shared in both liver sets that is phase shifted (left) and the direction of the phase shift (right). **(G)** Phase analysis of transcripts that oscillate only in NC or HF. **(H)** Circadian fluctuations of the metabolome relative to the transcriptome in both (left), NC-only (middle), or HF-only categories (right). **(I)** Extent of amplitude changes in transcript abundance (heat map and graph) and metabolites (graph) after HF feeding.

circadian. For example, lysine metabolism is highly rhythmic in normal feeding conditions [68]. In this study, lysine metabolism was highly rhythmic in both feeding conditions. Specifically, glutarate, lysine, 2-aminoadipate, and pipecolate showed oscillatory abundance in both conditions. On the other hand, pyrimidine metabolism displayed rhythmicity only under NC condition. For example, cytidine 5-monophosphate (5-CMP), 2-deoxycytidine, and 2-deoxycytidine 5-monophosphate all lost oscillation in HFD.

Strikingly, HFD completely blocked oscillation of nicotinamide adenine dinucleotide (NAD+). A previous report demonstrated reduced hepatic NAD+ under HFD [326]. Thus, HFD may modulate its negative influence on energy balance by eliminating circadian oscillations in NAD+ rather than inducing a static decrease in total NAD+ content. The lack of circadian NAD+ accumulation under HFD supports the observation that NAD+ is high during fasting [247]. Animals fed a HFD may never achieve such an energy-depleted state due to the constant and nonoscillatory levels of glucose. The molecular mechanism leading to the impairment in NAD+ oscillation in HFD constitutes a paradigm of clock transcriptional reprogramming through the control of the Nampt gene.

A large number of lipid metabolites were affected by HFD. Coenzyme A, a cofactor involved in fatty acid synthesis and B oxidation, displayed a circadian profile in HFD that was substantially increased in amplitude, as did its precursors phosphopanthetein and 3-dephosphocoenzyme A. Many amino acid metabolites continued to oscillate in both conditions, even though their relative abundance was substantially reduced by the HFD, likely due to increased gluconeogenesis. We conclude that the HFD impinges on the circadian metabolome in three possible manners: ablation, phase advancement, or promotion of oscillation for specific metabolites.

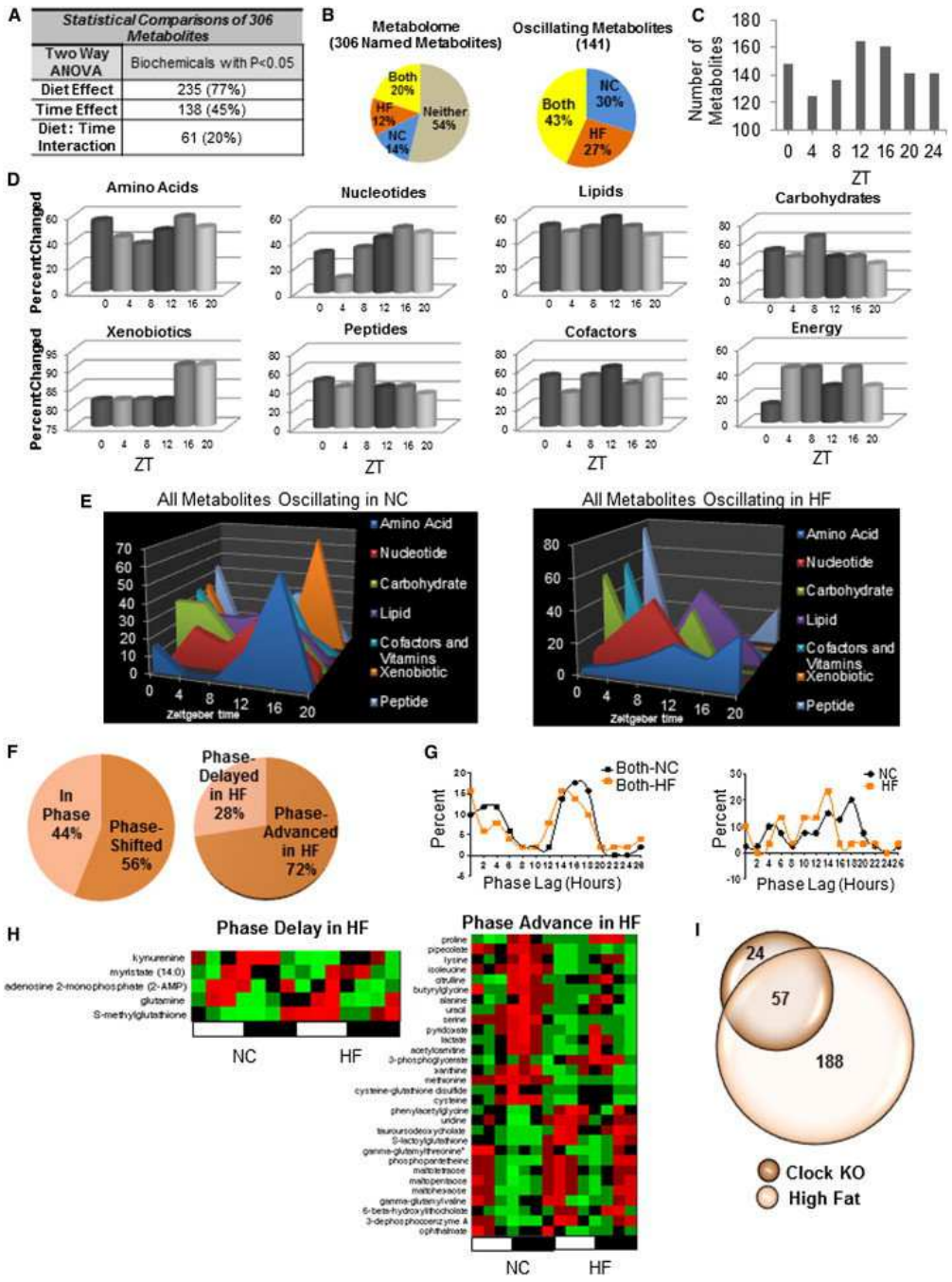

Figure 3.2: HDF alters the Circadian Profile of the Metabolome. **(A)** Number of hepatic metabolites affected by diet or time. **(B)** The hepatic circadian metabolome consists of metabolites that oscillate in both groups of animals regardless of diet (Both), metabolites that oscillate only in animals fed normal chow (NC), and metabolites that oscillate only in animals fed HFD (HF). p-value = 0.05, JTK_CYCLE, and n = 5 biological replicates. **(C)** The number of hepatic metabolites altered by the HFD at each zeitgeber time (ZT). **(D)** Percent of metabolites in a metabolic pathway changing at a specific ZT in HF animals. **(E)** Metabolic landscapes depict the percent of oscillatory metabolites that peak at a specific ZT for each feeding condition compared to the total number of oscillatory metabolites in that metabolic pathway. **(F)** Proportion of metabolites that oscillate on both diets that are in phase or phase shifted (left) and the direction of the phase shift (right). **(G)** Phase graph of metabolites that oscillate in both conditions (left) or only in the NC or HF conditions (right). **(H)** Heat maps depicting phase-delayed or phase-advanced metabolites in HF livers. **(I)** Overlap of metabolites that are both CLOCK dependent and sensitive to a HF diet.

3.1.2 Linking Circadian Metabolome and Transcriptome

We determined the relationship within metabolic pathways between the transcriptome (of the enzymes) and the metabolome on different diets by integrating the data into the bioinformatics resource, CircadiOmics [225, 34]. We classified and grouped metabolite-enzyme edges based on the presence or absence of oscillation, as well as additional characteristics of the oscillationspecifically, the phase and amplitude. The most common edge characterization (87 of 384 edges, 23%) revealed that the loss of oscillation for a particular metabolite usually was accompanied by a loss of oscillation for its related transcripts. Interestingly, the second most common edge classification involved the loss of oscillatory transcript abundance in HFD but an increase in the amplitude of oscillation in the related metabolite. No phase delay in the transcriptome or metabolome was observed within the top ten edge classification scenarios, suggesting again that a significant effect of HFD is to phase advance the remaining oscillatory metabolites. Edge classification reinforced the notion that one of the effects of HFD is to reorganize the temporal coherence between the metabolome and transcriptome. The most common relationships between related transcripts and metabolites involved an opposing state of oscillation in animals fed HFD.

A paradigmatic example of a metabolite whose loss of oscillation by HFD is accompanied by a dampened oscillation for its related transcript is NAD+. Circadian NAD+ synthesis depends on the transcriptional control by the clock of Nampt gene expression [206, 239]. HFD induces a loss of NAD+ oscillation that parallels a dampening of Nampt cyclic transcription. Additional case scenarios include ornithine decarboxylase 1 (Odc1) and ornithine (where a concomitant loss of oscillation occurs in HFD), acyl-CoA synthetase short-chain family member 2 (Acss2) and coenzyme A (where loss of oscillatory transcript in HFD corresponds to an increased metabolite amplitude), and cytochrome P450 monooxygenase (Cyp2a5) and arachidonate (where a phase advance in transcript in HFD corresponds to a lack of oscillation in its related metabolite).

Importantly, several metabolite and transcript edges within individual pathways mirror each other in HFD-induced gain of oscillation. Remarkable examples are within the amino acid subpathway of cysteine, methionine, S-adenosylmethionine (SAM), and taurine metabolism. Indeed, both SAM and S-adenosylhomocysteine (SAH) showed newly oscillating profiles in HFD. HFD-induced cycling of these metabolites was accompanied by de novo oscillation of several related enzymes, including Ehmt, Trmt2b, Whsc1, and Dph5genes whose products have known or predicted methyltransferase activity. A relevant case is Ahcyl2, the gene encoding the enzyme that catalyzes the reversible conversion of SAH to adenosine and homocysteine and whose oscillation parallels the one of SAH in HFD. Each metabolite and transcript identified in the livers of animals fed NC or HFD were integrated within the computational resource, CircadiOmics [68, 225, 34].

3.1.3 Disrupted CLOCK-BMAL1

[68, 206, 239]. Thus, we investigated the molecular mechanisms by which circadian oscillations are disrupted by HFD. First, we hypothesized that HFD might alter core clock gene expression. Importantly, most of the core circadian genes were rhythmic in the livers of HFD-fed mice, displaying only weak shifts or slightly dampened patterns of oscillation, results that are cohesive with previously published work [106, 144]. Per2 and Bmal1 mRNA showed mild dampening and phase advancement, whereas Clock expression was unaffected.

One case scenario is represented by the gene Dbp, whose robust circadian oscillation was phase advanced in HFD. Because Clock and Bmal1 cyclic transcription is similar in HFD-fed mice, we analyzed protein levels. Importantly, the levels of BMAL1 and CLOCK proteins were unaltered in livers of HFD-fed animals. Similarly, the phosphorylation profiles of BMAL1 in NC and HFD conditions were similar in different cellular fractions. We next explored whether CLOCK-BMAL1 chromatin recruitment might contribute to the altered

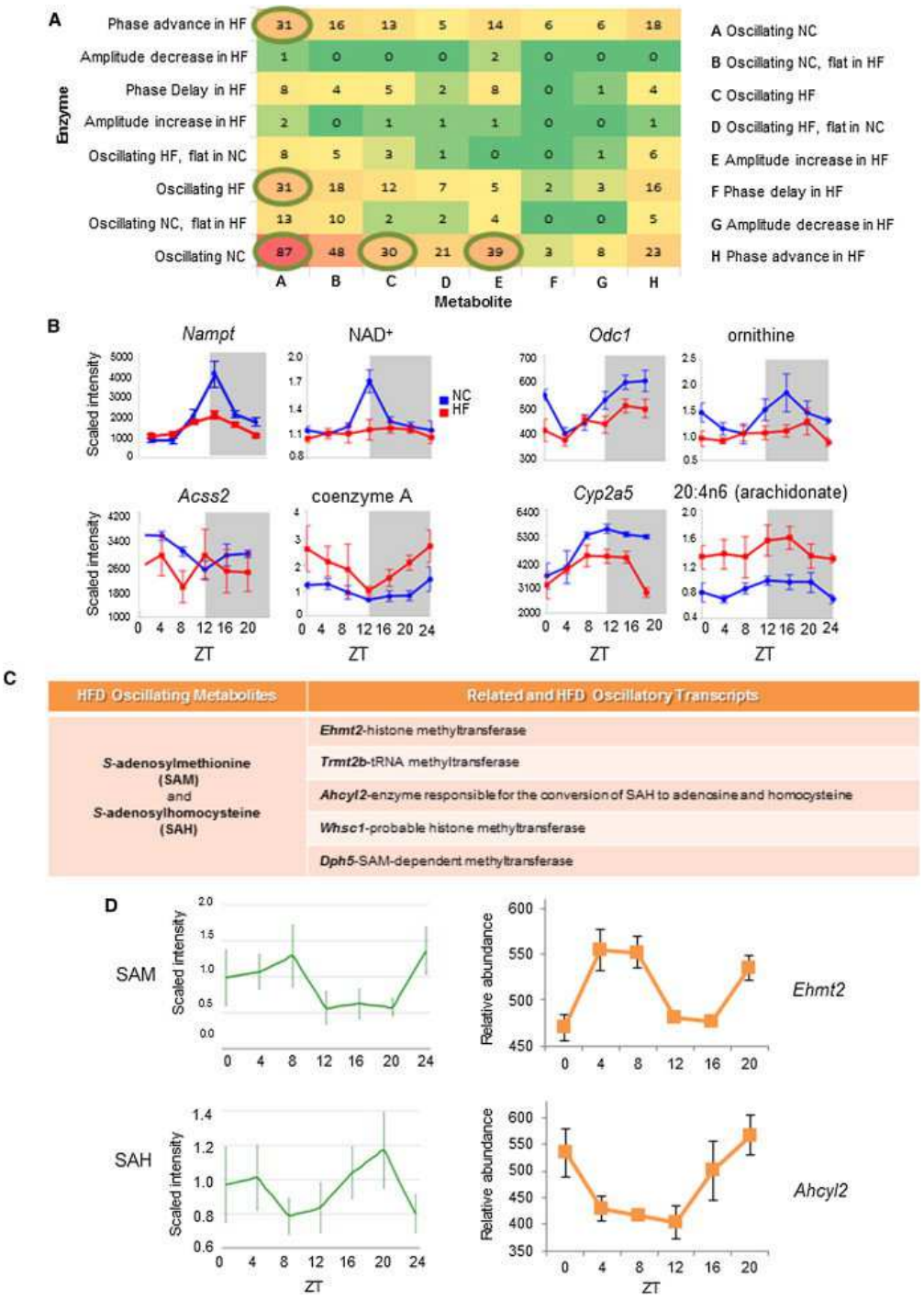

Figure 3.3: HFD Disrupts Circadian Organization between the Transcriptome and Metabolome. **(A)** Heat map showing the relationships between all pairs of metabolites and enzymes in KEGG. (Note: flat is a subset of not, where the maximum abundance does not exceed the minimum by 20%.) Circled are the numbers referring to the five most common relationships. **(B)** Related enzyme transcripts and metabolites (edges) that follow a particular temporal profile. **(C)** Metabolites and related transcripts within the SAM node that gain oscillation in HF.**(D)** Oscillatory abundance of SAM, SAH, and their related enzymes Ehmt2 and Ahcyl2 only in HF. Error bars, SEM.

pattern of Dbp expression by chromatin immunoprecipitation (ChIP) [244]. Remarkably, BMAL1 and CLOCK recruitment was shifted in livers of HFD-fed mice.

Interestingly, transcripts whose oscillation was lost in HFD were in large part peaking between ZT4 and ZT12, a time period that correlates with prominent CLOCK-BMAL1 recruitment to chromatin targets [105, 147, 201]. This parallels the dampening or abrogation of the oscillations of numerous metabolites previously shown to be CLOCK-BMAL1 regulated. A remarkable example is NAD+, whose cyclic levels become flat after HFD, paralleling the profile of Nampt transcription. Similarly, the oscillations of the metabolites uridine and uracil, the abundance of which is dependent on the enzymatic activity of CLOCK-BMAL1-driven uridine phosphorylase 2 (Upp2) [68], were depressed in the livers of HFD-fed animals. The amplitude of Upp2 expression was considerably reduced under HFD. Interestingly, we observed a substantial decrease in CLOCK and BMAL1 circadian occupancy on the Upp2 and Nampt promoters in livers of animals fed a HFD. Importantly, oscillation in H3K4me3, a histone modification tightly associated with circadian transcription [130, 244], significantly decreased at the Upp2 and Nampt promoters in HFD-fed animals. Thus, the profound effect elicited by HFD is caused by either phase-shifted or reduced recruitment of the CLOCK-BMAL1 complex to chromatin at the level of target promoters.

3.1.4 Diet-Induced Reprogramming and Obesity

Animals fed a HFD for 10 weeks become obese [311]. To discern whether clock reprogramming depends on the development of obesity rather than the HFD content, we fed mice a HFD for only 3 days and then analyzed the metabolome. Considering only metabolites that showed consistent circadian profiles in NC between the 10 week group and the 3 day groups at the zeitgeber times chosen (this comparison revealed 87.5% consistency between experiments), 131 metabolites showed a diet effect, whereas 80 showed a time effect. We

used NAD+, uridine, and uracil as metabolic markers as they were highly susceptible to 10 weeks of HFD. Notably, the abundance and oscillation of uracil and uridine was greatly reduced in amplitude, and the circadian oscillation of NAD+ was abolished within 3 days of HFD. Next, we determined the impact of the 3 day feeding paradigm on transcription. Bmal1 transcript and protein levels were unchanged by the 3 days of HFD, paralleling the scenario of the 10 week HFD. However, the amplitude of Upp2 and Nampt oscillation was already reduced after 3 days of HFD, as was the expression of Dbp at ZT12, a reflection of the phase shift observed in the 10 weeks HFD analysis. Finally, PPAR targets gained rhythmicity after acute HFD feeding as illustrated by Cidec expression.

In addition to the NC diet, a second low-fat diet was used to confirm that observed changes at 3 days were not simply due to variation in carbohydrate composition. Results were similar to NC-fed animals, underscoring the deleterious nature of HFD on the circadian clock. Chromatin immunoprecipitation experiments revealed that the occupancy of CLOCK and BMAL1 was reduced at their target sites on Upp2 and Dbp at ZT12, as was the H3K4me3 mark at these promoters. Thus, a short 3 day exposure to HFD initiates the reprogramming of the circadian clock.

3.1.5 Reversibility of Diet-Induced Remodeling

To determine whether the transcriptional state of HFD-fed mice is reversible, we fed a group of animals a HFD for 10 weeks followed by 2 weeks of NC feeding. Although animals lost some weight during the 2 week NC period, they remained significantly overweight relative to normal chow. Interestingly, after 2 weeks of NC feeding, circadian expression of Upp2 and Dbp was restored, as was Nampt. Expression of the PPAR target Pcx was not elevated relative to control livers at ZT12. Finally, BMAL1 occupancy at the Upp2 and Dbp promoters at ZT12 was identical in both liver groups, revealing a restoration of circadian BMAL1

presence at target promoters after the HFD challenge was removed. Thus, the HFD-induced transcriptional and epigenetic remodeling is reversible.

Metabolic and circadian processes are tightly linked, but the mechanisms by which altered nutrients influence the circadian clock have not been deciphered. We have explored the effects of nutrient challenge in the form of HFD on the circadian metabolome and transcriptome and found that HFD induces transcriptional reprogramming within the clock that reorganizes the relationships between the circadian transcriptome and the metabolome. We have unraveled at least three mechanisms by which this reprograming occurs: (1) loss of oscillation of a large number of normally oscillating genes; (2) a phase advance of an additional subset of oscillating transcripts; and (3) a massive induction of de novo oscillating gene transcripts.

We have demonstrated that HFD-induced changes in the circadian clock implicate a reprogramming of the transcriptional system that relies on at least two key mechanisms. The first mechanism is the lack of proper CLOCK-BMAL1 chromatin recruitment to genes that would normally be considered as clock controlled. This results in a decrease or abrogation of oscillation in transcription. The second, illustrated by the de novo oscillations in transcriptional networks otherwise considered arrhythmic, relies in large part on the robust, circadian accumulation in the nucleus and on chromatin of the transcription factor PPARy. Although we predict that other transcriptional pathways would contribute to clock reprogramming, including SREBP1, the role of PPAR appears prominent. This nuclear receptor has been linked to circadian control during adipogenesis and osteogenesis [133], whereas its role in the liver clock is not fully understood [91]. We determine that PPAR circadian function in HFD-fed mice relies on a clock-controlled nuclear translocation of the protein and rhythmic chromatin recruitment to target genes.

In contrast to the PPAR scenario, HFD does not affect CLOCK-BMAL1 nuclear translocation but impedes their specific chromatin recruitment. We speculate that additional regulatory pathways are implicated that might interplay with the ones described here. In

conclusion, the remarkable induction of de novo oscillation in both metabolites and transcripts under HFD indicates that a diet high in fat has previously unsuspected, potent, and pleiotropic effects on the circadian clock. Furthermore, the rapid influence of the diet on the clock (as demonstrated by the 3 day HFD experiment) reveals that this type of nutritional challengeand not merely the development of diet-associated complications such as obesityis capable of remodeling the clock. Further work will elucidate how the molecular composition of CLOCK-BMAL1 and PPAR chromatin complexes may be influenced by nutritional challenges, possibly leading to modulation of enzymatic activities of specific coregulators and modifiers.

An intriguing concept that may be derived from our study relates to the potential of specific genes to be circadian or not. Indeed, the transcriptional remodeling in the HFD raises the hypothesis that, given the right molecular environment, an extended array of transcripts and metabolites can oscillate. We speculate that this may be achieved through the coordinated harmonics of energy balance, transcriptional control, and epigenetic state. In summary, nutrients have powerful effects on the cellular clock, revealing its intrinsic plasticity. These effects consist not only of the abrogation of pre-existing rhythms but the genesis of rhythms where they do not normally exist. This induction is rapid and does not require the onset of obesity, and it is also reversible. The reversible nature of these effects gives hope for novel nutritional and pharmaceutical strategies.

3.2 Effects of Nutritional Challenge in the Serum

Diagnosis and therapeutic interventions in pathological conditions rely upon clinical monitoring of key metabolites in the serum. Recent studies show that a wide range of metabolic pathways are controlled by circadian rhythms whose oscillation is affected by nutritional challenges, underscoring the importance of assessing a temporal window for clinical testing and

thereby questioning the accuracy of the reading of critical pathological markers in circulation. We have been interested in studying the communication between peripheral tissues under metabolic homeostasis perturbation. Here we present a comparative circadian metabolomic analysis on serum and liver in mice under high fat diet. Our data reveal that the nutritional challenge induces a loss of serum metabolite rhythmicity compared with liver, indicating a circadian misalignment between the tissues analyzed. Importantly, our results show that the levels of serum metabolites do not reflect the circadian liver metabolic signature or the effect of nutritional challenge. This notion reveals the possibility that misleading reads of metabolites in circulation may result in misdiagnosis and improper treatments. Our findings also demonstrate a tissue-specific and time-dependent disruption of metabolic homeostasis in response to altered nutrition.

Circadian rhythms govern a large variety of behavioral, physiological, and metabolic processes [2, 238, 251, 57]. Recent advances reveal that a very large fraction of mammalian metabolism undergoes circadian oscillations [206, 227, 274, 145]. This notion is critical, and it raises awareness of the need for increased attention to the time of monitoring clinically relevant values in patients. Indeed, studies in humans show that levels of key markers oscillate significantly [49], possibly leading to false or misleading reads that may result in questionable therapeutic outcomes. Thus, a comprehensive comparative analysis of the circadian metabolome in the serum versus peripheral tissues is critical to decipher the circulating metabolites that constitute a specific signature of a given physiological state.

Circadian rhythms are under the control of clocks that ensure cyclic regulation of a large spectrum of cellular and molecular mechanisms. In mammals, the central clock is located in the suprachiasmatic nucleus (SCN)2 of the anterior hypothalamus. The SCN integrates external daily cues, such as the light-dark cycle, and operates as a synchronizer for a multitude of peripheral clocks located in most tissues [257]. Peripheral clocks respond to nutritional cues and can be uncoupled from the SCN by restricted feeding [274]. Recent studies have shown that

restriction of the time of feeding [274] as well as nutritional challenge by a high fat diet (HFD) [106, 144, 67] result in extensive modifications of liver metabolism. Furthermore, the liver clock displays a highly dynamic homeostasis associated with an elaborate reprogramming of its molecular gears under nutritional challenge [67]. Accumulating evidence underscores the intimate interplay between the circadian clock and cellular metabolism [91, 67, 18]. Indeed, many metabolic pathways are under circadian control and, in turn, may feedback to the clock system to assist in circadian timekeeping [206, 227, 251]. Although transcriptomics studies have extensively illustrated a substantial fraction of the genome controlled by the molecular clock [135, 196], analysis of the metabolome has lagged behind, mostly because of technical difficulties. The relatively recent use of technologies such as liquid chromatography-mass spectrometry (LC-MS) and the subsequent development of appropriate bioinformatics tools [225] have been valuable in starting to unraveling the contribution of the circadian clock to mouse and human metabolism in a number of tissues as well as in blood and saliva [50].

Analyses of serum metabolome in humans and mice have been performed in a variety of conditions (i.e. sleep deprivation, phase shifting, etc.) [118, 129, 52]. Because serum is a biological sample most often harvested in human patients and is also a critical linker between peripheral tissues as well as between peripheral tissues and the brain, we wanted to understand how a high fat diet affects the circadian clock at the level of serum metabolites. Here we reveal that, unlike in the liver, the overall effect of a high fat diet on the serum circadian metabolome is a profound loss of rhythmicity. Our results demonstrate that monitoring the levels of metabolites in the serum is a poor predictor of the metabolic landscape of the liver. Moreover, we underscore the possibility that the uncoupling of peripheral clocks from the SCN, known to be detrimental for energy balance [253], may occur through metabolic information present in the serum. Finally, we have identified specific serum metabolites diagnostic of the risk of diabetes, obesity, and other metabolic disorders that are associated with nutritional challenge.

We used LC-MS metabolomics to analyze the relative abundance of metabolites in the mouse serum and liver throughout the circadian cycle under NC and HFD conditions. Wild-type mice were divided in two experimental groups, the first fed an NC diet and the second fed an HFD (60% of calories from fat [67]) for 10 weeks. Liver and serum were harvested across the circadian cycle every 4 h. Although the hepatic circadian metabolome and transcriptome have been previously reported to undergo extensive reprogramming following nutritional challenge [67], the degree and specificity to which circulating metabolites oscillate have not been determined.

Our metabolome analysis identified 362 known metabolites in the serum, belonging to major metabolic pathways. Although a large fraction of metabolites are present in both tissues (222 metabolites), 140 metabolites, corresponding to 38.6% of the total, were detected only in serum and not in the liver. This indicates that either 1) their abundance is too low in the liver to be detected; 2) these metabolites are not typically made in or transported to the liver; or 3) due to technological variability, they were unable to be detected.

In both tissues, a large number of metabolites (62% in serum, 77% in the liver) were affected by HFD. When analyzed by analysis of variance, 40% of serum metabolites and 45% of liver metabolites deviated in abundance throughout the circadian cycle. However, when analyzed for circadian oscillation specifically (p value 0.05, JTK_CYCLE [67]), the fraction of oscillating metabolites was the same. Specifically, 46% oscillated in the serum, and 46% cycled in the liver under a distinct feeding condition. Strikingly, in serum, HFD induced an extensive disruption in the oscillation of metabolites that cycle in NC (55%). A smaller fraction of metabolites (27%) oscillated in both feeding conditions, and only 18% oscillated in HFD. This profile is in stark contrast to the situation in the liver, where 43% of metabolites oscillate in both feeding conditions, 30% oscillate only in NC (i.e. oscillation is lost under HFD), and 27% oscillate only in HFD [67]. Thus, although a similar number of metabolites oscillated in both feeding conditions in the liver, there was a 3-fold decrease in the number

of metabolites oscillating in HFD in the serum relative to NC. Thereby, it appears that the serum metabolome is much more sensitive to nutritional challenge than the liver. Moreover, an analysis of the phase of oscillation in both tissues under NC and HFD revealed some important differences. In serum, apart from the loss of oscillation in carbohydrates and cofactors in HFD, the remaining oscillatory metabolites were phase-delayed in HFD. Moreover, some variance was noted in the phase of oscillation for metabolites that oscillated in both diets. In particular, serum metabolites oscillating in both feeding conditions were phase-advanced in HFD, whereas, considering the phase of metabolites that oscillated only in NC or only in HFD, liver metabolites in HFD were somewhat phase-advanced compared with metabolites oscillating only in NC [67]. Also, we analyzed the relative abundance of major classes of metabolites at ZT0 and ZT12 for serum and liver [224]. Significant decreases in serum were detected at ZT0 under HFD compared with NC diet for peptides and xenobiotics. Moreover, lower levels of peptides were also found at ZT12 compared with ZT0 under NC. Interestingly, some major classes of metabolites showed a diet effect in the liver. This is the case for amino acids, xenobiotics, and nucleotides, with a marked decrease in their content under HFD for both of the time points analyzed.

By analyzing a variety of parameters, we have previously shown that, as expected, HFD-fed mice develop an obese phenotype [67]. Adipose tissue in mammals not only acts as storage for excess of nutrients; it also acts as an endocrine organ secreting adipokines that are involved in a wide range of functions [232, 293]. Specifically, obesity is associated with oxidative stress and inflammatory responses in adipose tissue (due to adipocytes hypertrophy and hyperplasia) with consequent increased levels of local and systemic pro-inflammatory cytokines. We analyzed the levels of IL-6, leptin, and adiponectin in serum and liver at two different time points (ZT4 and ZT16) to monitor whether the obese status elicited by the high fat diet could affect the circadian secretion of these adipokines. No changes or little change was observed in IL-6 and adiponectin levels between NC and HFD in both tissues. This could be due to various factors, such as the diet composition and/or the circadian

changes occurring at other ZTs. Importantly, the levels of leptin at ZT16 were significantly higher in HFD as compared with NC in both serum and liver. This result not only indicates a temporal disruption of this adipokine; it also suggests a misreading of the signal for the brain of the body's energy stores. Moreover, because leptin is implicated in the etiology of insulin resistance [158, 318, 202, 26], we extended our analysis by monitoring AKT and GSK3. As expected, we found that HFD induced an increase in basal (non-insulin-stimulated) AKT phosphorylation at Ser473 and GSK3 inactivation (as measured by phosphorylation at Ser9). Importantly, we also observed a complete loss of rhythmicity in AKT phosphorylation in the animals fed an HFD, whereas robust rhythmicity in phosphorylation of AKT is seen in NC-fed animals.

Next, in the pool of shared metabolites between serum and liver, we analyzed in detail the metabolites present in both tissues and oscillating only in NC. Of the eight metabolites oscillating in both tissues under NC, most were synchronous by showing a similar phase peak at ZT16. Importantly, there was a different composition of the metabolites shared between serum and liver in NC. Specifically, 75.5% of the serum lipids oscillated in NC versus 36.4% in the liver. Another striking difference relates to nucleotide metabolites; 18% of the shared nucleotide oscillated in the liver, whereas none oscillated in the serum. A parallel analysis for oscillating metabolites only in HFD revealed that only two are shared between liver and serum (allantoin and 2-oleoylglycerophosphoethanolamine).

Another revealing difference relates to metabolites oscillating in HFD, where 52% of liver lipid metabolites cycled, whereas only 33% did so in serum. Interestingly, 14 metabolites are shared and oscillate under both feeding conditions in both tissues, and most of them belong to the amino acid pathway. Analysis of the phase of oscillation for these shared metabolites revealed that, unlike the liver, the serum metabolome is not phase-advanced under HFD.

3.2.1 Pathway Analysis

Amino Acid

A significant fraction of amino acid metabolites are common to serum and liver, although some unique profiles are distinctive of the two tissues. Specifically, a number of amino acids were found exclusively in the serum (40% of all serum amino acid metabolites), including sarcosine, N6-acetyllysine, phenylpyruvate, and creatinine. A smaller fraction of amino acid metabolites are unique to the liver (17% of all liver amino acid metabolites), including glutarate, hypotaurine, and S-adenosylmethionine. Comparison of the profiles reveals that fewer amino acids oscillate in the serum than in the liver (48% versus 61.3%). In particular, we observed a 2-fold reduction in circadian amino acids affected by HFD in the serum as compared with the liver.

During the analysis of the amino acid pathway, we found that several amino acids, including glycine, serine, and threonine, display rhythmicity only under HFD in the serum. Conversely, metabolites belonging to the subpathway of the tryptophan metabolism, including tryptophan, indolelactate, indolepropionate, and kinurenine, completely lost oscillation in HFD. These metabolites, however, showed a significant decrease in levels, indicating that one of the effects of HFD is to influence the homeostasis of tryptophan metabolism. Moreover, HFD results in an increase of the overall levels of tyrosine and induces temporal regulation of tyrosine-related metabolites, such as cresol sulfates and 3-(4-hydroxyphenyl) lactate. Although HFD did not appear to regulate the circadian levels of other metabolites belonging to this pathway (phenol sulfates, 4-hydroxyphenylpyruvate), it decreased temporal aspects of their degradation. Interestingly, serotonin levels were significantly decreased in the serum under HFD compared with NC, in contrast to observations in human plasma following sleep deprivation [52].

The comparison between serum and liver amino acid metabolites revealed that some metabolites, including betaine, glutamate, glutamine, and 3-methylcrotonylglycine, are not oscillatory in serum, whereas they are robustly cyclic in the liver only in HFD. Similarly, amino acids of glutathione metabolism were devoid of oscillation in the serum (except for the ophthalmate and 5-oxoproline), in contrast to the liver, where they are highly oscillatory in both feeding conditions. In contrast, isobutyrylcarnitine, tyrosine, tryptophan, p-cresol sulfate, 3-indoxyl sulfate, and arginine were not cyclic in the liver but were cyclic in serum in NC or in HFD. Comparison of the oscillation phase revealed that metabolites of both tissues tended to peak later under HFD than what was typically observed in NC. Interestingly, under NC, most of serum and hepatic amino acids peaked at ZT16. Serum also showed an absence of fibrinogen cleavage peptides and dipeptide derivatives and a higher number of metabolites belonging to the dipeptide subpathway compared with the liver. Also, there was an increase in oscillating peptides in the serum compared with liver in HFD and a complete loss of rhythmicity for serum peptides that cycle only in NC as compared with liver. No temporal similarity for the oscillation phase was found between the two tissues analyzed.

Nucleotides

Most nucleotide metabolites are shared between liver and serum. The liver is the primary organ of de novo nucleotide synthesis, although many tissues use salvage pathways to generate nucleotide levels sufficient for cellular functions [26]. Several differences between liver and serum were, however, found, specifically in the content of the purine metabolites adenine and guanine. Interestingly, there was a loss in nucleotides oscillating in the serum compared with the liver (37% versus 54%). In particular, no oscillating nucleotide metabolites were found under NC conditions in the serum. Moreover, in the serum, nucleotide metabolites tended to peak mostly at ZT4 under both of the feeding conditions, whereas in the liver, they were phase-advanced under HFD.

Carbohydrates

Analysis of carbohydrate metabolites showed that 15 are shared between serum and liver. Almost one-third (29%) of the total serum carbohydrate metabolites were found exclusively in the serum, whereas 50% of total liver carbohydrates were found only in the liver. There was a striking difference in the number of carbohydrate metabolites whose levels changed in a circadian manner in the liver versus serum. Indeed, whereas only four metabolites (mannose, mannitol, sucrose, and xylose) oscillated in the serum (19%), 20 did so in the liver (61%). Moreover, all circadian serum carbohydrates in NC lost their cycling profile in HFD, whereas in the liver, the oscillations were conserved also under nutritional challenge. The cycling of carbohydrates in general appears to be more prominent in the liver, the primary site of both glucose uptake and glucose production. The loss of cycling under HFD of most carbohydrate metabolites in the serum reinforces the notion that the general effect of nutritional challenge is the disruption of homeostasis.

In addition to carbohydrates, another pathway that in the serum undergoes circadian disruption by HFD is glycolysis. Under nutritional challenge, all metabolites involved in glycolysis lost oscillation in the serum, including glucose 6-phosphate, lactate, glucose, and 3-phosphoglycerate, all of which remained oscillatory in the liver. An intriguing example is sucrose. A likely explanation could be that mice under HFD have a delay in glucose clearance compared with those in NC, mostly because of peripheral insulin resistance that results from higher levels of circulating free fatty acids.

Lipids

Many lipid metabolites are shared between serum and the liver. However, 33% of the lipid species found in the serum were not present in the liver. Most of these belong to the subpathways of medium-chain fatty acids, monohydroxy fatty acids, branched-chain fatty

acids, lysolipids, and metabolites in the carnitine metabolism pathway. Conversely, 18% of liver lipids are not found in the serum. Importantly, whereas more than half of the serum lipids oscillated across the circadian cycle, fewer did so in the liver (55% versus 33%). Diets also differentially affect lipid metabolites in the liver and serum. In particular, under NC, a higher number of lipids oscillated in the serum compared with the liver. Conversely, there was a massive loss of lipid metabolites under HFD in the serum as compared with the liver. Strikingly, most metabolites of the lysolipid pathway (55%) cycled in NC but lost oscillation in HFD, in striking contrast to the situation in the liver, in which only 28% of the lysolipids were shown to have a diet effect. Also, metabolites in the essential fatty acid and long chain fatty acid pathways oscillated in the serum only under NC, although they showed a non-cyclic trend in the liver under any diet condition. On the other hand, few lipids of the carnitine metabolism subpathway (e.g. myristate, carnitine, acetylcarnitine, and stearoylcarnitine) oscillated in the liver but not in the serum under HFD. For a number of metabolites, there were also changes in the phase. Some serum lipid metabolites were phase-delayed in HFD; also, whereas most of the liver metabolites oscillated in NC between ZT0 and ZT12, most serum lipids peaked at ZT8. Thus, circadian lipid profiles are profoundly affected by HFD and show loss of circadian oscillation in the serum.

Cofactors and Xenobiotics

The comparison between cofactors revealed the absence of vitamin B6, folate, and thiamine metabolites in the serum, whereas these metabolites were highly present in the liver. Interestingly, 91% of serum cofactor and vitamin-related metabolites were not oscillating throughout the circadian cycle compared with the liver (57%), whereas the remaining 9% oscillated only in NC conditions. This difference was inverted for xenobiotic metabolites. Indeed, 41% of serum xenobiotic metabolites were circadian versus only 27% in the liver, where there was a complete loss of oscillation under HFD. Moreover, serum xenobiotic-related metabolites

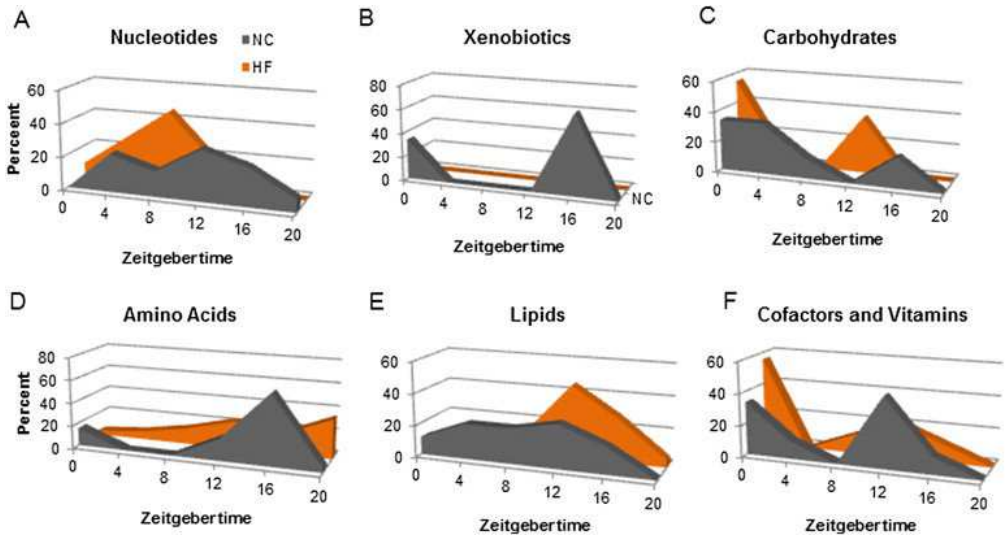

Figure 3.4: Comparison of Liver and Serum Oscillating Metabolites by KEGG Pathway.

were phase-advanced in NC compared with those in the liver.

Energy Metabolism

Metabolites related to the Krebs cycle and oxidative phosphorylation showed no major changes along the circadian cycle. Importantly, only two metabolites (22%) oscillated across the circadian cycle in the serum and only one in the liver (14%). These data suggest that these critical metabolites must maintain relatively stable levels throughout the circadian cycle and under nutritional challenge.

3.2.2 Metabolic Markers

The comparison between serum and liver metabolomes showed that almost 39% of the total metabolites identified, across most of the metabolic pathways, were exclusively present in serum. Most of the metabolites found in the serum are known to be present in all tissues and organs of the body, including intestine, muscle, brain, epidermis, and spleen, indicating that a given metabolite may be not specific to serum but rather present in low abundance or

is not found in the liver. Considering serum metabolites only, 60% of them undergo changes in response to the diet, independent of whether it is a decrease or an increase upon HFD. Interestingly, many of these metabolites can be considered as markers for various diseases, including cancer, cardiovascular and renal diseases, and metabolic disorders. For example, in our study, we found altered levels of arachidonate, cholesterol, stearate, betaine, glycerol, sucrose, 2-aminoadipate, eicosapentaenoate, 3-methyl-2-oxovalerate, and oleate. These metabolites have been shown to be associated with obesity, metabolic syndrome, or type II diabetes [272, 278, 208]. Moreover, the levels of several metabolites associated with cardiovascular diseases and/or renal failure/dysfunctions were significantly changed, such as, for example, fatty acid, p-cresol sulfate, inosine, genistein, and daidzain [210, 47]. Serotonin, which has a key role in appetite control, was severely affected by HFD, possibly underscoring the tight link between this neurotransmitter and obesity. Peripheral serotonin could be involved in the obesity-induced adipose tissue inflammation in our mice [45, 178].

3.2.3 Comparison of Liver and Serum Metabolic Reprogramming

The relevance of blood in clinical tests lies in the fact that tissue lesions, organ dysfunction, and pathological states alter metabolite composition in the serum, providing valuable information for diagnosis. Here we have presented a high throughput, comparative analysis of the serum metabolome as compared with the liver, along the circadian cycle and under nutritional challenge. In addition to its intrinsic clinical value, this study provides insights on the organism-wide processes of communication among tissues that may take place in a time-specific manner. Considerable advances in a variety of biochemical analytical techniques have allowed significant progress in the deciphering the metabolome in a number of physiological conditions. Specifically, metabolic changes throughout the circadian cycle in serum of both humans and rodents have been analyzed. In addition, a number of studies have detected metabolites that vary throughout the circadian cycle in other tissues, including

the liver [68]. These studies show that many metabolites cycle in abundance throughout the 24-h cycle and that many of these oscillations are subject to disruption in the liver following high fat feeding [67]. A number of studies support the notion that desynchrony between the central and peripheral clocks is disadvantageous for energy balance and homeostasis [9, 80], whereas normal rhythmicity can be altered by HFD administered ad libitum in some mouse models [106]. Also, phosphatidylcholine (18:0/18:1) has recently been shown to be a diurnal metabolite capable of integrating lipogenesis in the liver to the use of fatty acids peripherally [173]. In addition, circulating metabolites whose levels are disrupted as a result of the loss of adipose tissue-specific clock function have been shown to alter energy balance by disrupting the rhythmic expression of orexigenic and anorexigenic peptides in the hypothalamus [221]. To determine the extent and specificity to which diets affect the circadian metabolome in ways that might be disadvantageous to overall energy balance, we compared serum and liver metabolomes in mice made obese through a high fat diet. This comparison, the first of this type, has revealed that the serum is generally devoid of oscillation following nutritional challenge and that the remaining oscillatory events are not synchronized with the liver clock. A few previous studies have used a single time point (or non-circadian time points) to assess the metabolite profile of obese humans [136]. Some similarities between our results and these studies exist, specifically when analyzing metabolites of the glycerophospholipid and lysolipid pathways. In both obese humans and our obese mice, the abundance of many of these metabolites was substantially increased, supporting the notion that enhanced lipolysis constitutes a signature of the obese state. Unlike the liver, where only a few lipid metabolites showed circadian oscillation, over half of the lipids showed a circadian oscillation in the serum, the majority of which lose their oscillation after high fat feeding. Indeed, whereas de novo lipogenesis occurs in the liver after chronic high fat feeding, loss of oscillating lipids in the serum probably reflects constitutive breakdown of adipose tissue, which occurs in the insulin-resistant state [43]. Breakdown of adipose tissue causes the release of free fatty acids directly into the bloodstream, but it is not the only source of lipids in the blood. Indeed,

short- and medium-chain fatty acids can be absorbed directly from the intestine, so it is possible that with the large increase in dietary lipids, oscillations were lost or could not be detected. Moreover, loss of rhythmicity in this metabolite group may also reflect the fact that other peripheral clocks become misaligned under HFD. Another potential indication of this desynchrony between tissues is the total loss of carbohydrate oscillations after HFD in the serum but not in the liver. One remarkable effect of HFD on the serum metabolome is that, unlike in the liver, where numerous metabolites take on de novo oscillation only after HFD feeding [67], most serum metabolites lost their rhythmicity. Obviously, this has profound implications for the likelihood of synchronicity across peripheral tissues and between peripheral tissues and the brain. Whereas the SCN responds to light and functions as the central pacemaker [57, 257], clocks located in peripheral tissues can respond to other zeitgebers, such as nutrients during restricted feeding [274, 302]. These result in the uncoupling of peripheral clocks from the SCN, which has been shown to be highly disadvantageous for energy balance and to cause a variety of physiologic imbalances, as shown in both human and rodent studies [302, 106, 254, 138, 10]. Our results regarding the effect of HFD show some interesting similarities to the data of [52], who studied circadian metabolite profiles in humans after sleep deprivation. For example, whereas many amino acid-related metabolites generally have not been found to vary in a circadian fashion in humans, isoleucine and valine have both been shown to be rhythmic in human plasma, with both metabolites increasing in abundance after sleep deprivation. We have also found that rhythmicity of isoleucine and valine in mouse serum persists under HFD, although the overall levels of these amino acids and some of their related metabolites are significantly increased.

In addition, paralleling the effect of sleep deprivation, we observe increases in lysolipids under HFD. The increased abundance of lysolipids in the serum, as previously mentioned, may reflect breakdown of muscle and/or adipose tissue membranes. Thus, HFD and sleep deprivation appear to cause similar effects in terms of rhythmicity and abundance of several circulating metabolites.

Our study shows that HFD induces a misalignment between a peripheral tissue and the serum, where a significant fraction of circulating metabolites lose their rhythmicity under nutritional challenge. Also, peripheral clocks appear to respond in a highly tissue-specific manner to nutritional challenge. For example, unlike in the liver, a large number of circulating lipids are oscillatory only when mice are fed the normal chow diet.

Both nutritional challenge and disturbance of normal circadian patterns are risk factors for obesity [13]. Also, metabolic disruptions elicited by HFD lead to reprogramming of the circadian clock in the liver [67] and presumably in other tissues and serum, resulting in the uncoupling of peripheral clocks and SCN [13].

Thus, further investigations on the metabolome of other tissues along the circadian cycle and in response to different nutritional challenges will help in building a metabolic interconnective map of circadian metabolism. Indeed, loss of rhythmicity in fatty acids in the serum is likely to reflect the desynchronization of other peripheral clocks. A similar scenario seems to be present for carbohydrates, whose oscillation is lost under HFD only in serum and not in the liver. This result may suggest the presence of active lipogenesis along the circadian cycle under HFD. Indeed, it has been shown that excess of food intake is translated into altered expression levels of lipogenic genes [134]. Thus, a diet rich in fat could stimulate the conversion of carbohydrates into lipids for subsequent storage in the adipose tissue. A relevant effect of HFD on the liver clock is the phase advance of a group of metabolites and transcripts [67, 66]. This phenomenon appears to be inverted in serum, where in HFD, metabolites belonging to major metabolic pathways were generally phase-delayed. This type of misalignment across tissues may be responsible for lack of appropriate circadian communication, resulting in a loss of energy balance.

In conclusion, our study has profound implications for deciphering how circadian disruption is induced by nutrient challenge and its differential effect on serum or liver. A critical value of our findings relates to the application of this knowledge at the clinical level, by extending

these high throughput metabolomics studies to personalized medicine in various physiological conditions.

Chapter 4

Circadian Reprogramming and Metabolism

4.1 Circadian Metabolism in the Liver

Circadian rhythms are intimately linked to cellular metabolism. Specifically, the NAD+-dependent deacetylase SIRT1, the founding member of the sirtuin family, contributes to clock function. Whereas SIRT1 exhibits diversity in deacetylation targets and subcellular localization, SIRT6 is the only constitutively chromatin-associated sirtuin and is prominently present at transcriptionally active genomic loci. Comparison of the hepatic circadian transcriptomes reveals that SIRT6 and SIRT1 separately control transcriptional specificity and therefore define distinctly partitioned classes of circadian genes. SIRT6 interacts with CLOCK-BMAL1 and, differently from SIRT1, governs their chromatin recruitment to circadian gene promoters. Moreover, SIRT6 controls circadian chromatin recruitment of SREBP-1, resulting in the cyclic regulation of genes implicated in fatty acid and cholesterol metabolism. This mechanism parallels a phenotypic disruption in fatty acid metabolism in SIRT6 null mice as

revealed by circadian metabolome analyses. Thus, genomic partitioning by two independent sirtuins contributes to differential control of circadian metabolism.

The circadian clock regulates a host of physiological events required for energy balance [73, 251, 313]. These events provide remarkable plasticity for the organism to adapt to surrounding environmental changes, especially given the dynamic input of cellular metabolism on chromatin modifications [93, 130]. A functional link between the circadian clock and cellular metabolism was revealed by reports implicating the SIRT1 deacetylase in clock function [12, 205, 206]. Mammalian sirtuins constitute a family of seven NAD+-dependent deacetylases (SIRT17) that vary in potency of enzymatic activity and protein targets [38, 96, 113]. The subcellular localization of the sirtuins varies from cytoplasm, mitochondria, nucleus, and nucleolus [75].

Of the sirtuins, SIRT6 is unique in its constitutive localization to chromatin [203, 286], and its genome-wide occupancy is prominent at transcriptional start sites (TSSs) of active genomic loci, which coincides to serine 5 phosphorylated RNA polymerase II binding sites [259]. SIRT6 has also been reported to be dynamic in its chromatin binding in response to stimuli such as TNF, resulting in altering the transcriptional landscape of aging and stress-related genes [132]. SIRT6 deacetylates H3 lysine 9 (H3K9) [131, 194] and H3K56 [194], resulting in modulation of gene expression, telomere maintenance, and genomic stability [286] and the histone deacetylase (HDAC) activity of SIRT6 has been found to be nucleosome dependent [88]. Importantly, SIRT6 is also heavily implicated in metabolic regulation, as Sirt6/ mice die at 24 weeks of age due to severe accelerated aging and hypoglycemia as a result of altered rates of glycolysis, glucose uptake, and mitochondrial respiration [203]. SIRT6 also controls the acetylation state of PGC-1 in a GCN5-dependent manner that regulates blood glucose levels [62]. Liver-specific Sirt6/ mice develop fatty liver due to altered expression of genes involved in fatty acid beta oxidation and triglyceride synthesis [135].

The circadian transcriptome is thought to comprise at least 10% of all transcripts in a given

tissue, though genes can gain rhythmicity depending on a tissue-specific permissive environment [185]. Moreover, the potential for a specific gene to become circadian may be related to changes in the metabolic, nutritional, and epigenetic state [67]. A number of studies have revealed the role of chromatin remodeling in providing permissive genomic organization for circadian transcription [58, 19, 61]. We report that SIRT6 defines the circadian oscillation of a distinct group of hepatic genes, different from the ones under SIRT1 control. This partitioning of the circadian genome is achieved by controlling the recruitment to chromatin of the core circadian activators CLOCK-BMAL1, as well as SREBP-1. The sirtuin-dependent partitioning of circadian transcription leads to differential control of hepatic lipid metabolism related to fatty acid-dependent pathways.

4.1.1 Circadian Regulation of SIRT6 and SIRT1

Given the unique ability of SIRT6 to function as an HDAC [131, 194] and transcriptional facilitator at chromatin [132], we investigated its role in controlling hepatic circadian gene expression and metabolism. DNA microarrays were used to delineate the control of SIRT6 versus SIRT1 on the circadian genome. To do so, we used mice with liver-specific ablation of either Sirt1 or Sirt6 genes and their corresponding wild-type (WT) littermates. Livers were harvested every 4 hr over the circadian cycle, representing zeitgeber times (ZT) 0, 4, 8, 12, 16, and 20. Groups of genes were selected based on the following criteria: group 1 represents genes that oscillate in WT (SIRT6) liver and whose oscillation is dampened/disrupted in SIRT6 knockout (KO) mice. Group 2 represents genes that oscillate in SIRT6 KO, but not in their corresponding WT littermates. Group 3 represents genes that oscillate in WT (SIRT1) liver and whose oscillation is dampened/disrupted in SIRT1 KO mice (SIRT1 KO). Group 4 respresents genes that oscillate in SIRT1 KO, but not in their corresponding WT littermates. The group referred to as both includes genes that oscillate similarly in both WT and KO groups for either SIRT6 or SIRT1 data sets. Oscillating genes were selected based on

a 0.01 p-value cutoff. Of the SIRT6 transcriptome, 691 genes were identified in the WT group 1, with 779 genes oscillating more robustly in the SIRT6 KO group 2 and 506 genes oscillating similarly in both groups. Using the same criteria for the SIRT1 transcriptome, 703 genes oscillate in the WT group 3, with 1,126 genes oscillating with greater amplitude in the SIRT1 KO group 4 and 1,091 genes oscillating similarly in both groups. This analysis revealed that, of the 1,976 rhythmic genes identified in the SIRT6 transcriptome, the expression profile of 1,470 genes was altered by SIRT6 disruption (74%). In addition, of the 2,920 oscillating genes identified in the SIRT1 experiment, 1,829 genes were changed by SIRT1 disruption (63%). Thus, SIRT6, in addition to SIRT1, significantly regulates the expression of clock-controlled genes (CCGs).

Gene ontology (GO) analysis of genes with altered circadian oscillation in SIRT6 versus SIRT1 transcriptomes revealed some striking differences. The most highly represented biological processes are transcription, transcriptional regulation, and nuclear processes, enriched in both WT liver groups and SIRT1 KO livers but completely absent from the SIRT6 KO livers. In addition to transcription, enrichment in mitochondrial and intracellular non-membrane-bound organelle (GO term describing ribosomes, cytoskeleton, and chromosomes) was highly enriched. The SIRT6 KO group shared little homology with WT or SIRT1 KO groups in significantly selected biological pathways. GO terms enriched in SIRT6 KO were endoplasmic reticulum, Golgi apparatus, protein localization/catabolism, RNA processing, and translation. GO biological pathway analysis highlighted unique classes of genes represented exclusively in the SIRT6 KO group, indicating that disruption of hepatic SIRT6 results in altered circadian biological function.

Next, we focused on understanding how these two sirtuins differentially regulate distinct classes of circadian genes. Importantly, there is little overlap between the groups of SIRT1 and SIRT6 dependent circadian genes (160 common genes). These are mostly implicated in cytoplasmic and mitochondrial pathways and are linked to metabolic processes and stress

response, as described by GO biological pathway analysis. Thus, SIRT6 and SIRT1 regulate distinct biological classes of circadian genes. For a detailed view of these genes controlled by SIRT6 or SIRT1, refer to CircadiOmics [34, 224]. Analysis of the circadian phase of gene expression reveals a peak in phase of the genes oscillating in SIRT6 KO mice at ZT16 and ZT20, differently from the genes significantly expressed in SIRT1 KO mice peaking at ZT4 and ZT8.

Circadian expression was confirmed for distinct classes of genes based on their rhythmic profile: (1) genes whose expression profile is unaltered between WT versus SIRT6 KO and SIRT1 KO. Briefly, these genes are involved in transcription and regulation of rhythmic processes, as the bulk of core clock genes are generally resistant to change in expression. (2) Genes whose circadian expression is similarly regulated by SIRT6 and SIRT1. Examples include Nephronectin (Npnt), encoding an extracellular matrix protein, which oscillates in WT liver and is dampened similarly in both SIRT6 KO and SIRT1 KO mice. Conversely, circadian expression of Dbp is equally increased in amplitude at ZT 8 in both SIRT6 KO and SIRT1 KO animals. These genes, although responding in opposite manner to the ablation of either sirtuin, belong to the same class of genes similarly regulated by both sirtuins. (3) Genes whose amplitude in oscillation is more robust when either SIRT6 or SIRT1 is ablated. For example, fatty acid synthase (Fasn), 3-hydroxy-3-methyl-glutaryl-CoA reductase (Hmgcr), and lanosterol synthase (Lss) were uniquely regulated by SIRT6, as the amplitude of circadian oscillation was enhanced in SIRT6 KO. The circadian profiles of these genes were unaltered in SIRT1 KO, as compared to WT. Conversely, genes with enhanced circadian amplitude exclusively in SIRT1 KO, including regulator of G protein signaling 16 (Rgs16), serine dehydratase (Sds), and methylenetetrahydrofolate dehydrogenase 1-like (Mthfd1l), are shown. The profiles of Rgs16, Sds, and Mthfd1l genes are not altered in amplitude between WT and SIRT6 KO mice. Also, the expression of Sirt6 and Sirt1 is not altered in the SIRT1 KO and SIRT6 KO livers, respectively. Thus, control of circadian gene expression by SIRT6 and SIRT1 appears to define unique subdomains of oscillating CCGs that are involved in

distinct biological functions.

4.1.2 SIRT6 Interacts with CLOCK-BMAL1

Because SIRT6 is reported to localize to actively transcribed genomic loci [259], we sought to decipher the molecular mechanism by which SIRT6 controls circadian transcription. Fractionated liver extracts that lack SIRT6 result in a drastic increase in BMAL1 association to chromatin, though the total amount of nucleoplasmic BMAL1 was unaltered. Also, Bmal1 circadian expression is not altered in SIRT6 KO or SIRT1 KO, as compared to WT liver.

Because BMAL1 association at chromatin is enhanced in the absence of SIRT6, we analyzed promoter-specific recruitment of the circadian machinery. Chromatin immunoprecipitation (ChIP) analysis was performed to understand whether recruitment of the circadian machinery was altered in the absence of SIRT6 or SIRT1, which would therefore contribute to altered CCG expression observed in our microarray analysis. Circadian BMAL1 recruitment to the Rgs16 and Mthfd1l promoters is unaltered in the absence of SIRT1, despite the increased amplitude in gene expression in SIRT1 KO. Schematic representation of the promoter, as well as selective recruitment of BMAL1 to different putative E boxes in the Rgs16 and Mthfd1l promoters, illustrating that BMAL1 recruitment is virtually identical in WT and SIRT1 KO livers. In addition to Rgs16 and Mthfd1l, BMAL1 recruitment is also unaltered at Dbp and Per1 promoters in WT versus SIRT1 KO, despite the significant changes in circadian gene expression. In contrast, lack of SIRT6 results in a significant increase in circadian BMAL1 occupancy (ZT4 and ZT8) at the Dbp promoter. Also, an increase in Ac-H3K9 across all time points is seen. Additional data show altered BMAL1 recruitment to Per1 and Amd1 promoters in the absence of SIRT6. To further address the effect of SIRT6, we used a Dbp-luciferase reporter and found that ectopic expression of SIRT6 results in dose-dependent dampening of CLOCK-BMAL1-driven transcription, similar to results with

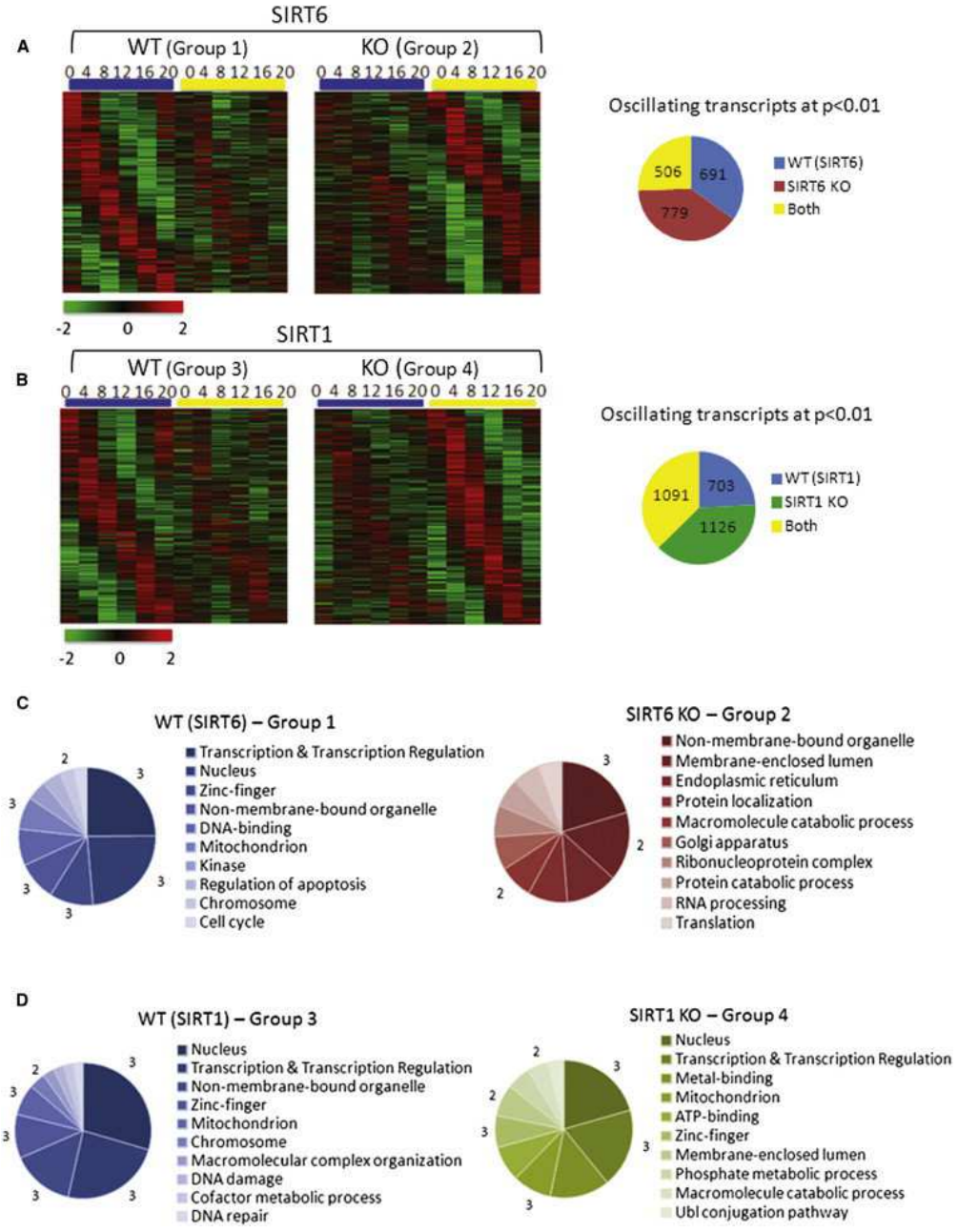

Figure 4.1: Paritioning Transcriptomic Oscillation by SIRT1 and SIRT6.

SIRT1 [21]. Thus, differently from SIRT1, SIRT6 controls circadian function by operating directly at the transcription level by recruiting the clock machinery to chromatin.

Moreover, we sought to confirm that SIRT6 interacts with the circadian transcription complex. SIRT6 physically interacts with CLOCK and BMAL1, individually or together, as shown by coimmunoprecipitation (co-IP). Also, SIRT6 does not interact directly with SIRT1 by co-IP. Furthermore, when CLOCK and BMAL1 are ectopically expressed with SIRT6 alone or in combination with both SIRT6 and SIRT1, the SIRT6 IP complex only interacts with CLOCK and BMAL1 and not SIRT1. Furthermore, by fractionating WT mouse liver, we reveal that subcellular localization of SIRT6 is predominantly in the nucleus and constitutively at chromatin at all ZTs, whereas SIRT1 is nuclear, but not chromatin bound [203, 286]. Likewise, co-IP experiments from chromatin fractions of HEK293 cells confirmed that SIRT1 does not reside at chromatin. Also, the SIRT6-dependent interaction with CLOCK and BMAL1 is found at chromatin. In addition, sequential co-IP experiments were performed to pull down the SIRT6- and SIRT1-dependent clock complexes from the same HEK293 cell lysates. Primary IP against Flag-SIRT1 revealed an interaction with CLOCK, and a secondary IP with HA-SIRT6 also revealed an interaction with CLOCK, which is in keeping with evidence showing that these two sirtuins independently interact with the clock machinery. Lastly, SIRT1 has been shown to deacetylate BMAL1 at lysine 537 [111, 206]. Whereas SIRT1 readily deacetylates BMAL1, SIRT6 is not able to do so, highlighting different mechanisms of action of these two sirtuins that reside in partitioned subcellular clock complexes.

4.1.3 SIRT6 Regulates SREBP-1-Dependent Circadian Transcription

Based on circadian gene expression profiles altered in SIRT6 KO liver, a number of genes were found to be SREBP targets such as Fasn, Hmgcr, and Lss. MotifMap [48, 315] was used to determine global transcription factor binding site enrichment in promoters with altered expression profiles when SIRT6 was disrupted. SREBP binding sites are highly enriched (137 sites) compared to serum response factor (SRF), peroxisome proliferator-activated receptor gamma (PPAR), forkhead box (FOXO), or E26 transformation-specific (ETS) family motifs. Next, genes whose expression is disrupted by loss of SIRT6 were compared to published ChIP-sequencing data [261, 260] to determine the extent of SREBP-1 and SREBP-2 gene targets that overlap with SIRT6. In addition to the genes already mentioned, other SREBP targets appear disrupted in SIRT6 KO, including fatty acid elongase family members (Elovl), low-density lipoprotein receptor (Ldlr), and acetoacetyl-CoA synthetase (Aacs) genes (which are also represented in MotifMap SREBP hits). As a role for SIRT1 in SREBP signaling cannot be excluded, we compared SREBP-1 target genes [260] to SIRT6- and SIRT1-dependent gene targets. Interestingly, overlapping genes between SIRT6/SREBP-1 targets were enriched in GO terms for fatty acid and lipid metabolism, whereas SIRT1/SREBP-1 overlapping targets were enriched in lipid and steroid metabolism, suggesting a partition in biological function in SIRT1- or SIRT6-specific control of SREBP.

As there are no significant changes in SREBP-1c circadian transcript and protein levels in SIRT6 KO livers, we carried out ChIP experiments. Strikingly, SREBP-1 circadian recruitment to the Fasn promoter, a known SREBP-responsive gene [260], is significantly increased in the absence of SIRT6, as compared to WT. The increase is prominent at ZT 4, thereby preceding the peak of Fasn transcription at ZT 16, a scenario in keeping with accumulated evidence, especially in a circadian context [145]. A schematic of the Fasn promoter illustrating selective SREBP-1 recruitment to the TSS versus negative control regions, as well as

recruitment to the Hmgcr and Lss promoters, is shown. Also, an increase in Ac-H3K9 levels is present at the Fasn promoter across most ZTs. Based on this evidence, it is expected that SREBP-1c contributes to Fasn circadian gene expression. To confirm this, we used livers from WT and SREBP-1c KO mice [260] at ZT 4 and ZT 16 and observed a significant dampening of Fasn circadian expression in SREBP-1c KO livers, whereas Dbp and Rev-Erb circadian expression remains unaltered. Thus, SIRT6 appears to define a class of genes whose amplitude in oscillation is directed by SREBP-1c. To functionally explore the effects of SIRT6 on SREBP-1c-mediated transcription, we used a luciferase reporter with either a full-length Fasn promoter (containing the previously described binding site of SREBP-1, referred to as Fas-Luc 1594/+65) or a mutant that disrupts SREBP-1 binding (Fas-Luc 65 MT). Coexpression with SREBP-1c showed robust Fasn promoter activation that is strongly repressed by increasing amounts of SIRT6. Importantly, the Fas-Luc 65 MT reporter is not sensitive to SIRT6-mediated repression. The effect is specific, as SIRT1 is not able to repress SREBP-1c-driven activation of Fasn. Thus, SIRT6 is implicated in regulating proper SREBP-1c chromatin recruitment, resulting in circadian transcription of its target genes.

4.1.4 Implications in Metabolic Phenotypes

Metabolomics analysis was used to determine in an unbiased manner the physiological consequences of SIRT6 or SIRT1 disruption along the hepatic circadian cycle. Heat maps highlight oscillating metabolites (JTK_CYCLE p-value 0.05) in WT livers that were disrupted in SIRT6 KO and metabolites that oscillated more robustly in SIRT6 KO livers, as compared to WT. In total, 77 metabolites displayed a genotype-dependent effect in the SIRT6 metabolome, and 142 metabolites were dependent on circadian rhythmicity. We also compared the metabolome profile obtained from the SIRT6 KO mice to livers from SIRT1 KO animals. Heat maps illustrate the metabolomics data for SIRT1, with oscillating metabolites only in WT livers (left) and those found to oscillate robustly in SIRT1 KO. In the SIRT1

metabolome, 42 metabolites displayed a genotype effect, whereas 199 show a time-of-day-dependent effect. In total, 85 metabolites robustly oscillate exclusively in SIRT6 KO, and 57 metabolites display strong rhythmicity in SIRT1 KO livers.

Metabolites were grouped into biological functional categories (peptides, cofactors and vitamins, lipids, nucleotides, amino acids, and carbohydrates) to determine where significant changes occurred in the livers from SIRT6 KO and SIRT1 KO mice versus their WT littermates. The most robust change was seen in lipid-related metabolites in SIRT6 KO livers. These lipids were heavily related to fatty acid metabolism, including circadian disruption of fatty acid synthesis (medium and long-chain fatty acids), storage, cellular membrane lipids, and signaling. Using SIRT6 microarray data, genes were run through DAVID to identify possible altered gene expression profiles that match in GO biological function with the metabolomics data set. A strong correlation in GO biological function was found, comparing the high-throughput metabolome and transcriptome data when SIRT6 is disrupted.

A group of lipids that displayed a strikingly enhanced circadian oscillation with a peak at ZT16 was membrane lysolipids that are related to cellular synthesis or degradation. Also, genes encoding phospholipases related to lipid signaling displayed altered expression profiles with a paralleled change in eicosanoid metabolite rhythms in response to SIRT6 disruption, indicating that signaling/inflammatory events are SIRT6 regulated. As an example, genes of the phospholipase A2 family (Pla2g2a and Pla2g12a) gained circadian oscillation in the absence of SIRT6, which corresponded with circadian upregulation of downstream 15-HETE levels. In addition to Fasn, fatty acid elongases and fatty acid transporters were significantly altered in response to SIRT6 disruption. Both carnitine and acetylcarnitine, which are important for beta oxidation of fatty acids in the mitochondria, gain circadian oscillation and peak at ZT16 in the SIRT6 KO livers. Although synthesis and breakdown of fatty acid pathways are related to SIRT6, storage of fatty acids into triglycerides was also altered as evidenced by a gain in oscillation of Agpat6 and glycerol-3-phosphate in the SIRT6 KO

mice. These metabolite pathways parallel the altered SREBP transcriptional response and indicate that SIRT6 is required for proper circadian regulation of fatty acid synthesis, storage, breakdown, and signaling.

Circadian control of metabolism is thought to be critical for organismal homeostasis [73, 251], and the identification of the molecular players implicated in this control is likely to reveal novel pharmacological strategies. Specifically, SIRT6 regulates hepatic circadian transcription consequently linked to downstream modulation of fatty acid metabolism. SIRT6 interacts with core clock proteins and controls circadian chromatin recruitment of BMAL1 to target promoters. Importantly, SIRT6 also controls SREBP1 recruitment to target promoters, such as Fasn, and helps maintain proper cyclic transcription. In fact, circadian metabolomics analyses reveal that SIRT6 controls lipid metabolism, contributing to the regulation of pathways involved in fatty acid synthesis and beta oxidation, triglyceride storage, signaling, and cellular membrane lipids.

One conclusion of this study is that two sirtuins, SIRT6 and SIRT1, control distinct subdomains of the circadian genome through different mechanisms. SIRT6 has been reported to reside at transcriptionally active loci, and its chromatin association is dynamic in response to stimuli so as to activate specific biological classes of genes [132]. It is tempting to speculate that SIRT6 operates as a transcriptional marker, and given its HDAC function, it may have multiple roles in dictating the boundaries of transcription. As supporting evidence of this notion, we show that SIRT6 contributes to chromatin recruitment of both the circadian machinery, as well as SREBP-1. There is no evidence that SIRT1 functions in the same manner. Indeed, SIRT1 is not implicated in chromatin recruitment of the clock machinery [21]. SIRT1 appears to modulate circadian transcription purely as a deacetylase by targeting both histone proteins and nonhistone proteins such as BMAL1 and PER2 [13, 206]. Intriguingly, free fatty acids (FFAs) are potent endogenous activators of SIRT6 HDAC activity, but not SIRT1. Thus, endogenous fatty acids could play a role in activating or sensitiz-

ing SIRT6, a notion that is particularly appealing, as our metabolomics data reveal that fatty acids peak in abundance at the beginning of the light phase (after feeding), which also coincides with peaks in BMAL1 and SREBP1 recruitment to chromatin. In keeping with this idea, the beginning of the light phase must therefore provide a permissive chromatin state, as recruitment of SIRT6-dependent transcription factors occurs primarily at ZT4 and ZT8 and in the case of SREBP-1 in advance of the peak in gene expression. Indeed, it has been proposed that an activated state of the circadian landscape exists between ZT4 and ZT12, when CLOCK-BMAL1 recruitment occurs and this active state is in advance of nascent transcription [145]. In virtue of its tight chromatin association, SIRT6 could thereby operate by sensing changing cellular metabolite levels (NAD+ or fatty acids) and translate this information to control circadian transcription. In this respect, SIRT6 would be unique among sirtuins because SIRT1 [13, 206] and SIRT3 [227] appear to be implicated in circadian regulation uniquely through their enzymatic function.

Aside from transcriptional/translational regulation of the clock, enzymatic activity of a number of factors influences circadian rhythms and could also contribute to SIRT6 function. SIRT6 was recently reported to directly regulate SREBP cleavage to its mature protein form as a result of SIRT6 localization to the promoters of genes such as SREBP cleavage-activating protein (SCAP) and site-1/2 proteases (S1P and S2P), which are involved in SREBP proteolytic cleavage and transport from the endoplasmic reticulum (ER)/Golgi apparatus. In addition to the circadian regulation of the SREBP lipogenic transcriptional program, enzymatic regulation at the ER has been described whereby a secondary 12 hr rhythm in the unfolded protein response (UPR) pathway activates SREBP signaling and deregulates lipid metabolism [46]. Though we are looking at 24 hr rhythms, these results highlight a possible connection that could further link SIRT6, SREBP, and ER-dependent enzymatic pathways that, in time, may contribute to the transcriptional role of SIRT6 and the clock described here.

Various mouse models have delineated the role of SREBP transcription factors in the lipogenic program [260, 261]. SREBP-1a and SREBP-1c (the form dominantly expressed in liver) activate both genes involved in fatty acid synthesis and the subsequent incorporation into triglycerides for storage and inclusion into cellular membranes. SREBP-2 is primarily implicated in cholesterol biosynthesis. Based on the results obtained by metabolomics analysis, our data indicate a disruption in fatty acid synthesis, breakdown, incorporation into membrane lipids, and storage with little disruption in cholesterol related pathways. Although we do not exclude the role of other factors such as hepatocyte nuclear factor 4 (HNF-4), liver X receptor (LXR), and peroxisome proliferator-activated receptors (PPARs), our results point to SREBP-1c as a dominant player implicated in SIRT6 circadian regulation of fatty acid metabolism. Intriguingly, [127] reported that, when transgenic mice overexpressing SIRT6 were challenged with a high-fat diet (HFD), these mice were protected from diet-induced obesity due to SIRT6 repression of PPAR-target genes. In this respect, recent results from our laboratory have shown that HFD regimen in mice reprograms the hepatic circadian transcriptome by inducing de novo oscillations of PPAR-dependent genes [67]. Given the seemingly ubiquitous localization of SIRT6 at transcriptionally active genomic loci and its role as a regulator of circadian transcription and SREBP signaling, SIRT6 could also be implicated in diet-induced metabolic regulation of SREBP, PPARs, or other factors. The remarkable role of SIRT6 in regulating the circadian transcriptome and defining a landscape for biologically relevant genomic loci places this epigenetic regulator in a central position to control the extensive circadian lipid metabolic program in the liver.

4.2 Circadian Control of Fatty Acid Elongation

4.2.1 SIRT1 Protein-mediated Deacetylation of Acetyl-CoA1

The circadian clock regulates a wide range of physiological and metabolic processes, and its disruption leads to metabolic disorders such as diabetes and obesity. Accumulating evidence reveals that the circadian clock regulates levels of metabolites that, in turn, may regulate the clock. Here we demonstrate that the circadian clock regulates the intracellular levels of acetyl-CoA by modulating the enzymatic activity of acetyl-CoA Synthetase 1 (AceCS1). Acetylation of AceCS1 controls the activity of the enzyme. We show that acetylation of AceCS1 is cyclic and that its rhythmicity requires a functional circadian clock and the NAD+-dependent deacetylase SIRT1. Cyclic acetylation of AceCS1 contributes to the rhythmicity of acetyl-CoA levels both in vivo and in cultured cells. Down-regulation of AceCS1 causes a significant decrease in the cellular acetyl-CoA pool, leading to reduction in circadian changes in fatty acid elongation. Thus, a nontranscriptional, enzymatic loop is governed by the circadian clock to control acetyl-CoA levels and fatty acid synthesis.

The circadian clock machinery is canonically described as a series of interconnected transcriptional and translational feedback loops [104, 220]. Additional findings indicate that the clock relies on multiple levels of control, including post-transcriptional [159], post-translational [191], metabolic [206, 239], and transcription-independent pathways [214, 215]. NAD+, a metabolite that acts as a critical coenzyme, has been shown to be an output of the circadian clock [206, 239]. Moreover, fluctuations in NAD+ can also modulate the clock through NAD+-dependent deacetylation of histones, BMAL1, and PER2 by the SIRT1 deacetylase [205, 111, 12]. SIRT1 has been shown to regulate several metabolic pathways and is implicated in controlling aging and inflammation through its deacetylase activity [37]. Interestingly, one of the proteins regulated by SIRT1-mediated deacetylation is acetyl-CoA synthetase 1 (AceCS1), a central enzyme involved in acetyl-CoA biosynthesis [97]. Deacety-

lation of Lys-661 on AceCS1 by SIRT1 leads to activation of AceCS1 [97]. Because SIRT1 activity, and the abundance of its cofactor NAD+, oscillate in a circadian manner [206, 205], we reasoned that AceCS1 acetylation, and in turn, acetyl-CoA abundance, may display circadian rhythmicity.

Acetyl-CoA, a metabolite that provides acetyl groups during the acetylation reaction, exists in two separate pools in the cell: a mitochondrial pool and a nuclear/cytosolic pool [6]. The mitochondrial pool is derived mainly from the action of the enzyme pyruvate dehydrogenase and from fatty acid oxidation. The nuclear/cytosolic pool, responsible for protein acetylation and fatty acid synthesis, is produced by two enzymes: AceCS1 and ATP-citrate lyase (ACLY). Whereas ACLY uses citrate (produced during the tricarboxylic acid cycle) as a substrate for the production of acetyl-CoA, AceCS1 uses acetate. In mammals, acetate can be produced physiologically by the intestinal flora, alcohol metabolism, prolonged fasting, and histone deacetylation [267]. In Saccharomyces cerevisiae, the homolog of AceCS1 (Acs2p), was shown to be the major source of acetyl-CoA [282]. Importantly, [310] have reported that ACLY and AceCS1 are present in both the cytosol and the nucleus of mammalian cells, and that the loss of either of these proteins leads to a reduction in global histone acetylation [310]. Moreover, reduction in histone acetylation upon loss of ACLY can be rescued by supplementing cells with acetate, supporting a critical role for AceCS1 in acetyl-CoA biosynthesis [310]. In this study, we demonstrate a novel regulation of the enzymatic activity of AceCS1 by the circadian clock that results in the rhythmicity of fatty acid elongation.

4.2.2 Rhythmic Acetylation of AceCS1 Controls Acetyl-CoA

To determine whether acetylation of AceCS1 changes with the time of the day, liver extracts were prepared at different zeitgeber times (ZTs) from mice entrained in 12-h light:12-h dark cycle. Using an anti-acetyl-AceCS1 antibody, specific to the acetylated Lys-661 residue [97],

we reveal that acetylation of AceCS1 oscillates in a circadian manner in the liver from wild-type (WT) mice. The highest level of acetylation was observed at ZT9, whereas AceCS1 was mostly deacetylated at ZT21. Total levels of AceCS1 did not display circadian rhythmicity, either in protein levels or in mRNA levels. Interestingly, the phase of oscillation of AceCS1 acetylation parallels that of BMAL1, another clock-related SIRT1 target [205, 111].

To evaluate whether the circadian clock drives AceCS1 acetylation, we used clock/clock (c/c) mutant mice [300] and found that acetylation is indeed drastically reduced in the liver of these mutant mice. We further analyzed the oscillation in AceCS1 acetylation in cultured cells by using MEFs. WT and Bmal1/ MEFs were synchronized by serum shock, and cells were harvested at different time intervals. Acetylated AceCS1 levels were rhythmic in the WT cells with a peak at 1824 h after synchronization, paralleling BMAL1 acetylation profile in MEFs [206, 205]. AceCS1 acetylation levels were almost undetectable in Bmal1/ MEFs, whereas total protein levels of AceCS1 in both cell types remained unchanged and nonrhythmic. Thus, AceCS1 acetylation oscillates in a circadian manner both in vivo and in cultured cells. Next we validated the role of SIRT1 in circadian deacetylation of AceCS1 by using EX527, a direct pharmacological inhibitor of SIRT1 [207]. Indeed, blocking SIRT1 functions leads to elevated and arrhythmic AceCS1 acetylation.

Because the acetylation status of AceCS1 controls its activity [97], we next sought to determine whether total cellular acetyl-CoA levels are also rhythmic. To do so, acetyl-CoA levels were measured by LC-MS/MS by using a modified version of the method described by Hayashi and Satoh [108]. We found that acetyl-CoA levels were rhythmic in the liver of WT mice, with highest levels observed at ZT3. This is in keeping with a scenario in which the peak of acetyl-CoA levels (ZT3) follows the peak of deacetylated (and hence, active) AceCS1 (ZT21). Next, we determined whether a functional circadian clock is important for the rhythmicity in the acetyl-CoA levels by analyzing the abundance of acetyl-CoA in the livers from Clock/ mice. The peripheral tissues of Clock/ mice have been shown to

be arrhythmic [55]. Consistent with a prominent role of the circadian clock machinery in regulating acetyl-CoA levels, there is no oscillation in the abundance of acetyl-CoA in the liver of Clock/ mice. We then measured acetyl-CoA levels in cultured cells by synchronizing MEFs. WT MEFs displayed robust oscillation in the acetyl-CoA levels, with a peak at 12-h post-synchronization and trough at 24 hour post-synchronization, in agreement with the cylic acetylation of AceCS1. Because acetylation of AceCS1 in Bmal1/ MEFs is low and noncyclic, we expected high and nonoscillating levels of acetyl-CoA in these cells, and this is in fact the case. Also, MEFs treated with EX527 displayed lower and nonoscillating levels of acetyl-CoA compared with untreated cells, paralleling the acetylation profile of AceCS1. These results indicate that acetyl-CoA levels are rhythmic in mouse liver and in MEFs, that this rhythmicity is clock-controlled, and that the clock-driven acetylation of AceCS1 contributes to the cyclic abundance of acetyl-CoA.

The relative contribution of ACLY and AceCS1 toward the intracellular abundance of acetyl-CoA is not fully understood. Blocking ACLY in cultured cells, either by RNAi [107] or by the specific inhibitor SB-204990 [44], has been shown to reduce the total cellular acetyl-CoA levels by roughly 50%. Moreover, knockdown of ACLY in mouse liver by adenovirus-mediated RNAi caused roughly 25% reduction in the hepatic acetyl-CoA levels [306]. To determine the relative contribution of ACLY and AceCS1 on total cellular acetyl-CoA levels, we transiently knocked down ACLY and AceCS1 by siRNAs in cultured cells. Our results show that both ACLY and AceCS1 contribute significantly, and in a similar extent, to the total cellular acetyl-CoA pool. We reproducibly observed a reduction of acetyl-CoA levels by 24 or 28% upon the knockdown of ACLY or AceCS1, respectively. Furthermore, total acetyl-CoA levels were also reduced by 31% in a cell line where AceCS1 was stably knocked down [325]. AceCS1 mRNA levels were reduced by about 90% in these cells. These results establish that AceCS1 is a major determinant of cellular acetyl-CoA.

Because acetyl-CoA levels could directly influence histone acetylation and thus, gene expres-

sion [310, 30], we analyzed changes in circadian gene expression after knocking down AceCS1 in MEFs. Using a lentiviral shRNA against AceCS1, we generated a MEF cell line that expressed significantly lower levels of AceCS1. When synchronized by dexamethasone, both control and AceCS1-knockdown MEFs displayed very similar, robust oscillation of core circadian gene expression. These results indicate that AceCS1 is not required for the regulation of circadian gene expression. Because the Km of histone acetyltransferases for acetyl-coA is relatively low [157], it is likely that modest fluctuations in acetyl-CoA levels might not be sufficient to alter histone acetylation and thus affect gene expression.

Acetyl-CoA is the carbon source for synthesis and elongation of fatty acids. Because AceCS1 is present predominantly in the cytosol [325] and the fatty acid synthesis is mostly dependent on cytosolic availability of acetyl-CoA, we explored whether fatty acid synthesis is under circadian control through the AceCS1-mediated oscillation in acetyl-CoA. Acetyl-CoA produced by AceCS1 has been shown to be utilized in lipid synthesis [97]. To validate the role of AceCS1 in lipid synthesis, we measured the incorporation of 14C-labeled acetate into lipids in AceCS1-knockdown and control cell lines. There is a remarkable decrease in 14C incorporation into lipids in AceCS1-knockdown cells compared with the control cells.

To further understand the role of AceCS1 in lipid metabolism, we used a lipidomics approach. We analyzed the levels of fatty acids of varying length and unsaturation at two time points in synchronized control and the AceCS1-knockdown cultured cells. The overall levels of fatty acids were significantly reduced in the AceCS1-knockdown cells. Interestingly, most fatty acids demonstrated a trend where the levels were higher at 12 h post-synchronization compared with the 24-h time point. These fatty acids included saturated and monounsaturated long chain fatty acids. This could be because the fatty acids are either oxidized during this time period and/or they are being converted to very long chain fatty acids (VLCFAs). Supporting the latter scenario, we observed that the levels of VLCFAs are higher at the 24-h time point. Importantly, the change in VLCFA levels is absent in AceCS1-knockdown

cells. These results suggest that the reduced level of acetyl-CoA in the AceCS1-knockdown cells leads to reduction in total fatty acid levels and also causes impaired elongation of long chain fatty acids into VLCFAs. To confirm that elongation of fatty acids is regulated by the circadian clock, we measured the levels of fatty acids in WT and c/c MEFs. Although there is a robust oscillation in VLCFAs in the WT MEFs, their levels are significantly lower and nonrhythmic in c/c MEFs. Our results demonstrate that the elongation of fatty acids, a process that requires acetyl-CoA, is under the control of the circadian clock machinery. These results also establish AceCS1 as an important contributor to fatty acid elongation.

4.2.3 Therapeutic Implications

Our findings provide evidence that AceCS1 functions as a circadian enzyme, thereby contributing to the cyclic cellular levels of acetyl-CoA. Rhythmicity in AceCS1 acetylation contributes to the oscillation of acetyl-coA levels and, in turn, regulates circadian fatty acid elongation. Acetate could also be converted to acetyl-CoA by the mitochondrial enzyme AceCS2. However, AceCS2 expression is significantly lower compared with AceCS1 in the mouse liver [82] and is almost undetectable in the MEFs. Furthermore, in our experiments where cells were treated with acetate-14C, knocking down AceCS1 is sufficient to reduce the acetate conversion to acetyl-CoA by roughly 10-fold, confirming the prominent role of AceCS1 in these cells.

Fatty acid synthesis constitutes a major process that utilizes acetyl-CoA in all cells. We have reported a unique pathway by which the circadian clock regulates the abundance of acetyl-CoA, leading to a clock-driven control of fatty acid elongation. Abolishing the activity of AceCS1 causes a significant decrease in the cellular pool of acetyl-CoA and leads to dampening of oscillations in fatty acid synthesis. This transcription-independent pathway is based solely on cyclic enzymatic function, utilizing the NAD+-dependent SIRT1 deacetylase

to control AceCS1 activity, and contributes to modulated biosynthesis of acetyl-CoA. Thus, our study adds another layer to important examples of transcription-independent control by the mammalian circadian clock [214, 215]. These findings underscore that the circadian clock occupies a central position in controlling both NAD+ and acetyl-CoA levels in the cell, linking SIRT1 to fatty acid elongation. Increasing evidence reveals the links between the circadian clock and lipid metabolism [74]. These may involve additional chromatin remodelers, such as HDAC3, whose recruitment to the genome and enzymatic output follow a circadian pattern. As many of the genes regulated by HDAC3 are involved in lipid metabolism, and loss of HDAC3 leads to increased de novo fatty acid synthesis and a fatty liver phenotype [74], future studies will need to explore its relationship with AceCS1 and the control by SIRT1. Our study has uncovered another level of interplay among the circadian clock, epigenetics, and metabolism. As de novo fatty acid synthesis is known to be increased in cancer [79] and obesity [276], our results might pave the way to future strategies for the use of sirtuin modulators [35] and chronotherapy in their treatment [252].

4.3 Fasting Induced Circadian Reprogramming

A variety of dietary regimens and time-restricted feeding have a profound impact on the circadian clock as well as cyclic gene expression in metabolic tissues [36, 67, 106, 144, 302]. Specifically, circadian gene expression in metabolic tissues can be differentially reprogrammed by various nutritional challenge, underscoring the plasticity of the clock system [67, 288]. In addition, the circadian clock regulates the expression of metabolic genes in a tissue-specific fashion, emphasizing the reciprocal link between the circadian clock and metabolism [64, 156, 206, 239]. Although the circadian clock plays an important role in rhythmic gene expression, time-restricted feeding restores cyclic gene expression even in arrhythmic Cry1 -/- , Cry2 -/- mutant mice, suggesting the presence of nutrient-responsive transcriptional

pathways that would contribute to the rhythmicity of circadian gene expression in a clock-independent manner [302]. Despite these findings, efforts to tease out how the circadian clock and nutrient-sensitive transcription factors (TFs) are functionally

coordinated at the level of gene regulation have not been satisfactory. Finally, while evidence on how food intake is integrated into circadian transcriptional regulation is accumulating [13], how lack of food operates on the clock remains virtually unexplored. Fasting is an adaptive state of metabolism when exogenous nutrient intake is limited [176, 177]. In mammals, a drastic shift in metabolism takes place so as to survive under low nutrient availability. For instance, skeletal muscles undergo protein breakdown and provide amino acids for the liver to implement gluconeogenesis, producing glucose to maintain appropriate blood glucose levels [176]. In parallel, the liver performs ketogenesis to supply ketone bodies to other vital organs including the brain, by harnessing free fatty acids from adipose tissue [176]. Such metabolic shifts across different tissues are achieved by fasting-induced TFs such as GR, CREB, FOXO, TFEB, and PPARs [89]. Recent studies suggest that fasting- mimicking diet and temporal feeding restriction have numerous health benefits including reduced adiposity, immune system change, and delayed aging, despite comparable calorie intake [25, 36, 106]. Moreover, temporal feeding restriction confers robustness to circadian rhythm, which could mediate protective effects of fasting against diverse diseases and aging [106]. Although several studies have described the link between fasting and the circadian clock [222, 317], it is still unclear how fasting by itself impinges on the circadian clock and clock-dependent gene regulation in concert with fasting induced TFs. Here we demonstrate that fasting has a drastic impact on circadian physiology by inducing a number of de novo oscillatory genes, which are distinct from those responsive to timed-feeding regimens [302]. We have identified specific classes of circadian genes whose regulation is dependent on distinct fasting- controlled TFs. Fasting significantly attenuates rhythmicity of BMAL1 and REV-ERBalpha protein expression levels both in liver and skeletal muscle, leading to repression and de-repression of their target genes, respectively. Also, fasting controls distinct classes of genes that are tem-

porally regulated by the clock and fasting-sensitive TFs. Furthermore, a number of genes are induced by fasting in a BMAL1-dependent manner, suggesting that the clock modulates the fasting response. Thus, fasting uncovers a previously unappreciated coordination between the circadian clock and nutrient sensing pathways leading to different classes of circadian gene expression.

In order to investigate how fasting influences circadian gene regulation and metabolism, we used 8-week old male C57BL/6 mice fed normal chow ad libitum and then subjected them to 24-hr fasting and performed indirect calorimetry analyses. There was a reduction in oxygen consumption, respiratory exchange ratio (RER), and energy expenditure by fastin. Notably, RER during fasting was lower than that during the resting phase under ad libitum feeding, likely because mice are still feeding during the resting phase, suggesting that fasting acts as a profound metabolic perturbation. We then collected tissues every 4-hr over the light/dark 12h/12h cycle from 24-hr fasted mice (FAST) or control mice fed ad libitum with normal chow (FED). As expected, body weight and epididymal white adipose tissue (eWAT) weight were reduced remarkably after fasting. To assess how fasting impacts circadian regulation, we analyzed the circadian transcriptome by RNA-seq. The analysis revealed that approximately 15% of hepatic transcripts and 4% of muscle transcripts are cyclic in FED mice based on JTK_CYCLE analysis [117]. Of the rhythmic transcripts in FED mice, about 80% and 66% of hepatic and muscle cyclic genes ceased oscillation after fasting, respectively, emphasizing the notion that the feeding- fasting cycle is a major environmental cue for peripheral tissues [51, 274, 302]. Strikingly, a number of genes, particularly in skeletal muscle, gained oscillation after fasting. The overall amplitude of hepatic oscillating genes in FAST mice was dampened, whereas that of muscle rhythmic genes was enhanced, as compared to FED mice. Moreover, phase analysis of the cycling genes revealed that the peak phase in skeletal muscle from FAST mice was highly centered around ZT12, while that in liver was more evenly distributed. Although some genes remained rhythmic both in FED and FAST mice, their peak phase was redistributed after fasting. Collectively, these data illustrate that fasting elicits tissue-specific

responses along the circadian cycle. Gene ontology analyses of the identified oscillatory genes revealed unique biological processes enriched in a tissue-specific manner. Notably, electron transport chain was highly enriched in FAST liver, in keeping with the pivotal role of mitochondrial oxidative metabolism under fasting [170]. Likewise, protein catabolic processes were enriched in FAST muscle, a well-documented metabolic adaptation upon fasting in the skeletal muscle [195]. In order to gain insight into whether lack of food operates as a metabolic cue, we compared hepatic genes cycling under time-restricted feeding [302], with genes oscillating in our FAST mice. Remarkably, only a small portion of genes display rhythmic expression in both groups, indicating that fasting is a metabolic cue distinct from time-restricted feeding. Furthermore, we investigated whether skeletal muscle from FAST mice shares transcriptional signatures with muscle from treadmill-exercised mice [231]. Intriguingly, approximately half of the exercise-induced genes and exercise-repressed genes in skeletal muscle were also induced and repressed by fasting, respectively. Supporting this notion, locomotor activity during fasting was enhanced particularly during the active phase, as described previously [1]. It has been shown that post-transcriptional regulation plays an important role in circadian gene expression in vivo [145]. Since gene ontology analysis of our fasting transcriptome data showed that RNA processing is enriched in cycling genes upon fasting, we tested whether post-transcriptional regulation participates in rhythmic gene expression upon fasting.

To address this question, we implemented Exon Intron Split Analysis (EISA) on our RNA-seq dataset to compare rhythmicity between intronic reads as a surrogate for precursor mRNA and exonic reads being representative of mature mRNA [84]. A large number of intronic and exonic transcripts displayed distinct oscillatory expression both in liver and skeletal muscle. Approximately 77% of the cycling exonic transcripts in FED liver were oscillatory only in exonic reads, which is in agreement with previous analysis [145]. By and large, this proportion appeared to be conserved in FED skeletal muscle as well as in FAST liver and skeletal muscle, suggesting a crucial role of post-transcriptional control in

circadian gene rhythmicity. We also focused on groups of genes oscillating both in intronic and exonic regions, and compared the peak phases between these two groups to explore the delay in the phase of exonic transcripts in comparison to that of intronic transcripts. The lag of peak phase disappeared after fasting in the liver, while becoming present after fasting in skeletal muscle, suggesting the presence of tissue-specific response of post-transcriptional control upon fasting. Overall, fasting appears to reprogram a number of cyclic genes through transcriptional and post-transcriptional mechanisms acting in a tissue-specific manner.

4.3.1 Fasting Targets Core Circadian Clock

Nutritional challenges in the form of high-fat [67] or ketogenic [288] diets reprogram circadian gene expression in the liver without an apparent effect on core clock components. Yet, because of the drastic effect on circadian transcription after fasting, we reasoned that lack of food could instead have a direct influence on core clock genes and proteins. Given the tissue-specific subset of cyclic genes in FED and FAST conditions, we compared the number of overlapping oscillating genes between liver and skeletal muscle. Only a small portion of cyclic genes were common in liver and skeletal muscle in any condition, manifesting tissue-specificity in circadian gene expression [185]. Among these genes, circadian regulation of gene expression was enriched in a group of genes oscillating in both tissues and both conditions, underscoring the resilient nature of the core clock oscillator. Therefore, we next explored the expression profiles of the core clock components in liver and skeletal muscle. Remarkably, gene expression of BMAL1-target genes was significantly attenuated (Dbp, Nr1d1, Bhlhe40, Per2, Per3), while REV-ERBa-target genes were de-repressed both in liver and skeletal muscle (Arntl, Cry1, Npas2, Nfil3). Phosphorylation of BMAL1 displays robust rhythmicity in FED mice, and is associated with active transcription of its target genes as reported in a previous study [285]. Rhythmic BMAL1 protein phosphorylation is significantly dampened in FAST mice, both in liver and skeletal muscle, in keeping with the attenuated gene expression

profiles of BMAL1-target genes. Furthermore, rhythmic acetylation of hepatic BMAL1 was mitigated in FAST mice, presumably as a result of increased deacetylation of BMAL1 by SIRT1 under fasting [205]. In support of this notion, acetyl-CoA synthetase 1 (ACS1) in liver, a known target of SIRT1 [97, 251], also exhibited dampened circadian acetylation in FAST mice. This dual alteration of cyclic phosphorylation and acetylation of BMAL1 could relate to the link between BMAL1 phosphorylation and acetylation [285]. Additionally, REV-ERBa and CRY1 protein expression in liver and skeletal muscle as well as hepatic PER2 expression were also dampened in rhythmicity in FAST mice. Thus, core clock components are significantly affected under fasting.

Fasting results in the activation of several nutrient-sensing factors, such as GR, CREB, FOXO, TFEB, and PPARs [177, 262]. We examined the expression levels of these regulators along the circadian cycle in FED or FAST mice, both in liver and muscle. Fasting induces these TFs in both tissues, though with distinct circadian patterns that implicate both gene and protein expression levels. In order to decipher whether the fasting-induced changes in the core clock impinge on temporal patterns of gene expression in concert with fasting-sensitive TFs on a genome-wide level, we examined publically available datasets. To do so, we analyzed gene targets for hepatic BMAL1 [145], REV-ERBa [72], and muscle BMAL1 [64], as well as hepatic GR [78], CREB [241, 329], FOXO [95], TFEB [263], PPARa [199], CREB [226], FOXO [195], TFEB [179], and PPARb [85]. We also paralleled muscle REV-ERBa target genes from muscle-specific Hdac3 -/- mice, based on the notion that muscle HDAC3 is primarily regulated by REV-ERBa [112]. We first explored the rhythmicity of target genes under the control of fasting- responsive TFs in liver and skeletal muscle. In the liver, most fasting-sensitive targets correspond to genes cycling in the FED condition, presumably because of the naturally occurring feeding-fasting cycle in ad libitum feeding. Furthermore, hepatic GR, CREB, and FOXO target genes oscillating in the FED condition were prone to peak at ZT8-12, consistent with the fasting phase in ad libitum feeding. Conversely, most fasting-sensitive targets in the muscle parallel a higher number of oscillatory genes in FAST

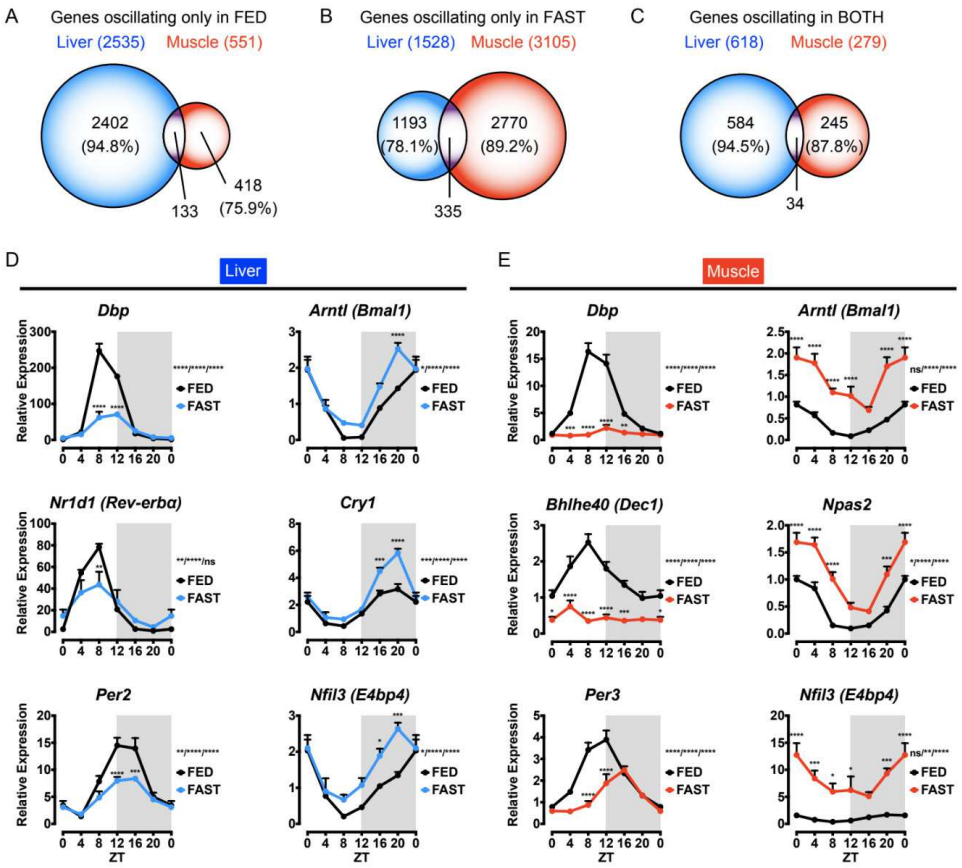

Figure 4.2: Overall Oscillation in Fasting Liver and Muscle. Specific Core Clock Repression in Liver and Muscle

condition and peak sharply at ZT12, since the response to fasting in skeletal muscle appears highly circadian. Collectively, these results suggest that each fasting-responsive TF drives rhythmic genes in a tissue-specific and phase-specific manner.

Next, we postulated that expression of BMAL1 target genes is likely to be higher in FED mice, since BMAL1 is a transcriptional activator [86] and its phosphorylation and acetylation display a stronger peak in FED mice. Also, we predicted that expression of REV-ERBa target genes may be higher in FAST mice because REV-ERBa is a transcriptional repressor [99] and its levels decrease under fasting. To validate our hypothesis, we carried out Gene Set Enrichment Analysis (GSEA) to test whether expression of BMAL1 and REV-ERBa gene targets is actually higher in FED and FAST mice at their peaks, respectively. Indeed,

hepatic BMAL1 target genes were significantly induced in FED mice at ZT8, although those at ZT12 were prone to be enriched, but not significantly. This observation was strengthened by the result showing that two- thirds of differentially expressed liver BMAL1-target genes displayed higher expression in FED mice both at ZT8 and ZT12. Similarly, muscle BMAL1-target genes were significantly enriched in FED mice both at ZT8 and ZT12, and approximately 70% of differentially expressed muscle BMAL1 targets also exhibited higher gene expression in FED mice at both time points. Notably, about 30% of differentially expressed BMAL1-target genes in both liver and muscle showed higher expression under fasting. These groups of genes have a significantly higher proportion of GR, CREB, FOXO, TFEB, hepatic PPAR, or muscle PPARa targets than those showing higher expression in FED mice, suggesting that a subgroup of BMAL1 target genes is also jointly regulated by fasting-sensitive TFs. Conversely, hepatic and muscle REV-ERBa target genes at ZT12 were significantly enriched in FAST mice, and approximately 60% of differentially expressed REV-ERBa targets displayed higher gene expression in FAST mice. These REV-ERBa target genes whose expression is induced by fasting are proportionally more likely to be GR, CREB, FOXO, TFEB, hepatic PPARa, or muscle PPARa targets. Among these fasting-sensitive TFs, PPAR was particularly enriched in hepatic REV-ERBa target genes, in keeping with the central role of REV-ERa in lipid metabolism [29, 42, 74]. In fact, known metabolic target genes of hepatic and muscle REV-ERBa were de-repressed under fasting [160]. Interestingly, it has been shown that REV- ERBa is also tethered to the genome by tissue-specific TFs such as HNF6 in liver [330]. Indeed, several HNF6/REV-ERBa targets, including Apoa4 and Cd36, are upregulated under fasting in the liver. Notably, hepatic Onecut1 (Hnf6) gene expression declined dramatically upon fasting, which could also expedite de-repression of HNF6/REV-ERBa target genes in liver. Taken together, these results support our hypothesis that attenuation of BMAL1 and REV-ERBa by fasting mediates changes in the temporal pattern of expression of their target genes on a genome-wide scale.

4.3.2 Fasting Sensitive Genes

As revealed by the transcriptome analysis, there is a group of BMAL1 target genes whose expression is enhanced by fasting and another group of BMAL1 target genes that instead displayed repression both in liver and skeletal muscle. In order to discern how BMAL1 and fasting-sensitive TFs coordinate gene transcription upon fasting, we classified genes into three groups according to the following criteria:

Class I BMAL1 target genes whose expression is repressed by fasting.

Class II BMAL1 target genes activated by fasting

Class III non-BMAL1 target genes whose expression is activated by fasting

Based on this classification, the number of genes in each class was similar between ZT8 and ZT12 both in liver and skeletal muscle, although the overall number of Class III genes is much higher than the other groups. We sought to examine whether this classification corresponds to unique transcriptional control mechanisms specific for each class of genes. We performed chromatin immunoprecipitation followed by real-time qPCR (ChIP-qPCR) in liver so as to explore the molecular mechanisms of genomic regulation by BMAL1 and fasting-induced TFs. Hepatic BMAL1 was less recruited to Class I genes such as Dbp and Per2 under fasting conditions, which was coherent to hepatic Dbp and Per2 gene expression, respectively. Notably, BMAL1 recruitment to Class II genes such as Cpt1a, Cidec, Acot4, and Gpt2 was still reduced by fasting despite increased expression of those genes upon fasting. Similarly, recruitment of BMAL1 to the Per1 promoter was also decreased upon fasting, despite induction of Per1 expression upon fasting. The induction of gene expression observed in Class II genes or Per1 is instead achieved through PPARa or CREB, whose recruitment to these promoters was increased by fasting. Recruitment of CREB and PPARa to the promoters of Class III genes, such as G6pc and Acot2 was also increased by fasting.

Although BMAL1 is known to occupy G6pc genomic region, deletion of Bmal1 in the liver does not alter G6pc gene expression, indicating that BMAL1 binding to the G6pc site is unlikely to be functional, leading to the categorization of G6pc as a non-BMAL1 target gene [145]. These results suggest that a temporal pattern of genomic recruitment of clock and fasting-sensitive TFs coordinately regulate specific classes of genes under fasting.

Next, we investigated the role of the circadian clock in fasting-induced gene regulation in liver and skeletal muscle. In order to address this question, we subjected Bmal1 -/- mice and their wild type (WT) littermates to 24-hr fasting or ad libitum feeding, and harvested liver and gastrocnemius muscle at ZT8, a time when BMAL1 recruitment to target promoters is at its peak. We explored the expression of genes belonging to the three classes we identified in fasted Bmal1 -/- mice. Expression of genes within Class I, such as Dbp, Nr1d1 (Rev-erba), and Per3, was abrogated by Bmal1 ablation as expected. Remarkably, genes within Class II were activated by fasting in a BMAL1-dependent manner despite the decreased recruitment of BMAL1 to their promoters under fasting. On the other hand, genes within Class III appeared to be activated by fasting in a BMAL1-independent fashion. We also confirmed that gene and protein expression of BMAL1 was abolished both in Bmal1 -/- liver and skeletal muscle. Under fasting, FOXO1 and GR expression in the hepatic nuclear fraction and PPARa and pCREB/CREB expression in skeletal muscle appeared higher in Bmal1 -/- mice. Conversely, hepatic nuclear PPARa expression was lower in Bmal1 -/- mice, presumably because hepatic PPARa is a direct target of BMAL1 [31, 212]. These results indicate that fasting sensing pathways are modulated by the circadian clock in a tissue-specific manner.

4.3.3 Implications in Disease

Circadian homeostasis is essential for the adaptation of all organisms to environmental changes as well as to nutritional challenges, pathologies and aging [2, 181, 182, 218, 228]. Food intake is considered as a major zeitgeber for clocks located in peripheral tissues [51, 274, 302]. Here we focused on the effect of fasting on circadian gene regulation to test whether lack of food merely reflects free running conditions, as observed in the SCN under constant darkness, or if rather fasting is capable of entraining a specific set of gene oscillations on its own. Our findings demonstrate that a significant number of genes gain rhythmicity upon fasting in a tissue-specific manner. Specifically, skeletal muscle gained almost twice as many newly oscillating genes after fasting as the liver, while a much higher number of hepatic genes are rhythmic when compared to skeletal muscle in FED mice, indicating that the skeletal muscle has an increased, intrinsic plasticity to fasting compared to the liver. Conversely, only 20% and 34% of hepatic and muscle cycling transcripts in FED mice preserved their rhythmicity under fasting. Among them, only a small fraction of genes were cyclic and in phase between FED and FAST (137 hepatic and 36 muscle genes, respectively). These resilient genes were presumably driven by a tissue-intrinsic clock, SCN derived systemic pathways, or the combination of both. As most cycling genes fail to sustain rhythmicity or to free-run under fasting, even in the presence of an intact SCN and functional clock, fasting appears to be a strong metabolic cue to entrain circadian gene expression.

Based on our observation that fasting attenuated the core clock oscillator, fasting appears to be a suppressive signal for the circadian clock. This may be partly accomplished by increased NAD+ levels and subsequent enhanced sirtuin activity by fasting [33, 247], that we have previously demonstrated to hinder BMAL1 recruitment to its genomic targets and BMAL1-dependent gene activation [184, 205]. Moreover, an additional layer of regulation by fasting could control clock protein translation, post-translational modifications, and degradation [12, 156]. Intriguingly, Per1 activation upon fasting is somewhat reminiscent of the effect elicited

by light, although it is still unclear whether Per1 induction by fasting contributes to the mitigation of BMAL1-dependent gene activation [266]. Feeding or insulin alone induces Per2 expression, suggesting that a switch from sufficient fasting to feeding could synergistically act as an entrainment signal by activating Per1 and Per2 [256].

Recent findings regarding chromatin accessibility demonstrated that PPAR, C/EBP, GR, and CREB motifs are particularly enriched in hepatic fasting-induced enhancers [90]. Moreover, CREB, FOX, and GR motifs are enriched in hepatic DNase I hypersensitive sites during the fasting phase of temporal feeding restriction even in Bmal1-null mice [270]. Therefore, it can be envisioned that these fasting-sensitive TFs may work in concert or independently of the circadian machinery. Taking these observations into account, we investigated the role and molecular mechanism of GR, CREB, FOXO, TFEB, and PPARs in the temporal pattern of differential gene expression upon fasting in concert with BMAL1 in the liver and skeletal muscle. This lead to a classification of fasting-dependent genes based on their differential gene expression. Our analysis revealed that there is a group of genes whose expression is dually controlled by fasting-sensitive TFs and BMAL1, both in liver and skeletal muscle. BMAL1 appears to play a dominant role in the expression of these genes in ad libitum fed condition, while fasting-responsive TFs take over BMAL1 upon nutritional deprivation to achieve a highly efficient gene induction. Notably, gene induction by fasting is dependent on BMAL1, suggesting that a functional clock is still necessary for the robust activation of these genes. Since physiological fasting is supposed to occur around ZT8-12, it could be speculated that BMAL1 and fasting-responsive TFs cooperatively produce robust oscillation in these dually controlled genes especially in the context of dark phase restricted feeding. On the other hand, the majority of genes activated by fasting are non-BMAL1 targets, supporting the notion that a number of genes would potentially be able to become oscillatory under forced feeding-fasting regimens, even without a functional intrinsic clock [302].

Accumulating evidence also suggests that post-transcriptional control plays an important

role in circadian gene expression [145, 83, 146, 193, 287]. A number of distinct genes were cycling only in exonic reads under fasting, indicating that nutrient-sensing signals could control the RNA processing machinery. Interestingly, the RNA editing activity on Apob mRNA and the excretion of small molecular weight ApoB are suppressed after fasting, though fasting does not affect the relative levels of Apob mRNA, indicating that RNA editing could sense fasting signals [102, 164]. Fasting also alters circadian alternative splicing and contributes to the temporal pattern of gene expression [188]. Intriguingly, peroxisome proliferator-activated receptor gamma co-activator 1a (PGC-1a) interacts with components of the RNA processing machinery, suggesting that PGC-1a could mediate fasting signal to post-transcriptional gene control [198, 303]. Since transcription and RNA processing are tightly coupled, it is tempting to speculate that fasting-sensitive TFs such as PPARs and FOXO also modulate post-transcriptional gene regulation in the context of fasting by employing co-activators and could use them to bridge transcription with post-transcriptional processes [22, 139].

Overall, our study shows that fasting entrains circadian gene expression through temporal reprograming of the circadian clock and fasting-sensitive TFs. This dramatic reorganization of gene regulation by fasting could prime the genome to a more permissive state to anticipate upcoming food intake and thereby drive a new rhythmic cycle of gene expression. Therefore, optimal fasting in a timed manner would be strategic to confer robust circadian oscillation that ultimately benefits health and protects against aging-associated diseases.

Chapter 5

Circadian Reprogramming and Development

5.1 Mir-132/212 and Depth Perception Development

5.1.1 MiR-132 Affects Visual Cortical Transcriptome

To investigate miRNA expression during postnatal development we performed RNA sequencing of small RNAs extracted from the visual cortex of P10 and P28 mice. A total of 176,228,828 raw reads were generated. On average 94.5% (SD = 0.64) of the reads could be aligned. 2,164 isomiRs and 299 precursors were found to have age-regulated expression. Mir-29a, miR-219, miR-338 and miR-132 were the miRNAs undergoing the strongest upregulation during development, a result confirmed by reverse transcription PCR and in agreement with previous data8, whereas miR-298, miR-149 and miR-331 were the top downregulated miRNAs. The corresponding miRNA families were also the strongest regulated families. Among the members of the miR-132 family, miR-132-3p and miR-212-5p were the

only miRNAs represented at high levels.

Then, we investigated the impact of developmental regulation of miR-132-3p and miR-212-5p on gene expression by analysing the transcriptome in the same samples used for the small RNA sequencing. 4,339 genes were significantly upregulated and 5,429 genes were downregulated in the P28 visual cortex with respect to the P10 cortex. Kyoto Encyclopedia of Genes and Genomes (KEGG) pathway analysis revealed that some pathways were in common between upregulated and downregulated genes, whereas other pathways were significantly enriched only in one of these groups. Many pathways previously involved in cortical development and plasticity were affected [165, 17, 294, 28, 143] strengthening the predictive validity of our analysis. Indeed, MAPK signalling, neurotrophin signalling, glutamatergic synapse, neuroactive ligand-receptor interaction, insulin signalling pathways were significantly enriched in both upregulated and downregulated genes; regulation of actin cytoskeleton, circadian rhythmmammal and chemokine signalling pathways were present only in upregulated genes; axon guidance, RNA transport, gap junction, long-term potentiation, long-term depression and mTOR signalling pathways were present only in the downregulated genes. Many of the developmentally regulated genes were predicted targets of multiple miRNAs. Importantly, there was a highly significant and specific overlap between the predicted targets of miR-132-3p and the genes downregulated with age (181 genes, odds ratio 2.10; Fisher exact test p-value = 0.0001). MiR-212-5p targets were also significantly enriched in age-downregulated genes albeit with a minor odds ratio than miR-132-3p (132 genes, odds ratio = 1.74; Fisher exact test p-value = 0.0001). This result is in agreement with the hypothesis that miR-132/212 age-regulated increase contributes to repress the expression of a significant number of genes during visual cortical development.

To independently test this hypothesis, we performed RNA sequencing on P28 visual cortical samples obtained from mice with germ-line deletion of the miR-132/212 locus. 1698 genes were differentially expressed between mutant and WT mice. Intriguingly, KEGG pathway

analysis revealed that 53 out of the 61 KEGG categories enriched with genes upregulated in miR-132/212 null mice were also present in the KEGG categories downregulated during normal development, suggesting that a substantial part of the rearrangement in molecular pathways occurring during normal development is altered in miR-132/212 mutants. Moreover, a significant enrichment in miR-132-3p targets was present in the genes upregulated in the miR-132/212 mutant cortex (54 genes, odds ratio 5.07; Fisher exact test p-value ¡ 0.0001), whereas the enrichment in miR-212-5p targets was not significant (14 genes, odds ratio 1.50; Fisher exact test p-value = 0.13). Importantly, there was an overlap (39 genes) between the miR-132-3p targets and genes that were both downregulated by age and upregulated by miR-132/212 deletion. This gene set included genes important for brain development such as MeCP2, Sox5, Sox11 and Pten. Thus, in the absence of miR-132 family the developmental downregulation of a significant number of miR-132-3p targets does not occur, confirming the importance of miR-132-3p developmental regulation in defining the transcriptomic changes occurring between P10 and P28 in the visual cortex.

5.1.2 Impaired Binocular Matching

We investigated whether the lack of miR-132/212 cluster was able to influence functional development of the visual cortex. We first analysed monocular tuning properties in sorted units recorded by multisite silicon electrode tetrodes inserted at depths sampling from layers III to V in binocular visual cortex of P27-28 WT and null mice. Orientation and direction selectivity was measured on responses to drifting sinusoidal gratings calculating three different parameters: orientation selectivity index (OSI), orientation tuning width and direction selectivity index (DSI) [114, 209]. Each index was separately computed for the contralateral and ipsilateral eye responses. No difference between WT and null mice was present for all these indexes (One-way analysis of variance (ANOVA), p-value = 0.159, p-value = 0.595 and p-value = 0.262 respectively) indicating that the maturation of these properties does

not require miR-132/212.

Previous data showed that after orientation selectivity completes its developmental trajectory, there is a process of binocular matching of preferred orientation19. To further analyse the role of miR-132/212 in visual cortical development, we assessed binocular matching of orientation preference in P27-28 null and WT mice. We found that mutant mice had a significantly worse binocular matching of orientation preference with respect to WT age-matched littermates (Two-way ANOVA, effect of genotype p-value = 0.001; post hoc Holm-Sidak test, p-value = 0.01), suggesting that the lack of miR-132 family specifically disrupts this late developing property of visual cortical neurons while keeping monocular tuning properties intact. Intriguingly, the defective binocular matching of orientation preference present in P27-28 miR-132/212 null mice persists into adulthood. Indeed, we measured binocular matching in adult P60 mutant and WT mice and we found that also at this age binocular matching was dramatically impaired in miR-132/212 null mice (post hoc Holm-Sidak test, p-value = 0.001), despite a normal orientation selectivity of visual cortical neurons (Two-way ANOVA, effect of genotype p-value = 0.133).

Single-unit data pooled from many animals can be biased towards those individual animals in which the largest number of units were studied. Therefore, we next analysed the results by case. Even with this analysis, binocular matching resulted to be strongly impaired in miR-132/212 null mice both at P27-28 and P60 (Two-way ANOVA, effect of genotype p-value = 0.001; post hoc Holm-Sidak test, WT versus KO: P27-28 p-value = 0.01, P60 p-value = 0.001).

Visual cortical neurons can be classified into simple and complex cells based on their response properties [209, 268]. Since it has been recently reported that during physiological development simple cells fulfil the process of binocular matching of orientation preference before complex cells [305, 255, 152, 153, 304], we studied the degree of binocular matching in simple and complex cells of null mice. Simple cells of null mice only showed a statis-

tically nonsignificant trend for binocular mismatching with respect to WT animals (t-test, P=0.07), while the binocular matching of complex cells was significantly disrupted (t-test, p-value = 0.01). Consistently with the results reported for the whole-cell population, monocular orientation tuning properties of both simple and complex cells were normal (One-way ANOVA P=0.624 and P=0.524, respectively). These results are in line with the hypothesis that miR-132 family is particularly important for the late development of binocular neuronal properties.

Since narrow-spiking units are known to be poorly orientation selective [209], an abnormally high presence of narrow-spiking units in miR-132/212 null mice could contribute to the low binocular matching of orientation preference observed in mutant mice. To test this possibility we classified neuronal units into two different classes, narrow spiking and broad spiking, on the basis of their spike waveform. This waveform signature is used to distinguish putative excitatory and fast spiking inhibitory neurons [209]. We found that 5.4% of miR-132/212 mutant units belonged to the narrow-spiking class. This percentage was not significantly different from that detected in the cortex of WT animals (8.4%; Fishers exact test p-value = 0.36) and in line with previous studies on mice of the same age [114, 142, 141]. These data show that the deletion of miR-132/212 locus does not impinge on the development of narrow-spiking units suggesting that the disruption of binocular matching in null mice was not due to an alteration of narrow-spiking inhibitory neurons. Consistently, the analysis of binocular matching of orientation preference exclusively in broad-spiking cells showed a significant disruption of this property in miR-132/212 mutants (t-test, p-value = 0.01) with no change in orientation selectivity (One-way ANOVA p-value = 0.165). These results also suggest that miR-132 could be mainly involved in the maturation of response properties of excitatory cortical neurons.

5.1.3 Ocular Dominance Placticity

It has been reported that binocular matching of orientation preference is an experience-dependent process [305] sharing molecular regulatory mechanisms with OD plasticity23. Thus, we decided to investigate whether OD plasticity was blocked in miR-132/212 null animals and whether the effects of MD on binocular matching could be occluded by miR-132/212 deletion. Previous work had already shown that miR-132 is necessary for OD plasticity [192], however a temporally restricted block of miR-132 availability using a miR-132 sponge was adopted. Therefore, we first controlled whether OD plasticity was also blocked by our genetic deletion of miR-132/212. We recorded visual evoked potentials (VEPs) and single units in WT and null mice MD for 3 days from P24-25. VEP recordings showed that non-deprived null mice have a normal OD ratio compared to age-matched WT littermates (Two-way ANOVA on rank transformed data, post hoc Holm-Sidak test p-value = 0.566), and that three days of MD were not able to induce OD shift in mutant mice (Two-way ANOVA on rank transformed data, post hoc Holm-Sidak test p-value = 0.958). MD in WT animals led to a significant decrease in the C/I VEP ratio (Two-way ANOVA on rank transformed data, genotype and condition interaction p-value = 0.01; post hoc Holm-Sidak test p-value = 0.001).

Single-unit analysis of the ocular dominance index (ODI) confirmed the lack of OD plasticity in null mice. ODI of null mice was not significantly different from that of WT animals (Two-way ANOVA, post hoc Holm-Sidak test p-value = 0.210) and from that of MD null mice (Two-way ANOVA, post hoc Holm-Sidak test p-value = 0.652), whereas MD WT mice displayed the typical OD shift towards the open eye (Two-way ANOVA, genotype condition interaction p-value = 0.05; post hoc Holm-Sidak test p-value = 0.01). Contralateral bias index (CBI) expressing the strength of contralaterally driven responses for each animal confirmed the results of unit-based analysis (Two-way ANOVA, genotype condition interaction p-value = 0.05; post hoc Holm-Sidak test: WT versus ko p-value = 0.96, ko versus ko-md

P=0.97, WT versus WT-md p-value = 0.05).

Then, we analysed the influence of visual experience on binocular matching level in P27-28 miR-132/212 null and WT mice subjected to a 3-days MD. We found that the effect of MD on binocular matching was occluded by the deletion of miR-132/212: while WT-md animals displayed a significant impairment of binocular matching with respect to non-deprived mice (Two-way ANOVA, genotype condition interaction p-value = 0.05, post hoc Holm-Sidak test p-value = 0.001), the closure of one eye did not further deteriorate the mismatch of orientation preference observed in miR-132/212 null animals (post hoc Holm-Sidak test P=0.767). The same conclusion emerged from the analysis of binocular matching by case (Two-way ANOVA, genotype condition interaction p-value = 0.01; post hoc Holm-Sidak test: WT versus WT-md p-value = 0.01, ko versus ko-md p-value = 0.795). These results demonstrate that miR-132/212 is necessary for experience-dependent development of binocular processes in the visual cortex.

5.1.4 Depth Perception Impairment

We then asked whether the disruption of binocular matching for orientation preference caused by miR-132/212 deletion in the visual cortex could affect animals perception abilities. We first performed an electrophysiological assessment of visual acuity (VA) in P27-28 miR-132/212 null mice [235]. No VA difference was present between mutant and WT animals (t-test, P=0.781), confirming that molecular mechanisms underlying experience-dependent regulation of binocularity of cortical neurons can be dissociated from those involved in VA maturation and plasticity [143, 305, 109, 187, 273].

We then focused on depth perception, given the importance of binocular cues for this visual function. We employed the visual cliff task to explore the effects of miR-132/212 deletion on stereoscopic visual abilities. This test exploits the spontaneous tendency of rodents to avoid

the deep side of a visual cliff arena. The construct validity of the visual cliff exploration test was first assessed investigating the behaviour of mice in monocular condition (that is, subjected to the closure of one eye obtained through eyelid suture). As previously reported38, animals in binocular condition (bin) spent a longer period of time on the shallow side of the arena, while monocular condition (mon) led to a significantly lower preference for the shallow side (t-test, p-value = 0.01). Total distance moved and velocity were comparable between the two groups (t-test, p-value = 0.123 and p-value = 0.142 respectively). These results confirmed that binocular vision is required for discrimination between the deep and the shallow side. To exclude the contribution of non-visual cues to the preferential exploration of the shallow side, we analysed the behaviour of binocular WT animals in the same visual cliff arena with the two visual stimuli placed at the same height immediately below the glass plates. In this condition, the differential exploration of the two sides of the arena shown by binocular WT mice in the visually cued version was completely eliminated (t-test, p-value = 0.01). Indeed, WT mice equally explored the two sides of the arena (one-sample t-test versus 50%; WT p-value = 0.514). The same was true for miR-132/212 null animals (one-sample t-test versus 50%; ko p-value = 0.622). These data demonstrate the tight relevance of visual cues in visual cliff test. No difference was present between WT and mutant mice in the time spent in the centre of the arena (t-test, p-value = 0.663) indicating similar levels of anxiety-like behavior in the two genotypes.

Next, we evaluated depth perception abilities of miR-132/212 null mice. We found that miR-132/212 mutant mice showed a significantly reduced preference for the shallow side with respect to WT mice (KruskalWallis One-way ANOVA on ranks, post hoc Dunns method, p-value = 0.05). Interestingly, the impairment in stereoscopic abilities detected in miR-132/212 null mice was reminiscent of that observed in animals subjected to a 3-day MD and tested after the restoration of binocular vision (that is, 2h after the reopening of the deprived eye, WT-md; KruskalWallis One-way ANOVA on ranks, post hoc Dunns method). To rule out the possibility that the significant difference in visual capacities reflect changes in the

ability to cope with stress in challenging task conditions, we analysed general activity and anxiety-related behaviour of WT and miR-132/212 mutant mice in the visual cliff arena. We found that total activity levels of animals were not affected by the deletion of miR-132/212 (distance moved: t-test, p-value = 0.285; velocity: t-test, p-value = 0.303). Moreover, the time spent by miR-132/212 mutant mice in the central portion of the apparatus was not different from that recorded for WT animals (t-test, p-value = 0.126), excluding the hypothesis that a combination of abnormal anxiety and activity levels might be related to their altered performance in the visual cliff arena.

In tight accordance with binocular matching results, depth perception impairment in miR-132/212 null mice persisted in adulthood: stereoscopic abilities of mutants at P60, indeed, appeared markedly altered with respect to age-matched WT animals (t-test, p-value = 0.05). Time spent in the central part of the arena, total activity and velocity of animals were comparable between genotypes also in this case (t-test, p-value = 0.767, p-value = 0.431 and p-value = 0.349, respectively). These results demonstrate that disruption of the binocular orientation tuning properties of neurons in the primary visual cortex is associated with behavioural deficits in depth perception.

Previous studies showed that miR-132 family is preferentially expressed by excitatory cells39. Moreover, we found that miR-132/212 deletion mainly affected the response properties of broad-spiking cells and morphological analysis of miR-132/212 null mice crossed with mice expressing green fluorescent protein in layer V pyramidal neurons showed a small but significant reduction spine density with respect to WT littermates (t-test, p-value = 0.05), suggesting that excitatory cells could be a specific cellular target of miR-132 family. To directly investigate this possibility, we generated a novel mouse model (Emx1:Cre-miR-132/212/) in which floxed miR-132/212 alleles are specifically deleted in forebrain glutamatergic neurons and in some glial cells by using the Emx1 promoter to drive Cre-recombinase expression [121]. The electrophysiological characterization of these mutants at P27-28 revealed no dif-

ferences in monocular properties, with OSI, tuning width and DSI being not significantly different between Emx1:Cre-miR-132/212/ mice and their age-matched littermates expressing exclusively the floxed miR-132/212 allele (miR-132/212fl/fl mice) or the Cre-recombinase allele (Emx1:Cre-WT mice; One-way ANOVA, p-value = 0.167, p-value = 0.300 and p-value = 0.893 respectively). In contrast, binocular orientation matching appeared to be significantly impaired in Emx1:Cre-miR-132/212/ animals (One-way ANOVA p-value = 0.01, post hoc Holm-Sidak test p-value = 0.01), thus recapitulating the phenotype of ubiquitary null mice. Analysis of average binocular matching of single mice confirmed the presence of an impairment exclusively in Emx1:Cre-miR-132/212/ mice (One-way ANOVA p-value 0.05, post hoc Holm-Sidak test, miR-132/212fl/fl versus Emx1:Cre-miR-132/212/ p-value= 0.05; Emx1:Cre-WT versus Emx1:Cre-miR-132/212/ p-value = 0.05; Emx1:Cre-WT versus miR-132/212fl/fl p-value = 0.808). These data indicate that the action of miR-132 family in excitatory forebrain cells is required for the normal development of binocular matching of orientation preference in the primary visual cortex.

5.1.5 Developmental Implications

During the first month of postnatal life the mouse visual cortex undergoes dramatic morphological and functional changes that leads to adult-like neuronal receptive fields17 and the maturation of visual function [32, 128]. We show that these changes are paralleled by a considerable transcriptome rearrangement: many miRNAs undergo a remarkable change of expression between P10 and P28 with the top hits being miR-29, that was previously involved in regulating epigenetic enzymes important for cortical plasticity [289]; miR-338 and miR-219, that were suggested to be key players in myelination; and miR-132/212, a miRNA family previously involved in synaptic plasticity [291, 192, 289, 290, 242, 110, 98, 307]. The combined analysis of miRNAs and mRNAs in the visual cortex of WT and miR-132/212 null mice revealed that genes downregulated with age and upregulated by miR-132/212 deletion

are highly enriched with miR-132-3p targets and, to a much lesser extent, with targets of miR-212-5p, the only two members of the miR-132 family abundantly expressed in the visual cortex. Taken together, these data demonstrate that miR-132 family contributes to shape the developmental regulation of visual cortex transcriptome and prompted us to analyse the effects of genetic deletion of the miR-132/212 locus on functional development of the visual cortex. We observed a specific deficit in the maturation of binocular matching of orientation preference in neurons of the binocular visual cortex of mutants accompanied by a remarkable impairment in depth perception.

OD plasticity is one the most studied models to understand how experience regulates brain development. A flurry of molecular mediators have been shown to be regulated by visual experience and involved in OD plasticity [165]. However, very little is known about the role of molecular factors involved in OD plasticity in normal visual development of non-deprived animals. A reasonable expectation would be that in absence of these factors visual development should be dramatically impaired. However, many studies have shown that functional development of cortical units is a multi-faceted process involving experience-independent and experience-dependent aspects occurring at specific time windows of development [141, 70, 128]. Thus, it is difficult to predict which features could be regulated by factors mediating experience-dependent plasticity. Recent work showed that a late occurring developmental process is the binocular matching of orientation preference [305, 152, 153, 304]. This process occurs in coincidence with the rise of miR-132 expression in the visual cortex8, with simple cells reaching adult levels of binocular matching of orientation preference before complex cells [304]. Importantly, this process is also temporally coincident with the CP for OD plasticity and is disrupted by MD19 suggesting that mechanisms underlying OD plasticity in deprived mice might overlap with those involved in development of binocular matching of orientation preference. Our data support this possibility by showing that the absence of miR-132/212, that resulted in no OD plasticity, was associated with a specific impairment of binocular matching of orientation preference. By contrast, early developing features of

cortical neuron RF, like orientation and direction selectivity, were unaffected. Moreover, the effects of MD on binocular matching were occluded by miR-132/212 deletion suggesting that MD might act on binocular matching by reducing miR-132/212 levels. This hypothesis is based on previous data showing that miR-132 and its primary precursor are strongly downregulated by MD. A possible scenario emerging from these observations is that visual experience after eye opening endows cortical cells with plasticity mechanisms, such as the post-transcriptional target regulation by miR-132/212, necessary for refinement of binocular connections onto visual cortical neurons. These mechanisms would overlap with those involved in changing OD in MD animals. MiR-132 family is expressed in an activity-dependent manner also in the monocular visual cortex [291] therefore it seems unlikely that these miRNAs are specifically dedicated to the formation of binocular cells. A more likely possibility is that miR-132 family could be involved in experience-dependent processes occurring also in this region [141] at the age when miR-132/212 is expressed.

Our data show that miR-132/212 mutants display an impaired maturation of binocular depth perception revealed using the visual cliff test that relies on binocular vision. This is the first time that an impairment of binocular matching of orientation preference of cortical neurons has been related to a behavioural failure, suggesting a physiological requirement of this neuronal feature in mouse vision.

We can exclude the contribution of non-visual cues to the preferential exploration of the shallow side because when we placed visual stimuli at the same height immediately below the glass plates, we did not detect any difference in the exploration of the two sides of the apparatus. In addition, the effect reported was not due to abnormal levels of anxiety or general exploratory activity in mutant mice as indicated by the equal time spent in the central and peripheral portion of the apparatus, and the comparable path length and locomotion velocity shown by WT and miR-132/212 null mice. Finally, the similar VA of WT and mutant mice excludes the possibility that the different performance in the visual

cliff test was due to blurring of the patterned visual stimuli in mutants.

It is well-known that depth perception exploits multiple visual cues, however binocular cues, such as disparity, are known to be particularly important also in mice [258]. It has been proposed that the response of visual cortical neurons to the inputs from the two eyes need to be tuned to similar orientations to encode binocular disparity of stimulus phase [305, 23], suggesting that impaired matching of binocular orientation preference induced by miR-132/212 deletion underlies the defective depth perception of mutants.

Our data also show that the impairment of binocular matching and depth perception due to miR-132/212 deletion is comparable to that observed in MD WT mice. By contrast, OD of cortical neurons is differentially affected by these two manipulations, suggesting that depth perception preferentially reflects the state of binocular interactions rather than the strength of the inputs of the two eyes onto cortical neurons.

How could the transcriptional regulation of miR-132/212 cluster control experience-dependent development of functional properties of visual cortical neurons? A series of in vitro and in vivo studies revealed that miR-132 family has an active role in brain structural plasticity. Indeed, miR-132 has been flagged as an important regulator of activity-dependent shaping of dendritic morphology and arborization, and spine density [291, 98, 301] acting through the activation of the Pac1-PAK-actin remodelling pathway [307, 119]. Moreover, miR-132 was found to mediate synaptic plasticity in the hippocampus [155, 312] and in the cortex [242], and alteration of its expression has been documented in several neuropsychiatric disorders [197, 233]. Most importantly, among the miR-132 target genes downregulated with age in WT mice, but remaining at significant high levels in miR-132/212 null mice, there are genes potentially involved in binocular matching like MeCP2, the mediator of brain-derived neurotrophic factor (BDNF) signalling Sos1, and phosphatase and tensin homolog (PTEN), an antagonist of the plasticity and groWTh mTOR/Akt pathway [28].

In conclusion, our study represents the first characterization of a miRNA role from its in vivo transcriptional and target regulation to its moulding action on cortical receptive fields and on its behavioural consequences on vision. Many microRNAs were found to be strongly regulated with age suggesting that they might contribute to the molecular regulation of the cortical transcriptome and eventually to functional development. Their number is likely to be underestimated by our study considering that cell-specific analyses could reveal additional regulated miRNA with highly selective expression. Thus, we surmise that miRNAs likely represent a novel molecular layer of control of postnatal cortical development. The pathogenetic relevance of miR-132 regulated processes during development is further supported by the presence of brain disease related genes among the developmentally regulated miR-132 targets altered in the miR-132/212 mutant including MeCP2, Pten, Ras-regulating genes Sos1 and Rasa1, Mmp16, Runx1t1, Sox11, Sox5, and Gpd2. Since many neurodevelopmental disorders including autism are related to alterations of neuronal connectivity and synaptic plasticity, miR-132 dysregulation and subsequent abnormal expression of miR-132 target genes could contribute to some pathological traits present in these diseases. Thus, a strategic modulation of miR-132/212 expression may offer a new therapeutic approach for these severe disorders.

5.2 Reprogramming Human Fibroblast to Myogenic Lineage

Genome architecture is important in transcriptional regulation, but its dynamics and role during reprogramming are not well understood. Over a time course, we captured genome-wide architecture and transcription during MYOD1-mediated reprogramming of human fibroblasts into the myogenic lineage. We found that chromatin reorganization occurred prior to significant transcriptional changes marking activation of the myogenic program. A global

bifurcation event delineated the transition into a myogenic cell identity 32 hours after exogenous MYOD1 activation, an event also reflected in the local dynamics of endogenous MYOD1 and MYOG. These data support a model in which master regulators induce lineage-specific nuclear architecture prior to fulfilling a transcriptional role. Interestingly, early in reprogramming, circadian genes that are MYOD1 targets synchronized their expression patterns. After the bifurcation, myogenic transcription factors that are MYOG targets synchronized their expression, suggesting a cell-type specific rhythm. These data support roles for MYOD1 and MYOG in entraining biological rhythms.

5.2.1 Cell Fate Determination

A comprehensive understanding of cell identity, how it is maintained and how it can be manipulated, remains elusive. Global analysis of the dynamical interplay between genome architecture (form) and transcription (function) brings us closer to this understanding [236]. This dynamical interaction creates a genomic signature that we can refer to as the four-dimensional organization of the nucleus, or 4D Nucleome (4DN) [39, 59, 77, 151]. Genome technologies such as genome-wide chromosome conformation capture (Hi-C) are yielding ever higher resolution data that give a more complete picture of the 4DN, allowing us to refine cell types, lineage differentiation, and pathological contributions of cells in different diseases. High time resolution on a global scale gives key insight into biological processes. Of interest in regenerative medicine is understanding the dynamical process of cellular reprogramming. Pioneering work by Weintraub et al. showed reprogramming of fibroblasts into muscle cells was possible through overexpression of a single transcription factor (TF), MYOD1, thus demonstrating that a different cell identity could supersede an established one [308, 309]. In 2007, when Yamanaka and colleagues reprogrammed human fibroblasts into an embryonic stem cell-like state with four TFs, POU5F1 (OCT4), SOX2, KLF4, and MYC, they showed that a pluripotent state could also supersede an established cell identity [284]. These remarkable

findings demonstrate the possibilities of controlling the genome and the cell identity through TFs. However, how TFs dynamically orchestrate genome architecture and transcription as a cell changes identities during reprogramming is not understood. One exciting finding in recent reports was that Hi-C contact maps can be used to divide the genome into two major compartments, termed A and B [39, 169]. Compartment A is associated with open chromatin (transcriptionally active), and compartment B with closed chromatin (transcriptionally inactive). The pattern of A/B compartmentalization is cell-type specific and reflects unique gene expression signatures. Studies show that A/B compartment switching occurs during differentiation and reprogramming, where genomic regions previously assigned to one compartment change to a different compartment to facilitate the gene expression associated with a new cell state [39, 59, 77, 151]. These studies support conjecture that A/B compartments have a contributory but not a deterministic role in establishing cell-type specific patterns of gene expression [59]. Previously we introduced a new technique from spectral graph theory to partition the genome into A/B compartments and identify topologically associating domains (TADs) [40]. This motivated us to study the 4DN from a network point of view, where nodes of the network correspond to genomic loci that can be partitioned at different scales: gene level, TAD level, and chromosome level. The edges of the network indicate contact between two loci, with contact weights given by Hi-C entries. Previous studies have extracted a single topological feature from the Hi-C matrix (e.g. A/B compartments), and then combined those results with gene expression [39, 56, 59, 77, 151, 169]. From the network perspective, A/B compartments are identified as distinct connected components of a network. As will be demonstrated here, other properties of the network topology, such as node centrality, can be extracted from the Hi-C matrix to yield further information about chromatin spatial organization. The utility of network centrality allows one to identify nodes that play influential topological roles in the network. A number of centrality measures exist, each specialized to a particular type of nodal influence. For example, degree centrality characterizes the local connectedness of a node as measured by the number of edges connecting to this node, while

closeness centrality is a global connectedness measure that characterizes the average distance of a given node to all other nodes. Eigenvector centrality is a neighborhood connectedness property in which a node has high centrality if many of its neighbors also have high centrality. Googles Page-rank algorithm uses a variant of eigenvector centrality [175]. In this work we investigated dynamics of topological features of genome architecture and explored how they varied with transcription during MYOD1-mediated reprogramming of human fibroblasts into the myogenic lineage. Sampling across a time course during reprogramming, we captured architecture by Hi-C, transcription by RNA-seq, and proteomics data. By combining different centrality measures we found important Hi-C features largely overlooked in previous studies, and this approach facilitated coordinated form-function analysis of chromatin conformation and gene expression in genome-wide data. Analyses of form-function dynamics revealed chromatin reorganization that occurred prior to changes in transcription. In this work, we introduce the concept of bifurcation to describe a critical transition from one cell identity to another. We detected a bifurcation in space-time 32 hours after activation of exogenous MYOD1 in fibroblasts that suggests a definitive transition into the myogenic lineage. Additionally we identified a core subset of myogenic genes that define this state. We further found robust synchronization of circadian gene expression, and determined that these genes are downstream targets of MYOD1, suggesting MYOD1 feedback onto circadian gene circuits. After the bifurcation, MYOG was associated with synchronization of a subset of important myogenic transcription factors. These findings support roles for MYOD1 and MYOG in entraining biological rhythms. Finally, our analysis of genomic regulatory elements such as chromatin remodeling genes, super enhancer regions and microRNAs provides additional clues toward understanding system-wide dynamics during reprogramming.

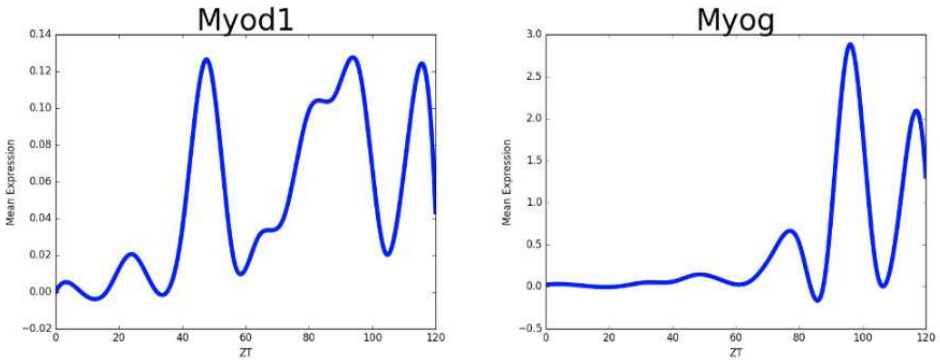

Figure 5.1: MYOD1 and MYOG Oscillation After Bifurcation Leading to Myogenic Lineage

5.2.2 MYOD1-mediated Direct Reprogramming

We converted primary human fibroblasts into the myogenic lineage using the transcription factor and master regulator MYOD1. In its native system, MYOD1 initiates the transcriptional program that turns muscle cell precursors into multinuclear muscle fibers. Fibroblasts were transduced with a lentiviral construct that expressed human MYOD1 fused with the tamoxifen-inducible mouse ER(T) domain (L-MYOD1) [137]. With 4-hydroxytamoxifen (4-OHT) treatment, transduced cells showed nuclear translocation of L-MYOD1 and morphological changes consistent with myogenic differentiation. We then validated the activation of two key myogenic genes downstream of MYOD1 (MYOG and MYH1). These results demonstrate successful conversion of fibroblasts into the myogenic lineage by L-MYOD1. Subsequent analyses were carried out on 4-OHT treated, transduced cells, sampling at 8 hour (hr) intervals for RNA-seq, small RNA-seq, and Hi-C analyses, and at 24 hr intervals for proteomics.

5.2.3 Synchronization of Circadian Rhythms

We observed that upon MYOD1 nucleus translocation, the population of cells exhibit robust synchronization in circadian gene expression. Upon further inspection this finding can be

interpreted as follows; a large portion of the core circadian gene network relies on E-box motif targets and transcription factors for control, the same motif that the bHLH protein MYOD1 targets [296]. This is further supported by the observation that known core circadian genes with E-box targets displayed the most profound synchronization initially, starting with an uptick in gene expression post MYOD1 addition. JTK_CYCLE confirmed this observation, as all E-box circadian genes were found to have a period of 24 hrs, with a maximum lag between any genes of 4 hrs (except for CRY1) [117].

Interestingly, the subset of transcripts displaying oscillatory behavior was different preand post- our identified bifurcation point. MYOD1 and MYOG expression began around our identified bifurcation point at 32 hrs and both transcripts displayed oscillatory expression. Additionally, circadian transcript oscillations dampened at time point 40 hr, corresponding with when the cells were given low-serum differentiation medium. We examined the subset of transcripts that were found to be only oscillatory after the bifurcation point and synchronous (in phase or antiphase) with MYOD1 and MYOG expression. Transcripts that were found to be oscillating in phase are potentially interacting in an excitatory fashion, and vice versa. Since both MYOD1 and MYOG are known transcription factors, we further investigated which newly oscillating transcripts may have motifs for either MYOD1 or MYOG binding sites in their promoter regions using MotifMap [48, 315]. For those genes that were found to oscillate only after the bifurcation point, 51 oscillating transcripts possessed upstream MYOG binding sites and were synchronous with MYOG. Similarly, 17 oscillating transcripts with MYOD1 binding sites were found to be synchronous with MYOD1. We found 23 known transcription factors to oscillate after the bifurcation point at our selected significance. Six of these oscillating transcription factors were synchronous and targeted by MYOG. Only a single oscillating transcription factor, ELF3, was found to be targeted and synchronous by MYOD1. Several of the six oscillatory transcription factors targeted by MYOG or MYOD1 have been shown to be related to cell differentiation in literature. Numerous studies have implicated the important role of SOX15 in muscle differentiation [190]. GATA6 has been

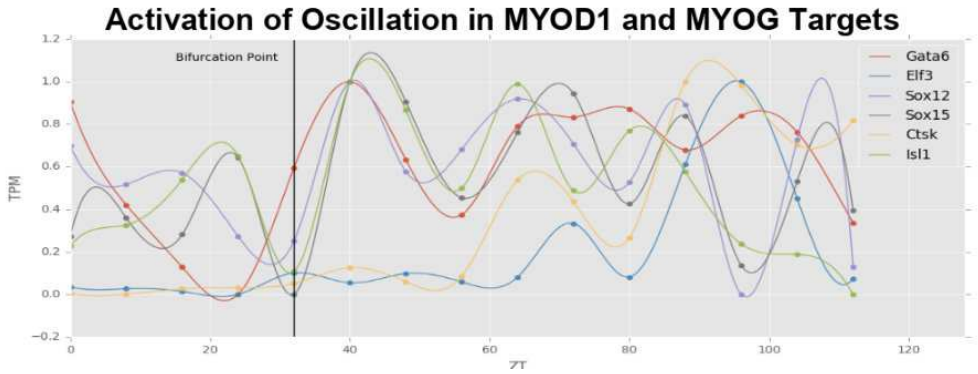

Figure 5.2: MYOD1 and MYOG Target Synchronized Oscillation

shown to regulate vascular smooth muscle development in several studies [316]. ISL1 has been shown to interact with CITED2 to induce cardiac cell differentiation in mouse embryonic cells [216]. ELF3 is found to play a diverse role in several types of cell differentiation [24].

5.2.4 MYOD1 and Core Circadian Clock

A number of studies have explored the link between MYOD1 and circadian genes ARNTL and CLOCK, revealing that ARNTL and CLOCK bind to the core enhancer of the MYOD1 promoter and subsequently induce rhythmic expression of MYOD1 [8]. We found that upon introduction of L-MYOD1, the population of cells exhibits robust synchronization in circadian E-box gene expression. Among these Ebox targets are the PER and CRY gene family, whose protein products are known to repress CLOCK-ARNTL function, thus repressing their own transcription. Additionally, E-box target NR1D1, which is synchronized upon addition of L-MYOD1, competes with ROR proteins to repress ARNTL transcription directly. This adds another gene network connection under MYOD1 influence, indirectly acting to repress ARNTL, leading us to posit that MYOD1 can affect CLOCK-ARNTL function through E-Box elements, in addition to CLOCK-ARNTLs established activation effect on MYOD1. Furthermore, these oscillations dampen post-bifurcation point, after which MYOG entrains the oscillations of a distinct subset of myogenic transcription factors. Therefore, MYOD1-

mediated reprogramming and circadian synchronization are mutually coupled, as is the case in many other studies of the reprogramming of cell fate [298].

Chapter 6

Mechanisms of Circadian Oscillation Reprogramming

6.1 Background

6.1.1 Oscillating Molecular Loops

The first observation is that a transcript (or any other molecular species) cannot oscillate in isolation. What really oscillate are entire loops of interacting molecular species comprising different kinds of interactions such as regulatory (transcriptional), proteinprotein and enzymatic interactions. Oscillatory loops typically contain an odd number of negative interactions. Biological network contain a large number of such directed loops and thus many potential oscillators. For instance, in a network consisting of 21,826 genes/proteins with 120,988 edges (114,493 regulatory edges and 6,495 physical proteinprotein interactions), we found over 3,600 directed loops of size 3 and over 71,100 directed loops of size 4. These numbers are not meant to be precise, as it is well known that there are several sources of

noise in reconstructed biological networks, but they are indicative of the general trends and it is reasonable to estimate that the number of potential oscillators in the cell is in the 105 range.

6.1.2 Periodicity and Evolution

In the complex molecular circuitry of a cell, having many loops, and thus many potential oscillators, does not explain why a large fraction of them would oscillate with a circadian frequency. When a complex physical system with many components is perturbed in many different ways, one does not expect to see each time a different subset of its component oscillating at the same constant frequency, unless this frequency is deeply built-in into the system as a resonant frequency. Indeed, high time resolution circadian data [116] show that most oscillating genes have a period of about 24h, with some genes oscillating at harmonic periods of about 12hours and 8hours. Very short periods (e.g. periodicity of one hour or less) and periods not commensurate with the daynight cycle (e.g. periodicity of 7h) are not observed as they are probably not physiological. The key question then is why so many loops exhibit the same 24-h periodicity? We believe evolution provides the answer to this question as the world is drastically different during the day and the night, for instance in terms of temperature, light, winds and predators. Thus paying attention to these differences is likely to have conferred major survival benefits to the corresponding organisms in the course of evolution. It is important to note that some of the earliest unicellular precursors of current living systems were highly circadian. For example, Cyanobacteria which were present 3.4 billion years ago are highly circadian [299] since they use photosynthesis. Thus circadian oscillations at the molecular level were discovered very early by evolution and subsequently refined and propagated throughout the tree of life over two trillion daynight cycles. Thus evolution has deeply sculpted the relentless circadian rhythm into many of the molecular oscillators present in each cell, so that the circadian frequency is the main resonant

frequency of these networks

6.1.3 Network of Coupled Oscillators

Armed with an understanding or what the oscillators are and why they may have a built-in resonant period of 24h, we can now consider how these oscillators are coupled to each other and how biological systems can manipulate the oscillatory landscape and its couplings to adapt to internal or external perturbations.

Many different biological mechanisms couple these oscillators together, but at the root of the coupling, there is always the sharing of vertices (or even edges or paths) between oscillating loops forming an intricate network of coupled circadian oscillators. The couplings in such a network are likely to be non-linear, heterogeneous and condition specific. Reprogramming at the cellular level (obviously reprogramming occurs at many levels and may involve, for instance hormonal signals triggered by the SCN and cell-to-cell communication within a tissue) occurs by **(i)** suppressing existing molecular interactions thereby breaking loops; **(ii)** enabling new molecular interactions thereby creating new loops or **(iii)** changing the sign of existing molecular interactions thereby modifying the oscillatory behavior of existing loops.

There are several possible non-exclusive mechanisms by which the cell can create, suppress or modify interactions between the different species to rapidly reprogram its oscillatory repertoire. For instance, dynamic changes in the epigenome, like methylation, acetylation and chromatin remodeling can play a central role in selecting the fraction of oscillating species. An epigenetic modification in the promoter of a gene can prevent the expression of a gene permanently, thus suppressing the oscillatory behavior of all the loops containing the corresponding transcript or protein. Removing the modification has the opposite effect. Recent studies have also identified circadian long-range interactions [4] and the role of CLOCK protein as a histone acetyltransferase [60]. Similarly, a post-translational mod-

ification may enable the interaction of two proteins and thus the creation of corresponding loops. Furthermore, nodes or edges associated with many loops act as hubs that can couple and simultaneously influence many other oscillators.

Circadian rhythms are pervasive and play a key role in ensuring homeostatic balance with the environment and coordinating many aspects of physiology including the sleep/wake cycle, eating, hormone and neurotransmitter secretion and even memory and cognitive function [65, 80, 87, 283]. Disruption of circadian rhythms has been directly linked to health problems ranging from cancer, to insulin resistance, to diabetes, to obesity and to premature ageing [9, 80, 138, 156]. Research has shown that these circadian rhythms are genetically encoded by a molecular clock found in nearly every cell, with a master clock located in the suprachiasmatic nucleus (SCN) [200, 237] of the hypothalamus, coordinating and interacting with peripheral clocks throughout the body [283, 324]. Central to the cellular clock and the rhythmicity of SCN neurons as well as other cells are transcription factors that drive the expression of their own negative regulators [219, 257]. This results in a negative transcriptional and translational feedback loop, highly conserved across species, that perpetuates oscillations in gene expression that occur every 24hours. In mammals, two bHLH transcription factors, CLOCK and BMAL1 heterodimerize and bind to conserved E-box sequences in target gene promoters, thus driving the rhythmic expression of mammalian Period (Per1, Per2 and Per3) and Cryptochrome (Cry1 and Cry2) genes [277]. PER and CRY proteins form a complex that inhibits subsequent CLOCKBMAL1-mediated gene expression [27, 57, 219]. In short, the core of the clock is driven by only a dozen genes [321].

In contrast, gene expression experiments [68, 67, 116, 184, 196] reveal that a much larger fraction, on the order of 10%, of all transcripts in the cell are oscillating in a circadian manner and that the oscillating transcripts differ by cell or tissue type [217, 275, 321]. Thus, the number of oscillating transcripts typically extends beyond the core clock. However, the precise extent of this phenomenon, or its applicability to other molecular species such

as metabolites, has not been investigated systematically. While researchers have looked at the common denominator (the master clock genes and its interactors), little has been done to systematically understand the unique and possibly novel oscillations observed in a specific tissue or under a specific set of perturbations. In a recent study [67] where we contrasted the circadian profiles of both transcripts and metabolites in the liver of mice fed normal-chow and high-fat diets, we noticed considerable differences associated with a massive reprogramming occurring within the cell. By analyzing not only the transcripts and metabolites that lost their circadian oscillations as a result of the high-fat diet but also the transcripts and metabolites that gained novel circadian oscillations as a result of the perturbation, we were able to discover compensatory oscillations in important molecular species like SREBP1, a transcription factor responsible for lipid synthesis.

In combination, these results raise several fundamental questions [223]. Exactly how pervasive are circadian oscillations at the molecular level, i.e. how far do they extend beyond the core clock? What is the overlap in circadian oscillations across different tissues and conditions? How flexible and programmable are these oscillations and what are the underlying mechanisms controlling rhythmicity? To begin to address these questions, we conduct a large-scale aggregated analysis of multiple circadian transcriptome and metabolome datasets.

6.1.4 Effects of Perturbation

We observe that genetic or environmental perturbations tend to disrupt circadian oscillations in given system in several ways. As expected, such perturbations can:

1. Change the amplitude of pre-existing circadian oscillations for some of the molecular species;

2. Change the phase of pre-existing circadian oscillations for some of the molecular species;

3. Disrupt or even suppress the pre-existing oscillations of some of the molecular species.

Indeed, experiments involving genetic knockouts, diet changes or even simply different mice strains, show these effects. For instance, when comparing gene expression in liver tissue from Clock mutant and wild-type mice [196], about 1160 genes show a loss of circadian rhythmicity. However, about 400 genes oscillate in both conditions but with a difference in amplitude or phase. Similarly, when comparing gene expression and metabolite levels in liver tissue from 10-week high-fat-fed versus normal-chow-fed mice [67], about 2200 genes and about 40 measured metabolites show a loss of circadian rhythmicity, whereas about 1520 genes and about 60 measured metabolites oscillate in both conditions, but with a difference in amplitude or phase.

6.2 Importance of the Core Circadian Clock

Molecular hubs associated with highly connected species usually affect many oscillating loops and are capable of setting up cascades of changes in amplitude, phase and oscillatory behavior. An example is provided by nicotinamide adenine dinucleotide+, a metabolite that participates in many reactions and plays a central role in regulating circadian rhythms [206, 227, 238]. Not surprisingly, transcription factors also tend to behave like hubs, and the clock itself behaves as a central hub intersecting many loops and helping cellular reprogramming and the selection of a significant fraction of which loops actually oscillate under a given set of internal and external conditions.

In particular, the main transcription factors in the clock, Clock and Bmal1, are densely connected. They are known to bind to a single or pair of E-box sites. E-box sites are short (canonical sequence CACGTG) and frequent in the genome. With a stringent Bayesian Branch Length Score [315, 48] greater than 1, we found over 23800 conserved E-box sites

in the mouse genome using MotifMap several of which are in the promoters of transcription factors. Using time-resolved ChIP-seq data for BMAL1, Rey etal. (2011) identified 2049 E-box binding sites in mouse liver. Among these, about 60% (1319) showed a rhythmic binding of BMAL1 and 13% of all BMAL1 sites had a pair of E-box elements with spacers of 67 base pairs. Thus, in a given environment, cells can reveal or hide a fraction of E-box sites thereby controlling which loops are directly, or indirectly, affected and possibly entrained by Clock and Bmal1.

To further understand the factors that confer to the cell its circadian reprogramming capabilities, we analyzed the role of the core clock genes in the context of the underlying global molecular network. Using a network with regulatory and proteinprotein interaction edges, we calculated the distance of all nodes from Clock or Bmal1 and also the total number of directed loops that contain Clock or Bmal1. We found that about 10% of genes are one hop away and about 6070% genes are two hops away from Clock or Bmal1. In addition, about 10% of genes are connected to Clock or Bmal1 through a directed loop of size 6 or less. In short, in this network of coupled oscillators, Clock and Bmal1 form a central hub coupling and modulating many other circadian oscillators

6.3 Developing a Model of Transcriptional Organization

To identify a model of organization for transcriptomic circadian oscillations, we perform a series of analyses of increasing sophistication using novel computation metrics. To achieve robustness and overcome noise in the data and incomplete knowledge, we present results obtained consistently at different statistical threshold as well as results that are supported by multiple lines of evidence. In total, 87 datasets from mouse were used to generate each

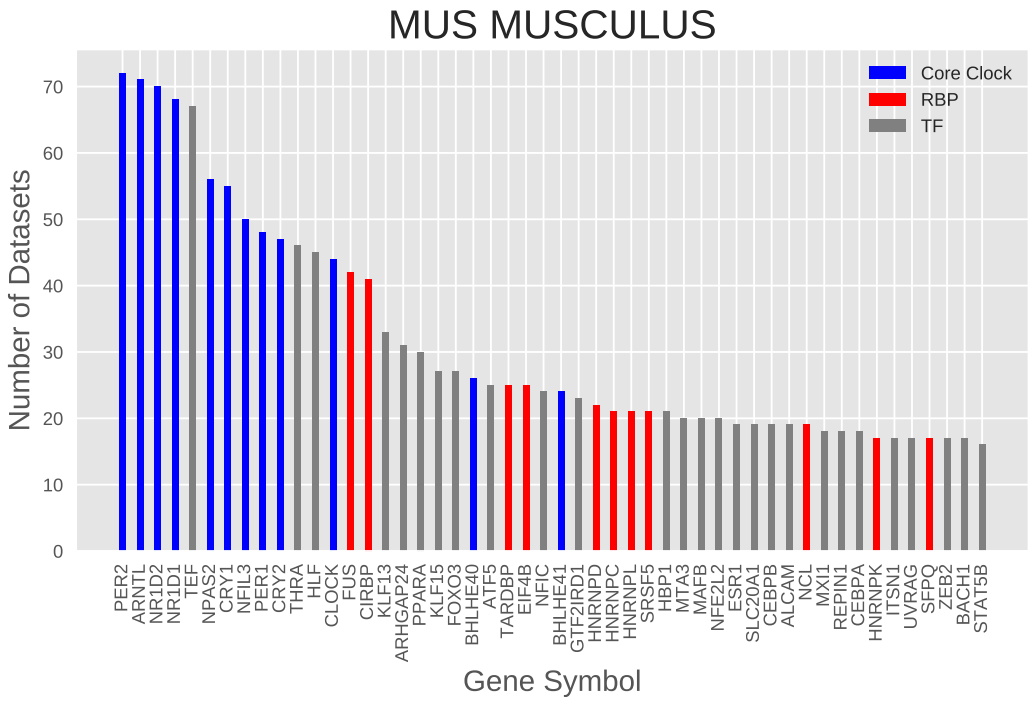

Figure 6.1: Most Frequent Oscillating TFs and RBPs

set of results. The most represented tissues are liver (37 datasets), skin (14 datasets) and brain (13 datasets). Aggregated results as well as tissue specific results were generated.

6.3.1 Frequency Analysis

The frequency at which a TF or RBP is found to oscillate in a collection of datasets provides a simple metric for estimating its consistency in circadian oscillation. 6.1 illustrates this frequency distribution for mouse at a BIO_CYCLE p-value < 0.01. Additionally, 64 datasets from Papio anubis (baboon) were used for comparison to validate the methods. Both analyses show that TFs involved in the circadian core clock are found to be the most frequently oscillating. This purely data-driven approach automatically discovers the circadian core clock. Furthermore, it identifies additional TFs and RBPs that must play an important role in circadian oscillation.

Transcript frequency is defined as the total number of datasets where a given protein coding transcript is found to be oscillating at a BIO_CYCLE predicted p-value < 0.01. Protein-coding transcripts were identified from BioMart ENSEMBL gene database [269].

6.3.2 Regulation Analysis

Measuring the circadian regulatory influence of the TFs and RBPs identified in the previous analysis requires further investigation using more sophisticated computational methods. To this end, a novel computational method was used to identify and score directed regulatory edges in oscillating loops. The Circadian Regulatory Control (CRC) method can be understood as a proxy for circadian regulation between a TF or RBP (source) and a transcript (target). There are three major components of the CRC method. First, as a prerequisite, the source and target must be oscillating, as assessed by BIO_CYCLE. Second, the source must have at least one high quality binding site on the target for transcriptional or post-transcriptional regulation, as assessed by MotifMap and MotifMap-RNA [315, 48, 174]. For a TF, binding sites were assessed at the promoter region of the target transcript. For an RBP, binding sites were assessed at the introns or UTRs of the target transcript. Third, there must be a correlative relationship between the phases of the source and the target. Recent studies have shown a significant lag between the transcript expression and the concentration of the corresponding protein [246]. We addressed this issue by computing and modeling the distribution of this lag, using transcriptomic and proteomic datasets produced from the same study on CircadiOmics (Methods 4.2).

After filtering on p-value for the first criteria, the remaining two criteria were combined into two different CRC scores. The *B-score* is a binary indicator of circadian regulation at various filtering thresholds for the number of high quality binding sites and the likelihood of phase correlation. The *E-score* is an exponentially weighted combination of these two criteria. In

Mouse All (n=81)		
TF/RBP	All Score	All Ranking
FUS	8.83	9
THRA	8.44	10
BHLHE40	8.30	11
NFIC	8.09	12
HNRPDL	7.56	15
CIRBP	7.42	16
MXI1	7.35	17
EIF4B	7.34	18
CEBPB	6.65	20
HNRNPK	5.61	21
TARDBP	5.40	22
KLF13	4.75	23
PPARA	4.73	24
FOXO3	4.64	25
RAD21	4.56	26
KHDRBS1	4.38	27
ALCAM	4.30	28
MTA3	4.25	29
ARHGAP24	4.23	30
YY1	4.22	31
HNRNPL	4.15	32
NFYA	4.14	33
MAFK	4.12	34
KLF15	4.12	35
PCBP4	4.06	36
HNRNPC	4.06	37
ESR1	4.00	38
SREBF2	3.92	39
BACH1	3.77	40

Mouse Brain (n=13)		
TF/RBP	Brain Score	Brain Rank
CIRBP	1.54	2
SFPQ	1.20	6
KLF15	0.96	8
FUS	0.94	9
ZC3H11A	0.88	10
MXI1	0.86	11
RBM28	0.81	14
EGR1	0.75	15
CHD1	0.71	16
CREB1	0.71	17
HIF1A	0.67	18
HNRPDL	0.66	19
CEBPG	0.65	20
BHLHE40	0.64	21
HNRNPK	0.63	22
SP2	0.63	23
RAD21	0.62	24
NFE2L2	0.60	25
EGR2	0.59	26
GTF2I	0.58	28
KLF12	0.58	29
HCFC1	0.58	30
CHD2	0.57	31
GTF2F1	0.56	32
SRPR	0.54	33
CEBPD	0.53	34
ETV1	0.49	35
GABPA	0.49	36
A1CF	0.49	37

Mouse Skin (n=14)		
TF/RBP	Skin Score	Skin Rank
NFIC	3.44	6
E2F1	2.68	7
MXI1	2.34	10
RUNX1	1.59	13
BRCA1	1.55	14
TCF4	1.46	15
HCFC1	1.41	16
MEF2A	1.32	17
ETV5	1.27	18
THRA	1.17	19
CHD1	1.16	20
FOXM1	1.12	21
NFATC1	1.12	22
FUS	1.12	23
ALCAM	1.11	24
HNRPDL	1.08	25
NFYA	1.03	26
ZFP161	1.00	27
CHD2	0.98	28
RBM5	0.97	29
TCF12	0.95	30
SREBF2	0.94	31
KHDRBS1	0.91	32
EIF4B	0.87	33
KLF13	0.85	34
ELK4	0.85	35
RFX5	0.83	36
SF1	0.81	37
ELAVL1	0.79	38

Mouse Liver (n=31)		
TF/RBP	Liver Score	Liver Rank
CEBPB	4.25	4
BHLHE40	4.22	5
FUS	3.92	7
HNRNPK	3.58	10
EIF4B	3.51	12
PCBP4	3.45	14
THRA	3.30	15
MXI1	2.83	18
YY1	2.80	19
MAFK	2.79	20
ATF5	2.75	21
MTA3	2.75	22
PPARA	2.63	23
BACH1	2.59	24
RXRA	2.58	25
ESR1	2.57	26
RFX4	2.54	27
HNRPDL	2.53	28
FOXO3	2.52	29
CIRBP	2.52	30
STAT5B	2.49	31
CRP	2.43	32
TARDBP	2.37	33
HNRNPC	2.35	34
ARHGAP24	2.33	35
DCTN2	2.28	36
NFIC	2.27	37
KLF1	2.25	38
USF2	2.25	39

Figure 6.2: Tables showing the ranking of circadian TFs and RBPs by CRC E-score in different tissue types. The leftmost table shows ranking in mouse transcriptome across all datasets. RBPs are labeled in red, while TFs are labeled in black. Core clock TFs have been removed from the listing.

general, results generated using both scores tend to agree. However, *B-score*, as a binary indicator, is more convenient for large scale analysis of graph structures. In contrast, *E-score*, as a real valued metric, has more sensitivity and is used for ranking nodes and edges. For each source TF or RBP, a CRC score was computed by aggregating all the CRC E-scores from all its outgoing edges either in all experiments or in tissue-specific experiments. The highest scoring TFs and RBPs are shown in Table 6.2.

When looking at aggregated results, core clock TFs such as CLOCK and BMAL1 were found to have the largest scores, a finding consistent with both the frequency of oscillation and previous literature [297]. Extended members of the core clock were also identified in the ranking including THRA and BHLHE40 [275, 166].

In the results across all datasets, additional TFs and RBPs were identified that seem to have a much broader regulatory role than what is reported in the literature. For instance,

FUS and CIRBP have been reported to affect the core circadian factor PER2 via alternative splicing, but only in the mouse liver [150, 201, 213]. In contrast, we find that FUS and CIRBP are found to be high scoring also in both brain and skin. EIF4B has been identified in the circadian regulation of translation in mouse liver [125]. We find that EIF4B is also top scoring in skin. HNRPDL is listed as a potential target of circadian regulation via microRNA in the brain [41]. Strikingly, these RBPs and TFs are found to have very high CRC scores across all mouse datasets. This suggest that they play a broader, previously uncharacterized role in circadian regulation.

When looking at tissue specific results, many additional TFs and RBPs with high CRC scores are discovered. Although literature evidence has shown that these factors interact with circadian pathways, they are not known to be regulators of oscillation. These TFs may explain tissue specific circadian reprogramming. Within brain tissue, SFPQ is functionally involved in the cell cycle pathway, which also includes NONO and PER2 [92]. EGR1 has been found to oscillate and regulated by the core clock [162]. Within our results, EGR1 potentially regulates a large number of downstream transcripts in the brain. CHD1 is known to be involved in circadian chromatin remodeling in brain [19]. KLF15 is well known to be regulated by the peripheral clock in relation to circadian nitrogen homeostatis in liver and muscle [123]. Within skin tissue, RUNX is a top TF and is known to be regulated in a circadian fashion in epidermal cells [122]. E2F1 is regulated by circadian factors SIRT1 and CLOCK[205]. BRCA1 is known to interact with core clock TFs such as PER2 [314]. Within liver tissue, CEBPB is top ranking excluding core clock TFs. This agrees with the literature finding that it interacts with the core clock through REV-ERB [115]. PCBP4 is known to be involved in circadian alternative splicing in the liver [189].

Additionally, there are many other novel findings that have been linked to very few circadian studies. These findings include: NFIC, RAD21, MXI1, and TARDBP across all tissues; ZC3H11A, RBM28, and CEBPG in brain; HCFC1 and ETV5 in skin; and HNRNPK, ATF5,

and BACH1/MAFK in liver, and may provide leads for investigations of previously unknown circadian regulatory mechanisms.

While these results have focused on individual TFs and RBPs, the identification of a model of transcriptomic organization requires a global view of circadian regulation. Using the CRC method, we introduce the concept of a CRC graph. A CRC graph is a directed weighted graph where nodes are defined as oscillating transcripts and edges are defined by a CRC *B-Score* or *E-Score*. A dataset CRC graph was built for each of the 87 mouse datasets separately. Additionally, a single aggregate graph was generated from the superimposition of all individual dataset CRC graphs. Analysis of the CRC graphs explores the regulatory relationship between oscillating transcripts within the network of coupled circadian oscillators.

The Circadian Regulation Control method is a measure of circadian regulation from a source TF/RBP to a target transcript, consisting of three components of evidence. First, both the source and the target are predicted to be oscillatory by BIO_CYCLE [3] with p$\leq$ 0.01. Second, if the source is a TF, there exist at least one high quality binding site ($BBLS \geq 1, NLOD \geq 0.9$ and $FDR \leq 0.25$) in the promoter region of the targeted (defined as -5,000 to +500 bp to the TSS) predicted by MotifMap [315, 48]. For RBP sources, there are high quality binding sites ($BBLS \geq 1, NLOD \geq 0.9$) predicted by MotifMap-RNA [174] in the introns or UTRs of target transcript. In both cases, the number of high quality binding sites is aggregated for each individual regulatory edge per dataset. Third, the lag between the expression phases of the source and the target is used to assess the degree of phase matching. The distribution of experimental lag between the transcript and the protein product of 2,400 genes [50] was modeled as a beta distribution with $\mu = 0.35, SD = 0.25$. Given a lag between any circadian source and target, we estimate the likelihood of positive or inverse phase-correlation. In particular, the highest probability density interval (HPD) of the given lag is calculated with respect to the mode of the beta distribution, which is a

value between 0 and 1 (exactly at the mode).

Furthermore, the values of these two components are summarized in two ways. First, a binary score, *B-score*, was calculated by imposing a specific threshold for each values. We use a threshold of binding sites ≥ 1 and an $HPD \geq 0.8$, which corresponds to 2-6 hourrs. Second, an exponentially weighted score, *E-score*, is defined as $E = 0.5 * HPD - 0.5 * exp(-NumberOfBindingSites)$. This score was shown in empirical testing to produce reasonable rankings between core clock TFs and was used for ranking TFs and RBPs.

6.3.3 Correlation Analysis

While previous analysis was performed on nodes on a CRC graph, to further understand the organization of circadian transcripts, it is necessary to study the regulatory edges. We reduced the complexity of this analysis by focusing on the regulatory edges between TFs and RBPs, which form a subgraph of the whole CRC graph.

A correlation analysis was performed using CRC E-scores associated with these edges. An edge score matrix was constructed using the sum of CRC scores for all edges between interacting TFs and RBPs in the aggregated CRC graph. The results compiled from all mouse datasets are shown in Figure 6.3. The heatmap demonstrates strong correlation within core clock TFs, as well as between the core clock and other top CRC scoring TFs and RBPs such as FUS and CIRBP. Figure 6.3 B lists some of the top interactions. Many of the findings are consistent with literature.

However, some top interactions are relatively unseen in circadian literature, such as the potential regulation of PER2 by NFIX, or TEF by NFYA and RXRA. These novel interactions may be important in circadian regulation. Overall, correlation analysis shows that most of the top circadian regulation between factors centers around the core clock. However, the

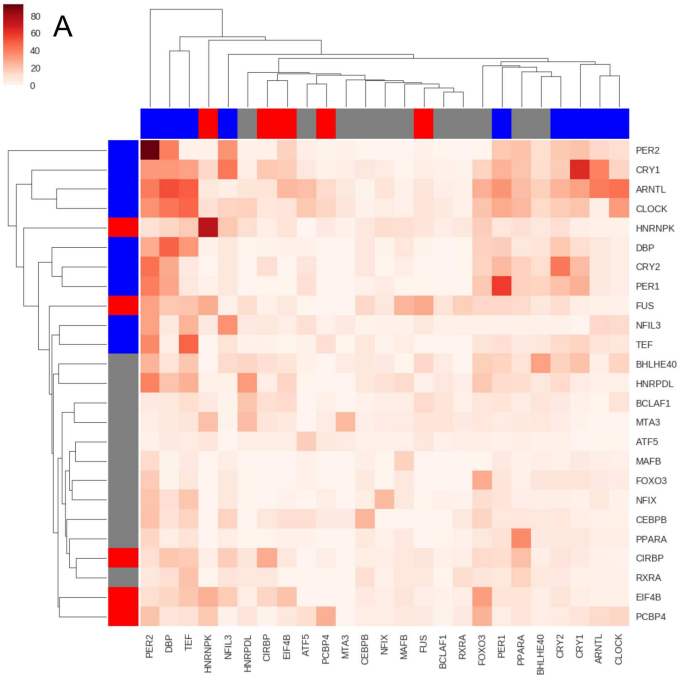

B

Regulation	Mouse Score	Ranking	Type
FUS->PER2	29.49	19	RBP->Core Clock TF
ARNTL->NFIC	24.13	28	Core Clock TF->TF
BHLHE40->PER2	23.64	29	TF->Core Clock TF
ARNTL->FOXO3	22.41	31	Core Clock TF->TF
NFIX->PER2	21.03	36	TF->Core Clock TF
MXI1->PER2	20.54	37	TF->Core Clock TF
CEBPB->PER2	17.59	48	TF->Core Clock TF
NFYA->TEF	17.42	50	TF->Core Clock TF
ARNTL->KLF13	16.61	52	Core Clock TF->TF
ARNTL->BHLHE41	15.91	53	Core Clock TF->TF
KLF15->ARNTL	15.59	55	TF->Core Clock TF
RXRA->TEF	15.37	56	TF->Core Clock TF
ARNTL->KLF15	14.84	60	Core Clock TF->TF
PER2->KLF15	14.76	61	Core Clock TF->TF
ARNTL->NCL	14.67	62	Core Clock TF->RBP
NFYA->ARNTL	14.63	63	TF->Core Clock TF
PER1->FOXO3	14.52	64	Core Clock TF->TF
ARNTL->BHLHE40	14.52	65	Core Clock TF->TF
REPIN1->TEF	14.09	66	TF->Core Clock TF
ARNTL->SLC20A1	13.94	68	Core Clock TF->TF
USF2->TEF	11.65	72	TF->Core Clock TF
ARNTL->XBP1	11.29	73	Core Clock TF->TF
CEBPB->NFIL3	10.63	74	TF->Core Clock TF
PER1->KLF15	9.40	75	Core Clock TF->TF
ARNTL->UVRAG	9.39	76	Core Clock TF->TF
CRY1->REPIN1	9.34	77	Core Clock TF->TF
NFYA->PER2	9.30	78	TF->Core Clock TF
ARNTL->MAFK	8.58	79	Core Clock TF->TF
BHLHE41->CRY1	8.55	80	TF->Core Clock TF

Figure 6.3: Correlation analysis. **(A)** Edge Score Heatmap of inter-regulator (TF/RBP) circadian CRC score (E-score aggregates) in mouse with hierarchical clustering. The score is calculated by aggregating CRC scores from the directed edges starting from row TF/RBP to the column TF/RBP across all datasets. Stronger colors in the heatmap indicate higher total scores (normalized for visualization). Color on row and column indicates the type of regulators: blue indicates core clock TF, red indicates RBP and gray indicates regular TF. There is a strong cluster of core circadian TFs and RBPs (e.g. CIRBP, FUS). **(B)** Ranking of top regulations between TFs and RBPs. Regulations between core clock TFs have been omitted.

core clock only strongly interacts with a relatively small set of TFs.

For each dataset, the CRC score between a source TF or RBP and all its possible targets, as quantified by E-score, are aggregated across all outgoing edges. Total results from all 87 mouse datasets are organized by tissue type (e.g. all, liver, brain, skin).

Regulatory correlation results are derived from a subgraph of the total CRC graph, where only regulatory edges between TF and RBPs are included. Similarly, results from different datasets are combined by aggregating the scores from individual datasets. Partial results derived from E-scores are shown in 6.3.

6.3.4 CRC Graph

The CRC graph can be seen as representation of the structure of circadian transcriptomic regulation based on the evidence presented in previous results. Here we analyze this representation by combining results from both nodes and regulatory edges. The following results were generated from both individual dataset CRC graphs and the aggregate CRC graph. The CRC *B-score* was used in place of a weighted *E-score* to discretely determine the presence of a regulatory edge.

Regulatory distance was computed as the length of the shortest directed path in the CRC graph between a source TF or RBP and a target transcript. The set of oscillating transcripts that are found to have a regulatory distance-one from the core clock were considered to be directly regulated by the core clock. The mean percentage of distance-one transcripts across all dataset CRC graphs is roughly 35%. While the majority of transcripts are not found to be directly regulated by the core clock, almost any transcript can be connected through a regulatory path in the CRC graph to the core clock. On average, greater than 80% of oscillating transcripts in a dataset CRC graph can be connected within distance-three from

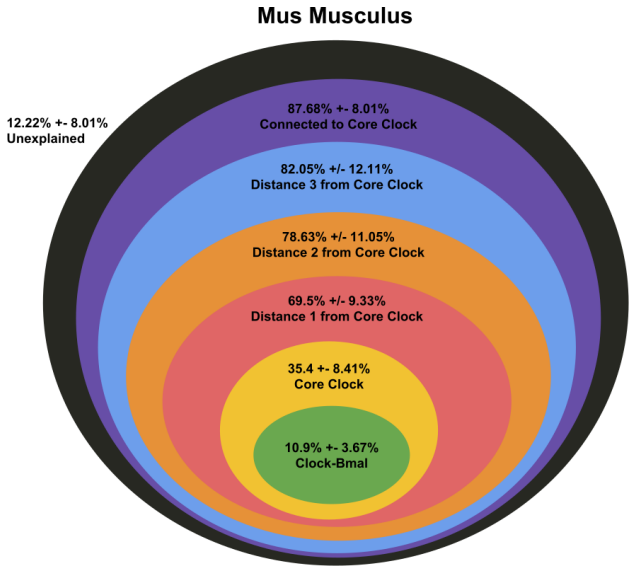

Figure 6.4: Mean percentages of transcriptome explained by TF/RBP at fixed regulatory distances from the core clock across mouse datasets.

the core clock. The mean percentage of oscillating transcripts found at increasing regulatory distances across all mouse datasets is shown in 6.4.

Within a dataset CRC graph, each oscillating TF or RBP has an average branching factor of nine. This large branching factor has an important implication in the global set of oscillating transcripts found in any experiment. Perturbations in TFs and RBPs can potentially be amplified to changes in over 700 transcripts over a regulatory distance-two. Regulatory feedback that is known to exist within the core circadian clock can be identified within most dataset CRC graphs. For the set of TFs or RBPs at regulatory distance-one or greater, feedback exists between transcripts at the same regulatory distance and between transcripts at lower regulatory distances. This feedback, on average, only extends backwards a single regulatory step. In this way, the CRC graph can be seen as a cascading hierarchy of oscillating regulatory loops.

Functional enrichment by Gene Ontology (GO) term was performed on the subset of transcripts found at each regulatory distance. Transcripts found at regulatory distance-1 from

the core clock exhibited significant enrichment for terms related to Circadian Rhythms, Cell Cycle, Metabolic Processes, and Neuronal Processes. The sets of transcription factors found at this distance were grouped into these broad functional categories including the set of known RBPs. These functional related TFs and RBPs are found to regulate a much larger set of downstream transcripts at increasing regulatory distances, which are not directly regulated by the core clock. TFs and RBPs with larger regulatory distances correlate strongly with decreasing CRC scores (Supplementary Table 2). To observe the significant shifts in the set of oscillating transcripts found in reprogramming events, a perturbation must occur in the expression of TFs and RBPs with small regulatory distances and, consequently, a high CRC score. Perturbations affecting low CRC scoring TFs and RBPs at large regulatory distances can only induce changes in proportionally smaller sets of oscillating transcripts. Therefore, it is reasonable to conclude that experimental conditions that relate to changes in metabolism, neuron function, cell cycle and development, or RBP modification likely instigate large reprogramming events through perturbations found in distance-one TFs or RBPs.

CRC Graphs are constructed for each of the 87 mouse datasets. Nodes are defined as oscillating transcripts using a threshold BIO_CYCLE p-value ≤ 0.01. Edges with a CRC *B-score* $= 1$ are included. The shortest path length, used to define regulatory distance, between a TF and RBP and a target transcript and the average branching factor for each TF and RBP was computed by https://networkx.github.io/. Results for mouse liver, skin, and brain tissue are provided in Supplementary Table 4. GO enrichment analysis and functional annotation for transcripts found at each distance was completed using the Python library https://github.com/tanghaibao/goatools using NCBI gene to GO term associations. The enrichment results provided in Supplementary Table 1 were performed at an adjusted p-value ≤ 0.01.

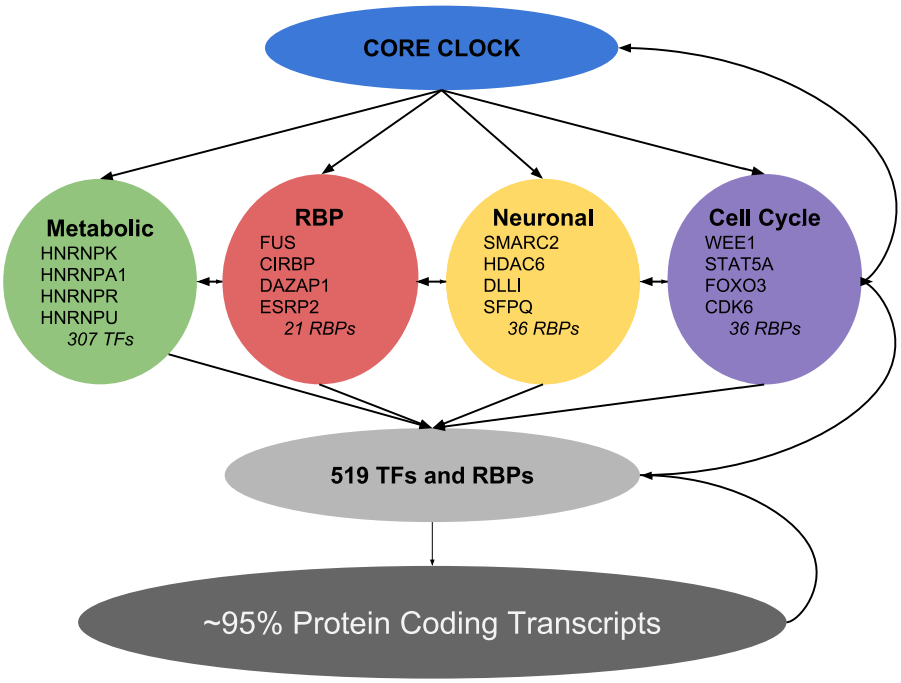

Figure 6.5: Network view of TFs and RBPs that are found at regulatory distance = 0. These TFs predominantly fall into three broad categories labeled from GO annotations that includes *Cell Cycle*, *Neuronal Function*, and *Metabolic Process*.

6.3.5 Interpretation

The question of how specific subsets of oscillators are selected under specific genetic, epigenetic, and environmental conditions has remained an open question in the study of circadian rhythms. An organizational model that allows this selection within the network of coupled oscillators must exist on a spectrum from centralized organization orchestrated by the core circadian clock and to complete self-organization through the competition of many circadian oscillating loops. In order to determine where in this spectrum the network of coupled oscillators operates, we obtained results using the CRC method and CRC graph with the large collection of mouse transcriptomic data available on CircadiOmics. To begin, we analyzed the frequency of all oscillating transcripts. With no prior information, this method identifies TFs known to be components in the core circadian clock including CLOCK, BMAL1, CRY1/2, PER1/2, NRD1D1/2, and DBP. This result was again reproduced using 64 transcriptomic datasets from baboon tissues. Finally, many TFs and RBPs that must be important circadian regulators are identified in both this analysis and subsequent analyses.

We formulated the Circadian Regulatory Control (CRC) method for identification of regulatory edges in circadian feedback loops. Two CRC scores, *B-Score* and *E-score*, incorporate multiple sources of evidence including statistical significant of transcript oscillation and high quality predicted binding sites. These scores further take into account the delay between transcript and protein abundance using available proteomic datasets included in CircadiOmics. CRC scores provide evidence for circadian regulation from a TF or RBP to a specific target. Additionally, an aggregated score provides a measure of the regulatory influence of a TF or RBP by combining the scores of all outgoing edges. Using aggregated CRC scores, we conducted a robust quantitative analysis of the most influential circadian TFs and RBPs across all 87 mouse datasets. These results identified multiple TFs and RBPs important to circadian regulation that were corroborated by literature evidence. Furthermore, we identified multiple novel circadian TFs and RBPs with limited evidence for circadian

regulation.

Using the CRC method, we introduced the concept of the CRC graph as a directed weighted graph where nodes are oscillating transcripts and regulatory edges are measured by CRC scores. We constructed CRC graphs from both single experimental datasets and the total collection of 87 mouse datasets. We studied the correlation between top TFs and RBPs using aggregated edge scores. We observed that the most influential TFs and RBPs interact with the core circadian clock. However, the core clock directly regulates a relatively small set of TFs and RBPs. This finding hints at a hierarchical organization of circadian regulation centering around the core clock, where regulation can occur through steps represented as edges in the CRC graph.

Oscillating transcripts within the aggregated CRC graph were separated by regulatory distances from the core circadian clock. At some regulatory distance, over 95% of all oscillating protein coding transcripts can be connected to the core clock. Functional annotation by GO terms reveals that at a regulatory distance-one, TFs can be grouped together into three categories: Cell Cycle, Metabolic Process, and Neuronal Function. These sets, along with the set of RBPs found at distance-one, are functionally related and highly influential circadian regulators of a large collection of downstream oscillating transcripts. We conclude that reprogramming events,, where the core circadian clock continues to oscillate, must originate from perturbations of expression in these TFs and RBPs.

Bibliography

[1] V. A. Acosta-Rodríguez, M. H. de Groot, F. Rijo-Ferreira, C. B. Green, and J. S. Takahashi. Mice under caloric restriction self-impose a temporal restriction of food intake as revealed by an automated feeder system. *Cell metabolism*, 26(1):267–277, 2017.

[2] Y. Adamovich, L. Rousso-Noori, Z. Zwighaft, A. Neufeld-Cohen, M. Golik, J. Kraut-Cohen, M. Wang, X. Han, and G. Asher. Circadian clocks and feeding time regulate the oscillations and levels of hepatic triglycerides. *Cell metabolism*, 19(2):319–330, 2014.

[3] F. Agostinelli, N. Ceglia, B. Shahbaba, P. Sassone-Corsi, and P. Baldi. What time is it? Deep learning approaches for circadian rhythms. *Bioinformatics*, 32(12):i8–i17, 2016. [PubMed:27307647] [PubMed Central:PMC4908327] [doi:10.1093/bioinformatics/btw243].

[4] L. Aguilar-Arnal and P. Sassone-Corsi. The circadian epigenome: how metabolism talks to chromatin remodeling. *Current opinion in cell biology*, 25(2):170–176, 2013.

[5] M. Ahmadian, J. M. Suh, N. Hah, C. Liddle, A. R. Atkins, M. Downes, and R. M. Evans. Pparγ signaling and metabolism: the good, the bad and the future. *Nature medicine*, 19(5):557, 2013.

[6] B. N. Albaugh, K. M. Arnold, and J. M. Denu. Kat (ching) metabolism by the tail: insight into the links between lysine acetyltransferases and metabolism. *Chembiochem*, 12(2):290–298, 2011.

[7] J. Alvarez, A. Hansen, T. Ord, P. Bebas, P. E. Chappell, J. M. Giebultowicz, C. Williams, S. Moss, and A. Sehgal. The circadian clock protein bmal1 is necessary for fertility and proper testosterone production in mice. *Journal of biological rhythms*, 23(1):26–36, 2008.

[8] J. L. Andrews, X. Zhang, J. J. McCarthy, E. L. McDearmon, T. A. Hornberger, B. Russell, K. S. Campbell, S. Arbogast, M. B. Reid, J. R. Walker, et al. Clock and bmal1 regulate myod and are necessary for maintenance of skeletal muscle phenotype and function. *Proceedings of the National Academy of Sciences*, page 201014523, 2010.

[9] L. Antunes, R. Levandovski, G. Dantas, W. Caumo, and M. Hidalgo. Obesity and shift work: chronobiological aspects. *Nutrition research reviews*, 23(1):155–168, 2010.

[10] L. d. C. Antunes, M. N. d. Jornada, L. Ramalho, and M. P. L. Hidalgo. Correlation of shift work and waist circumference, body mass index, chronotype and depressive symptoms. *Arquivos Brasileiros de Endocrinologia & Metabologia*, 54(7):652–656, 2010.

[11] D. M. Arble, J. Bass, A. D. Laposky, M. H. Vitaterna, and F. W. Turek. Circadian timing of food intake contributes to weight gain. *Obesity*, 17(11):2100–2102, 2009.

[12] G. Asher, D. Gatfield, M. Stratmann, H. Reinke, C. Dibner, F. Kreppel, R. Mostoslavsky, F. W. Alt, and U. Schibler. Sirt1 regulates circadian clock gene expression through per2 deacetylation. *Cell*, 134(2):317–328, 2008.

[13] G. Asher and P. Sassone-Corsi. Time for food: The intimate interplay between nutrition, metabolism, and the circadian clock. *Cell*, 161(1):84–92, 2015. [PubMed:25815987] [doi:10.1016/j.cell.2015.03.015].

[14] A. Azzi, R. Dallmann, A. Casserly, H. Rehrauer, A. Patrignani, B. Maier, A. Kramer, and S. A. Brown. Circadian behavior is light-reprogrammed by plastic DNA methylation. *Nature Neuroscience*, 17(3):377–382, 2014. [PubMed:24531307] [doi:10.1038/nn.3651].

[15] P. Baldi, S. Brunak, Y. Chauvin, C. A. Andersen, and H. Nielsen. Assessing the accuracy of prediction algorithms for classification: an overview. *Bioinformatics*, 16(5):412–424, 2000.

[16] P. Baldi and P. J. Sadowski. Understanding dropout. In *Advances in neural information processing systems*, pages 2814–2822, 2013.

[17] L. Baroncelli, M. C. Cenni, R. Melani, G. Deidda, S. Landi, R. Narducci, L. Cancedda, L. Maffei, and N. Berardi. Early igf-1 primes visual cortex maturation and accelerates developmental switch between nkcc1 and kcc2 chloride transporters in enriched animals. *Neuropharmacology*, 113:167–177, 2017.

[18] J. Bass. Circadian topology of metabolism. *Nature*, 491(7424):348–356, 2012. [PubMed:23151577] [doi:10.1038/nature11704].

[19] W. J. Belden, Z. A. Lewis, E. U. Selker, J. J. Loros, and J. C. Dunlap. Chd1 remodels chromatin and influences transient dna methylation at the clock gene frequency. *PLoS genetics*, 7(7):e1002166, 2011.

[20] D. Bell-Pedersen, V. M. Cassone, D. J. Earnest, S. S. Golden, P. E. Hardin, T. L. Thomas, and M. J. Zoran. Circadian rhythms from multiple oscillators: lessons from diverse organisms. *Nature Reviews Genetics*, 6(7):544, 2005.

[21] M. M. Bellet, E. Deriu, J. Z. Liu, B. Grimaldi, C. Blaschitz, M. Zeller, R. A. Edwards, S. Sahar, S. Dandekar, P. Baldi, et al. Circadian clock regulates the host response to salmonella. *Proceedings of the National Academy of Sciences*, 110(24):9897–9902, 2013.

[22] D. L. Bentley. Coupling mrna processing with transcription in time and space. *Nature Reviews Genetics*, 15(3):163, 2014.

[23] B. Bhaumik and N. P. Shah. Development and matching of binocular orientation preference in mouse v1. *Frontiers in systems neuroscience*, 8:128, 2014.

[24] M. Böck, J. Hinley, C. Schmitt, T. Wahlicht, S. Kramer, and J. Southgate. Identification of elf3 as an early transcriptional regulator of human urothelium. *Developmental biology*, 386(2):321–330, 2014.

[25] S. Brandhorst, I. Y. Choi, M. Wei, C. W. Cheng, S. Sedrakyan, G. Navarrete, L. Dubeau, L. P. Yap, R. Park, M. Vinciguerra, et al. A periodic diet that mimics fasting promotes multi-system regeneration, enhanced cognitive performance, and healthspan. *Cell metabolism*, 22(1):86–99, 2015.

[26] J. J. Brault and R. L. Terjung. Purine salvage to adenine nucleotides in different skeletal muscle fiber types. *Journal of Applied Physiology*, 91(1):231–238, 2001.

[27] S. A. Brown, E. Kowalska, and R. Dallmann. (re) inventing the circadian feedback loop. *Developmental cell*, 22(3):477–487, 2012.

[28] S. A. Buffington, W. Huang, and M. Costa-Mattioli. Translational control in synaptic plasticity and cognitive dysfunction. *Annual review of neuroscience*, 37:17–38, 2014.

[29] A. Bugge, D. Feng, L. J. Everett, E. R. Briggs, S. E. Mullican, F. Wang, J. Jager, and M. A. Lazar. Rev-erbα and rev-erbβ coordinately protect the circadian clock and normal metabolic function. *Genes & development*, 26(7):657–667, 2012.

[30] L. Cai, B. M. Sutter, B. Li, and B. P. Tu. Acetyl-coa induces cell growth and proliferation by promoting the acetylation of histones at growth genes. *Molecular cell*, 42(4):426–437, 2011.

[31] L. Canaple, J. Rambaud, O. Dkhissi-Benyahya, B. Rayet, N. S. Tan, L. Michalik, F. Delaunay, W. Wahli, and V. Laudet. Reciprocal regulation of brain and muscle arnt-like protein 1 and peroxisome proliferator-activated receptor α defines a novel positive feedback loop in the rodent liver circadian clock. *Molecular Endocrinology*, 20(8):1715–1727, 2006.

[32] L. Cancedda, E. Putignano, A. Sale, A. Viegi, N. Berardi, and L. Maffei. Acceleration of visual system development by environmental enrichment. *Journal of Neuroscience*, 24(20):4840–4848, 2004.

[33] C. Cantó, L. Q. Jiang, A. S. Deshmukh, C. Mataki, A. Coste, M. Lagouge, J. R. Zierath, and J. Auwerx. Interdependence of ampk and sirt1 for metabolic adaptation to fasting and exercise in skeletal muscle. *Cell metabolism*, 11(3):213–219, 2010.

[34] N. Ceglia, Y. Liu, S. Chen, F. Agostinelli, K. Eckel-Mahan, P. Sassone-Corsi, and P. F. Baldi. Circadiomics: Circadian omic web portal. *Nucleic Acid Research*, 2018.

[35] Y. Cen, D. Y Youn, and A. A Sauve. Advances in characterization of human sirtuin isoforms: chemistries, targets and therapeutic applications. *Current medicinal chemistry*, 18(13):1919–1935, 2011.

[36] A. Chaix, A. Zarrinpar, P. Miu, and S. Panda. Time-restricted feeding is a preventative and therapeutic intervention against diverse nutritional challenges. *Cell metabolism*, 20(6):991–1005, 2014.

[37] A. Chalkiadaki and L. Guarente. Sirtuins mediate mammalian metabolic responses to nutrient availability. *Nature Reviews Endocrinology*, 8(5):287, 2012.

[38] H.-C. Chang and L. Guarente. Sirt1 and other sirtuins in metabolism. *Trends in Endocrinology & Metabolism*, 25(3):138–145, 2014.

[39] H. Chen, J. Chen, L. A. Muir, S. Ronquist, W. Meixner, M. Ljungman, T. Ried, S. Smale, and I. Rajapakse. Functional organization of the human 4d nucleome. *Proceedings of the National Academy of Sciences*, 112(26):8002–8007, 2015.

[40] J. Chen, A. O. Hero III, and I. Rajapakse. Spectral identification of topological domains. *Bioinformatics*, 32(14):2151–2158, 2016.

[41] H.-Y. M. Cheng, J. W. Papp, O. Varlamova, H. Dziema, B. Russell, J. P. Curfman, T. Nakazawa, K. Shimizu, H. Okamura, S. Impey, et al. microrna modulation of circadian-clock period and entrainment. *Neuron*, 54(5):813–829, 2007.

[42] I. Cho and M. J. Blaser. The human microbiome: at the interface of health and disease. *Nature Reviews Genetics*, 13(4):260, 2012.

[43] S. M. Choi, D. F. Tucker, D. N. Gross, R. M. Easton, L. M. DiPilato, A. S. Dean, B. R. Monks, and M. J. Birnbaum. Insulin regulates adipocyte lipolysis via an akt-independent signaling pathway. *Molecular and cellular biology*, 30(21):5009–5020, 2010.

[44] K. Y. Chu, Y. Lin, A. Hendel, J. E. Kulpa, R. W. Brownsey, and J. D. Johnson. Atp-citrate lyase reduction mediates palmitate-induced apoptosis in pancreatic beta-cells. *Journal of Biological Chemistry*, pages jbc–M110, 2010.

[45] J. D. Crane, R. Palanivel, E. P. Mottillo, A. L. Bujak, H. Wang, R. J. Ford, A. Collins, R. M. Blümer, M. D. Fullerton, J. M. Yabut, et al. Inhibiting peripheral serotonin synthesis reduces obesity and metabolic dysfunction by promoting brown adipose tissue thermogenesis. *Nature medicine*, 21(2):166, 2015.

[46] G. Cretenet, M. Le Clech, and F. Gachon. Circadian clock-coordinated 12 hr period rhythmic activation of the ire1α pathway controls lipid metabolism in mouse liver. *Cell metabolism*, 11(1):47–57, 2010.

[47] A. Crisafulli, D. Altavilla, H. Marini, A. Bitto, D. Cucinotta, N. Frisina, F. Corrado, R. D'anna, G. Squadrito, E. B. Adamo, et al. Effects of the phytoestrogen genistein on cardiovascular risk factors in postmenopausal women. *Menopause*, 12(2):186–192, 2005.

[48] K. Daily, V. R. Patel, P. Rigor, X. Xie, and P. Baldi. MotifMap: integrative genome-wide maps of regulatory motif sites for model species, 2011.

[49] R. Dallmann, A. U. Viola, L. Tarokh, C. Cajochen, and S. A. Brown. The human circadian metabolome. *Proceedings of the National Academy of Sciences*, 109(7):2625–2629, 2012.

[50] R. Dallmann, A. U. Viola, L. Tarokh, C. Cajochen, and S. A. Brown. The human circadian metabolome. *Proceedings of the National Academy of Sciences*, 109(7):2625–2629, 2012. [PubMed:22308371] [PubMed Central:22308371] [doi:10.1073/pnas.1114410109].

[51] F. Damiola, N. Le Minh, N. Preitner, B. Kornmann, F. Fleury-Olela, and U. Schibler. Restricted feeding uncouples circadian oscillators in peripheral tissues from the central pacemaker in the suprachiasmatic nucleus. *Genes & development*, 14(23):2950–2961, 2000.

[52] S. K. Davies, J. E. Ang, V. L. Revell, B. Holmes, A. Mann, F. P. Robertson, N. Cui, B. Middleton, K. Ackermann, M. Kayser, et al. Effect of sleep deprivation on the human metabolome. *Proceedings of the National Academy of Sciences*, page 201402663, 2014.

[53] K. Deater-Deckard, M. Chang, and M. E. Evans. Engagement states and learning from educational games. *New directions for child and adolescent development*, 2013(139):21–30, 2013.

[54] J. P. DeBruyne, D. R. Weaver, and S. M. Reppert. Clock and npas2 have overlapping roles in the suprachiasmatic circadian clock. *Nature neuroscience*, 10(5):543, 2007.

[55] J. P. DeBruyne, D. R. Weaver, and S. M. Reppert. Peripheral circadian oscillators require clock. *Current Biology*, 17(14):R538–R539, 2007.

[56] R. Dekker, M. Fleischmann, K. Inderfurth, and L. N. van Wassenhove. *Reverse logistics: quantitative models for closed-loop supply chains*. Springer Science & Business Media, 2013.

[57] C. Dibner, U. Schibler, and U. Albrecht. *The Mammalian Circadian Timing System: Organization and Coordination of Central and Peripheral Clocks*, volume 72. 2010. [PubMed:20148687] [doi:10.1146/annurev-physiol-021909-135821].

[58] L. DiTacchio, H. D. Le, C. Vollmers, M. Hatori, M. Witcher, J. Secombe, and S. Panda. Histone lysine demethylase jarid1a activates clock-bmal1 and influences the circadian clock. *Science*, 333(6051):1881–1885, 2011.

[59] J. R. Dixon, I. Jung, S. Selvaraj, Y. Shen, J. E. Antosiewicz-Bourget, A. Y. Lee, Z. Ye, A. Kim, N. Rajagopal, W. Xie, et al. Chromatin architecture reorganization during stem cell differentiation. *Nature*, 518(7539):331, 2015.

[60] M. Doi, J. Hirayama, and P. Sassone-Corsi. Circadian regulator clock is a histone acetyltransferase. *Cell*, 125(3):497–508, 2006.

[61] M. Doi, Y. Takahashi, R. Komatsu, F. Yamazaki, H. Yamada, S. Haraguchi, N. Emoto, Y. Okuno, G. Tsujimoto, A. Kanematsu, et al. Salt-sensitive hypertension in circadian clock–deficient cry-null mice involves dysregulated adrenal hsd3b6. *Nature medicine*, 16(1):67, 2010.

[62] J. E. Dominy, Y. Lee, M. P. Jedrychowski, H. Chim, M. J. Jurczak, J. P. Camporez, H.-B. Ruan, J. Feldman, K. Pierce, R. Mostoslavsky, et al. The deacetylase sirt6 activates the acetyltransferase gcn5 and suppresses hepatic gluconeogenesis. *Molecular cell*, 48(6):900–913, 2012.

[63] C. L. Drake, T. Roehrs, G. Richardson, J. K. Walsh, and T. Roth. Shift work sleep disorder: prevalence and consequences beyond that of symptomatic day workers. *Sleep*, 27(8):1453–1462, 2004.

[64] K. A. Dyar, S. Ciciliot, L. E. Wright, R. S. Biensø, G. M. Tagliazucchi, V. R. Patel, M. Forcato, M. I. Paz, A. Gudiksen, F. Solagna, et al. Muscle insulin sensitivity and glucose metabolism are controlled by the intrinsic muscle clock. *Molecular metabolism*, 3(1):29–41, 2014.

[65] K. Eckel-Mahan and P. Sassone-Corsi. Metabolism control by the circadian clock and vice versa. *Nature structural & molecular biology*, 16(5):462, 2009.

[66] K. Eckel-Mahan and P. Sassone-Corsi. Metabolism and the circadian clock converge. *Physiological reviews*, 93(1):107–135, 2013.

[67] K. L. Eckel-Mahan, V. R. Patel, S. De Mateo, R. Orozco-Solis, N. J. Ceglia, S. Sahar, S. A. Dilag-Penilla, K. A. Dyar, P. Baldi, and P. Sassone-Corsi. Reprogramming of the circadian clock by nutritional challenge. *Cell*, 155(7):1464–1478, 2013. [PubMed:24360271] [PubMed Central:24360271] [doi:10.1016/j.cell.2013.11.034].

[68] K. L. Eckel-Mahan, V. R. Patel, R. P. Mohney, K. S. Vignola, P. Baldi, and P. Sassone-Corsi. Coordination of the transcriptome and metabolome by the circadian clock. *Proceedings of the National Academy of Sciences*, 109(14):5541–5546, 2012. [PubMed:22431615] [PubMed Central:PMC3325727] [doi:10.1073/pnas.1118726109].

[69] R. Edgar, M. Domrachev, and A. E. Lash. Gene expression omnibus: Ncbi gene expression and hybridization array data repository. *Nucleic acids research*, 30(1):207–210, 2002.

[70] J. S. Espinosa and M. P. Stryker. Development and plasticity of the primary visual cortex. *Neuron*, 75(2):230–249, 2012.

[71] L. Fajas, M. Debril, and J. Auwerx. Ppar gamma: an essential role in metabolic control. *Nutrition, metabolism, and cardiovascular diseases: NMCD*, 11(1):64–69, 2001.

[72] B. Fang, L. J. Everett, J. Jager, E. Briggs, S. M. Armour, D. Feng, A. Roy, Z. Gerhart-Hines, Z. Sun, and M. A. Lazar. Circadian enhancers coordinate multiple phases of rhythmic gene transcription in vivo. *Cell*, 159(5):1140–1152, 2014.

[73] D. Feng and M. A. Lazar. Clocks, Metabolism, and the Epigenome. *Molecular Cell*, 47(2):158–167, jul 2012. [PubMed:22841001] [PubMed Central:PMC3408602] [doi:10.1016/j.molcel.2012.06.026].

[74] D. Feng, T. Liu, Z. Sun, A. Bugge, S. E. Mullican, T. Alenghat, X. S. Liu, and M. A. Lazar. A circadian rhythm orchestrated by histone deacetylase 3 controls hepatic lipid metabolism. *Science*, 331(6022):1315–1319, 2011.

[75] T. Finkel, C.-X. Deng, and R. Mostoslavsky. Recent progress in the biology and physiology of sirtuins. *Nature*, 460(7255):587, 2009.

[76] L. K. Fonken, J. L. Workman, J. C. Walton, Z. M. Weil, J. S. Morris, A. Haim, and R. J. Nelson. Light at night increases body mass by shifting the time of food intake. *Proceedings of the National Academy of Sciences*, 107(43):18664–18669, 2010.

[77] J.-P. Fortin and K. D. Hansen. Reconstructing a/b compartments as revealed by hi-c using long-range correlations in epigenetic data. *Genome biology*, 16(1):180, 2015.

[78] R. Frijters, W. Fleuren, E. J. Toonen, J. P. Tuckermann, H. M. Reichardt, H. Van der Maaden, A. Van Elsas, M.-J. Van Lierop, W. Dokter, J. De Vlieg, et al. Prednisolone-induced differential gene expression in mouse liver carrying wild type or a dimerization-defective glucocorticoid receptor. *BMC genomics*, 11(1):359, 2010.

[79] V. Fritz and L. Fajas. Metabolism and proliferation share common regulatory pathways in cancer cells. *Oncogene*, 29(31):4369, 2010.

[80] O. Froy. Metabolism and circadian rhythmsimplications for obesity. *Endocrine reviews*, 31(1):1–24, 2009.

[81] O. Froy and R. Miskin. Effect of feeding regimens on circadian rhythms: implications for aging and longevity. *Aging (Albany NY)*, 2(1):7, 2010.

[82] T. Fujino, J. Kondo, M. Ishikawa, K. Morikawa, and T. T. Yamamoto. Acetyl-coa synthetase 2, a mitochondrial matrix enzyme involved in the oxidation of acetate. *Journal of Biological Chemistry*, 2001.

[83] J.-M. Fustin, M. Doi, Y. Yamaguchi, H. Hida, S. Nishimura, M. Yoshida, T. Isagawa, M. S. Morioka, H. Kakeya, I. Manabe, et al. Rna-methylation-dependent rna processing controls the speed of the circadian clock. *Cell*, 155(4):793–806, 2013.

[84] D. Gaidatzis, L. Burger, M. Florescu, and M. B. Stadler. Analysis of intronic and exonic reads in rna-seq data characterizes transcriptional and post-transcriptional regulation. *Nature biotechnology*, 33(7):722, 2015.

[85] Z. Gan, E. M. Burkart-Hartman, D.-H. Han, B. Finck, T. C. Leone, E. Y. Smith, J. E. Ayala, J. Holloszy, and D. P. Kelly. The nuclear receptor pparβ/δ programs muscle glucose metabolism in cooperation with ampk and mef2. *Genes & development*, 2011.

[86] N. Gekakis, D. Staknis, H. B. Nguyen, F. C. Davis, L. D. Wilsbacher, D. P. King, J. S. Takahashi, and C. J. Weitz. Role of the clock protein in the mammalian circadian mechanism. *Science*, 280(5369):1564–1569, 1998.

[87] J. R. Gerstner, L. C. Lyons, K. P. Wright, D. H. Loh, O. Rawashdeh, K. L. Eckel-Mahan, and G. W. Roman. Cycling Behavior and Memory Formation. *Journal of Neuroscience*, 29(41):12824–12830, oct 2009. [PubMed:19828795] [PubMed Central:PMC4077269] [doi:10.1523/JNEUROSCI.3353-09.2009].

[88] J. Gil, A. Ramírez-Torres, and S. Encarnación-Guevara. Lysine acetylation and cancer: A proteomics perspective. *Journal of proteomics*, 150:297–309, 2017.

[89] B. J. Goldstein, L. Zhu, R. Hager, A. Zilbering, Y. Sun, and J. B. Vincent. Enhancement of post-receptor insulin signaling by trivalent chromium in hepatoma cells is associated with differential inhibition of specific protein-tyrosine phosphatases. *The Journal of Trace Elements in Experimental Medicine: The Official Publication of the International Society for Trace Element Research in Humans*, 14(4):393–404, 2001.

[90] I. Goldstein, S. Baek, D. M. Presman, V. Paakinaho, E. E. Swinstead, and G. L. Hager. Transcription factor assisted loading and enhancer dynamics dictate the hepatic fasting response. *Genome research*, 27(3):427–439, 2017.

[91] C. B. Green, N. Douris, S. Kojima, C. A. Strayer, J. Fogerty, D. Lourim, S. R. Keller, and J. C. Besharse. Loss of nocturnin, a circadian deadenylase, confers resistance to hepatic steatosis and diet-induced obesity. *Proceedings of the National Academy of Sciences*, 104(23):9888–9893, 2007.

[92] F. Guillaumond, B. Boyer, D. Becquet, S. Guillen, L. Kuhn, J. Garin, M. Belghazi, O. Bosler, J.-L. Franc, and A.-M. François-Bellan. Chromatin remodeling as a mechanism for circadian prolactin transcription: rhythmic nono and sfpq recruitment to hltf. *The FASEB Journal*, 25(8):2740–2756, 2011.

[93] P. Gut and E. Verdin. The nexus of chromatin regulation and intermediary metabolism. *Nature*, 502(7472):489, 2013.

[94] M. A. Gutiérrez-Monreal, V. Treviño, J. E. Moreno-Cuevas, and S.-P. Scott. Identification of circadian-related gene expression profiles in entrained breast cancer cell lines. *Chronobiology international*, 33(4):392–405, 2016. [PubMed:27010605], [doi:10.3109/07420528.2016.1152976].

[95] A. R. Haeusler, C. J. Donnelly, G. Periz, E. A. Simko, P. G. Shaw, M.-S. Kim, N. J. Maragakis, J. C. Troncoso, A. Pandey, R. Sattler, et al. C9orf72 nucleotide repeat structures initiate molecular cascades of disease. *Nature*, 507(7491):195, 2014.

[96] J. A. Hall, J. E. Dominy, Y. Lee, and P. Puigserver. The sirtuin familys role in aging and age-associated pathologies. *The Journal of clinical investigation*, 123(3):973–979, 2013.

[97] W. C. Hallows, S. Lee, and J. M. Denu. Sirtuins deacetylate and activate mammalian acetyl-coa synthetases. *Proceedings of the National Academy of Sciences*, 103(27):10230–10235, 2006.

[98] K. F. Hansen, K. Sakamoto, S. Aten, K. H. Snider, J. Loeser, A. M. Hesse, C. E. Page, C. Pelz, J. S. C. Arthur, S. Impey, et al. Targeted deletion of mir-132/-212 impairs memory and alters the hippocampal transcriptome. *Learning & Memory*, 23(2):61–71, 2016.

[99] H. P. Harding and M. A. Lazar. The monomer-binding orphan receptor rev-erb represses transcription as a dimer on a novel direct repeat. *Molecular and cellular biology*, 15(9):4791–4802, 1995.

[100] S. L. Harmer, J. B. Hogenesch, M. Straume, H.-S. Chang, B. Han, T. Zhu, X. Wang, J. A. Kreps, and S. A. Kay. Orchestrated transcription of key pathways in arabidopsis by the circadian clock. *Science*, 290(5499):2110–2113, 2000.

[101] S. L. Harmer, S. Panda, and S. A. Kay. Molecular bases of circadian rhythms. *Annual review of cell and developmental biology*, 17(1):215–253, 2001.

[102] S. G. Harris and H. C. Smith. In vitro apolipoprotein b mrna editing activity can be modulated by fasting and refeeding rats with a high carbohydrate diet. *Biochemical and biophysical research communications*, 183(2):899–903, 1992.

[103] J. A. Haspel, S. Chettimada, R. S. Shaik, J. H. Chu, B. A. Raby, M. Cernadas, V. Carey, V. Process, G. M. Hunninghake, E. Ifedigbo, J. A. Lederer, J. Englert, A. Pelton, A. Coronata, L. E. Fredenburgh, and A. M. Choi. Circadian rhythm reprogramming during lung inflammation. *Nature Communications*, 5(May):1–15, 2014. [PubMed:25208554] [PubMed Central:PMC4162491] [doi:10.1093/10.1038/ncomms5753].

[104] M. H. Hastings, A. B. Reddy, and E. S. Maywood. A clockwork web: circadian timing in brain and periphery, in health and disease. *Nature Reviews Neuroscience*, 4(8):649, 2003.

[105] F. Hatanaka, C. Matsubara, J. Myung, T. Yoritaka, N. Kamimura, S. Tsutsumi, A. Kanai, Y. Suzuki, P. Sassone-Corsi, H. Aburatani, et al. Genome-wide profiling of the core clock protein bmal1 targets reveals a strict relationship with metabolism. *Molecular and cellular biology*, 30(24):5636–5648, 2010.

[106] M. Hatori, C. Vollmers, A. Zarrinpar, L. DiTacchio, E. A. Bushong, S. Gill, M. Leblanc, A. Chaix, M. Joens, J. A. Fitzpatrick, et al. Time-restricted feeding without reducing caloric intake prevents metabolic diseases in mice fed a high-fat diet. *Cell metabolism*, 15(6):848–860, 2012.

[107] G. Hatzivassiliou, F. Zhao, D. E. Bauer, C. Andreadis, A. N. Shaw, D. Dhanak, S. R. Hingorani, D. A. Tuveson, and C. B. Thompson. Atp citrate lyase inhibition can suppress tumor cell growth. *Cancer cell*, 8(4):311–321, 2005.

[108] O. Hayashi and K. Satoh. Determination of acetyl-coa and malonyl-coa in germinating rice seeds using the lc-ms/ms technique. *Bioscience, biotechnology, and biochemistry*, 70(11):2676–2681, 2006.

[109] J. A. Heimel, M. H. Saiepour, S. Chakravarthy, J. M. Hermans, and C. N. Levelt. Contrast gain control and cortical trkb signaling shape visual acuity. *Nature neuroscience*, 13(5):642, 2010.

[110] J. Hernandez-Rapp, P. Y. Smith, M. Filali, C. Goupil, E. Planel, S. T. Magill, R. H. Goodman, and S. S. Hébert. Memory formation and retention are affected in adult mir-132/212 knockout mice. *Behavioural brain research*, 287:15–26, 2015.

[111] J. Hirayama, S. Sahar, B. Grimaldi, T. Tamaru, K. Takamatsu, Y. Nakahata, and P. Sassone-Corsi. Clock-mediated acetylation of bmal1 controls circadian function. *Nature*, 450(7172):1086, 2007.

[112] S. Hong, W. Zhou, B. Fang, W. Lu, E. Loro, M. Damle, G. Ding, J. Jager, S. Zhang, Y. Zhang, et al. Dissociation of muscle insulin sensitivity from exercise endurance in mice by hdac3 depletion. *Nature medicine*, 23(2):223, 2017.

[113] R. H. Houtkooper, E. Pirinen, and J. Auwerx. Sirtuins as regulators of metabolism and healthspan. *Nature reviews Molecular cell biology*, 13(4):225, 2012.

[114] J. L. Hoy and C. M. Niell. Layer-specific refinement of visual cortex function after eye opening in the awake mouse. *Journal of Neuroscience*, 35(8):3370–3383, 2015.

[115] G. Huang, F. Zhang, Q. Ye, and H. Wang. The circadian clock regulates autophagy directly through the nuclear hormone receptor nr1d1/rev-erbα and indirectly via cebpb/(c/ebpβ) in zebrafish. *Autophagy*, 12(8):1292–1309, 2016.

[116] M. E. Hughes, L. DiTacchio, K. R. Hayes, C. Vollmers, S. Pulivarthy, J. E. Baggs, S. Panda, and J. B. Hogenesch. Harmonics of circadian gene transcription in mammals. *PLoS genetics*, 5(4):e1000442, 2009.

[117] M. E. Hughes, J. B. Hogenesch, and K. Kornacker. JTK_CYCLE: An Efficient Nonparametric Algorithm for Detecting Rhythmic Components in Genome-Scale Data Sets. *Journal of Biological Rhythms*, 25(5):372–380, oct 2010. [PubMed:19772347] [PubMed Central:PMC2761978] [doi:10.1177/0748730410379711].

[118] Y. Imai, K. Abe, S. Sasaki, N. Minami, M. Nihei, M. Munakata, O. Murakami, K. Matsue, H. Sekino, and Y. Miura. Altered circadian blood pressure rhythm in patients with cushing's syndrome. *Hypertension*, 12(1):11–19, 1988.

[119] S. Impey, M. Davare, A. Lasiek, D. Fortin, H. Ando, O. Varlamova, K. Obrietan, T. R. Soderling, R. H. Goodman, and G. A. Wayman. An activity-induced microrna controls dendritic spine formation by regulating rac1-pak signaling. *Molecular and Cellular Neuroscience*, 43(1):146–156, 2010.

[120] M. Inoue, T. Ohtake, W. Motomura, N. Takahashi, Y. Hosoki, S. Miyoshi, Y. Suzuki, H. Saito, Y. Kohgo, and T. Okumura. Increased expression of pparγ in high fat diet-induced liver steatosis in mice. *Biochemical and biophysical research communications*, 336(1):215–222, 2005.

[121] T. Iwasato, A. Datwani, A. M. Wolf, H. Nishiyama, Y. Taguchi, S. Tonegawa, T. Knöpfel, R. S. Erzurumlu, and S. Itohara. Cortex-restricted disruption of nmdar1 impairs neuronal patterns in the barrel cortex. *Nature*, 406(6797):726, 2000.

[122] P. Janich, K. Toufighi, G. Solanas, N. M. Luis, S. Minkwitz, L. Serrano, B. Lehner, and S. A. Benitah. Human epidermal stem cell function is regulated by circadian oscillations. *Cell stem cell*, 13(6):745–753, 2013.

[123] D. Jeyaraj, F. A. Scheer, J. A. Ripperger, S. M. Haldar, Y. Lu, D. A. Prosdocimo, S. J. Eapen, B. L. Eapen, Y. Cui, G. H. Mahabeleshwar, et al. Klf15 orchestrates circadian nitrogen homeostasis. *Cell metabolism*, 15(3):311–323, 2012.

[124] S. Jitrapakdee, A. Vidal-Puig, and J. Wallace. Anaplerotic roles of pyruvate carboxylase in mammalian tissues. *Cellular and Molecular Life Sciences CMLS*, 63(7-8):843–854, 2006.

[125] C. Jouffe, G. Cretenet, L. Symul, E. Martin, F. Atger, F. Naef, and F. Gachon. The circadian clock coordinates ribosome biogenesis. *PLoS biology*, 11(1):e1001455, 2013.

[126] M. Kanehisa and S. Goto. Kegg: kyoto encyclopedia of genes and genomes. *Nucleic acids research*, 28(1):27–30, 2000.

[127] Y. Kanfi, V. Peshti, R. Gil, S. Naiman, L. Nahum, E. Levin, N. Kronfeld-Schor, and H. Y. Cohen. Sirt6 protects against pathological damage caused by diet-induced obesity. *Aging cell*, 9(2):162–173, 2010.

[128] E. Kang, S. Durand, J. J. LeBlanc, T. K. Hensch, C. Chen, and M. Fagiolini. Visual acuity development and plasticity in the absence of sensory experience. *Journal of Neuroscience*, 33(45):17789–17796, 2013.

[129] Y. Kasukawa, N. Miyakoshi, T. Ebina, T. Aizawa, M. Hongo, K. Nozaka, Y. Ishikawa, H. Saito, S. Chida, and Y. Shimada. Effects of risedronate alone or combined with vitamin k 2 on serum undercarboxylated osteocalcin and osteocalcin levels in postmenopausal osteoporosis. *Journal of bone and mineral metabolism*, 32(3):290–297, 2014.

[130] S. Katada and P. Sassone-Corsi. The histone methyltransferase mll1 permits the oscillation of circadian gene expression. *Nature Structural and Molecular Biology*, 17(12):1414, 2010.

[131] T. L. Kawahara, E. Michishita, A. S. Adler, M. Damian, E. Berber, M. Lin, R. A. McCord, K. C. Ongaigui, L. D. Boxer, H. Y. Chang, et al. Sirt6 links histone h3 lysine 9 deacetylation to nf-κb-dependent gene expression and organismal life span. *Cell*, 136(1):62–74, 2009.

[132] T. L. Kawahara, N. A. Rapicavoli, A. R. Wu, K. Qu, S. R. Quake, and H. Y. Chang. Dynamic chromatin localization of sirt6 shapes stress-and aging-related transcriptional networks. *PLoS genetics*, 7(6):e1002153, 2011.

[133] T. Kawai and S. Akira. The role of pattern-recognition receptors in innate immunity: update on toll-like receptors. *Nature immunology*, 11(5):373, 2010.

[134] S. Kersten. Mechanisms of nutritional and hormonal regulation of lipogenesis. *EMBO reports*, 2(4):282–286, 2001.

[135] H.-S. Kim, C. Xiao, R.-H. Wang, T. Lahusen, X. Xu, A. Vassilopoulos, G. Vazquez-Ortiz, W.-I. Jeong, O. Park, S. H. Ki, et al. Hepatic-specific disruption of sirt6 in mice results in fatty liver formation due to enhanced glycolysis and triglyceride synthesis. *Cell metabolism*, 12(3):224–236, 2010.

[136] J. Y. Kim, J. Y. Park, O. Y. Kim, B. M. Ham, H.-J. Kim, D. Y. Kwon, Y. Jang, and J. H. Lee. Metabolic profiling of plasma in overweight/obese and lean men using ultra performance liquid chromatography and q-tof mass spectrometry (uplc- q-tof ms). *Journal of proteome research*, 9(9):4368–4375, 2010.

[137] K. Kimura, H. Jin, M. Ogawa, and T. Aoe. Dysfunction of the er chaperone bip accelerates the renal tubular injury. *Biochemical and biophysical research communications*, 366(4):1048–1053, 2008.

[138] A. Knutsson. Health disorders of shift workers. *Occupational medicine*, 53(2):103–108, 2003.

[139] D. Knutti and A. Kralli. Pgc-1, a versatile coactivator. *Trends in Endocrinology & Metabolism*, 12(8):360–365, 2001.

[140] C. H. Ko and J. S. Takahashi. Molecular components of the mammalian circadian clock. *Human Molecular Genetics*, 15(SUPPL. 2):271–277, 2006. [PubMed:16987893] [doi:10.1093/hmg/ddl207].

[141] H. Ko, L. Cossell, C. Baragli, J. Antolik, C. Clopath, S. B. Hofer, and T. D. Mrsic-Flogel. The emergence of functional microcircuits in visual cortex. *Nature*, 496(7443):96, 2013.

[142] H. Ko, T. D. Mrsic-Flogel, and S. B. Hofer. Emergence of feature-specific connectivity in cortical microcircuits in the absence of visual experience. *Journal of Neuroscience*, 34(29):9812–9816, 2014.

[143] Y. Kobayashi, Z. Ye, and T. K. Hensch. Clock genes control cortical critical period timing. *Neuron*, 86(1):264–275, 2015.

[144] A. Kohsaka, A. D. Laposky, K. M. Ramsey, C. Estrada, C. Joshu, Y. Kobayashi, F. W. Turek, and J. Bass. High-fat diet disrupts behavioral and molecular circadian rhythms in mice. *Cell metabolism*, 6(5):414–421, 2007.

[145] N. Koike, S.-H. Yoo, H.-C. Huang, V. Kumar, C. Lee, T.-K. Kim, and J. S. Takahashi. Transcriptional Architecture and Chromatin Landscape of the Core Circadian Clock in Mammals. *Science*, 338(6105):349–354, oct 2012. [PubMed:22936566] [PubMed Central:PMC3694775] [doi:10.1126/science.1226339].

[146] A. Kojima, M. Ikegami, K. Teshima, and T. Miyasaka. Highly luminescent lead bromide perovskite nanoparticles synthesized with porous alumina media. *Chemistry Letters*, 41(4):397–399, 2012.

[147] R. V. Kondratov, A. A. Kondratova, V. Y. Gorbacheva, O. V. Vykhovanets, and M. P. Antoch. Early aging and age-related pathologies in mice deficient in bmal1, the core componentof the circadian clock. *Genes & development*, 20(14):1868–1873, 2006.

[148] R. V. Kondratov, A. A. Kondratova, V. Y. Gorbacheva, O. V. Vykhovanets, and M. P. Antoch. Early aging and age-related pathologies in mice deficient in bmal1, the core componentof the circadian clock. *Genes & development*, 20(14):1868–1873, 2006.

[149] R. V. Kondratov, A. A. Kondratova, V. Y. Gorbacheva, O. V. Vykhovanets, and M. P. Antoch. Early aging and age-related pathologies in mice deficient in bmal1, the core componentof the circadian clock. *Genes & development*, 20(14):1868–1873, 2006.

[150] B. Kornmann, O. Schaad, H. Bujard, J. S. Takahashi, and U. Schibler. System-driven and oscillator-dependent circadian transcription in mice with a conditionally active liver clock. *PLoS biology*, 5(2):e34, 2007.

[151] P. H. L. Krijger, B. Di Stefano, E. de Wit, F. Limone, C. Van Oevelen, W. De Laat, and T. Graf. Cell-of-origin-specific 3d genome structure acquired during somatic cell reprogramming. *Cell Stem Cell*, 18(5):597–610, 2016.

[152] K. Krishnan, B.-S. Wang, J. Lu, L. Wang, A. Maffei, J. Cang, and Z. J. Huang. Mecp2 regulates the timing of critical period plasticity that shapes functional connectivity in primary visual cortex. *Proceedings of the National Academy of Sciences*, 112(34):E4782–E4791, 2015.

[153] S. J. Kuhlman, E. Tring, and J. T. Trachtenberg. Fast-spiking interneurons have an initial orientation bias that is lost with vision. *Nature neuroscience*, 14(9):1121, 2011.

[154] N. Kumashiro, T. Yoshimura, J. L. Cantley, S. K. Majumdar, F. Guebre-Egziabher, R. Kursawe, D. F. Vatner, I. Fat, M. Kahn, D. M. Erion, et al. Role of patatin-like phospholipase domain-containing 3 on lipid-induced hepatic steatosis and insulin resistance in rats. *Hepatology*, 57(5):1763–1772, 2013.

[155] T. J. Lambert, D. R. Storm, and J. M. Sullivan. Microrna132 modulates short-term synaptic plasticity but not basal release probability in hippocampal neurons. *PloS one*, 5(12):e15182, 2010.

[156] K. A. Lamia, K.-F. Storch, and C. J. Weitz. Physiological significance of a peripheral tissue circadian clock. *Proceedings of the national academy of sciences*, 105(39):15172–15177, 2008.

[157] M. R. Langer, C. J. Fry, C. L. Peterson, and J. M. Denu. Modulating acetyl-coa binding in the gcn5 family of histone acetyltransferases. *Journal of Biological Chemistry*, 2002.

[158] O. Le Bacquer, E. Petroulakis, S. Paglialunga, F. Poulin, D. Richard, K. Cianflone, and N. Sonenberg. Elevated sensitivity to diet-induced obesity and insulin resistance in mice lacking 4e-bp1 and 4e-bp2. *The Journal of clinical investigation*, 117(2):387–396, 2007.

[159] G. Le Martelot, D. Canella, L. Symul, E. Migliavacca, F. Gilardi, R. Liechti, O. Martin, K. Harshman, M. Delorenzi, B. Desvergne, et al. Genome-wide rna polymerase ii profiles and rna accumulation reveal kinetics of transcription and associated epigenetic changes during diurnal cycles. *PLoS biology*, 10(11):e1001442, 2012.

[160] G. Le Martelot, T. Claudel, D. Gatfield, O. Schaad, B. Kornmann, G. L. Sasso, A. Moschetta, and U. Schibler. Rev-erbα participates in circadian srebp signaling and bile acid homeostasis. *PLoS biology*, 7(9):e1000181, 2009.

[161] H.-m. Lee, R. Chen, H. Kim, J.-P. Etchegaray, D. R. Weaver, and C. Lee. The period of the circadian oscillator is primarily determined by the balance between casein kinase 1 and protein phosphatase 1. *Proceedings of the National Academy of Sciences*, 108(39):16451–16456, 2011.

[162] J. H. Lee and A. Sancar. Circadian clock disruption improves the efficacy of chemotherapy through p73-mediated apoptosis. *Proceedings of the National Academy of Sciences*, 108(26):10668–10672, 2011.

[163] L. M. Leesnitzer, D. J. Parks, R. K. Bledsoe, J. E. Cobb, J. L. Collins, T. G. Consler, R. G. Davis, E. A. Hull-Ryde, J. M. Lenhard, L. Patel, et al. Functional consequences of cysteine modification in the ligand binding sites of peroxisome proliferator activated receptors by gw9662. *Biochemistry*, 41(21):6640–6650, 2002.

[164] J. K. Leighton, J. Joyner, J. Zamarripa, M. Deines, and R. A. Davis. Fasting decreases apolipoprotein b mrna editing and the secretion of small molecular weight apob by rat hepatocytes: evidence that the total amount of apob secreted is regulated post-transcriptionally. *Journal of Lipid Research*, 31(9):1663–1668, 1990.

[165] C. N. Levelt and M. Hübener. Critical-period plasticity in the visual cortex. *Annual review of neuroscience*, 35:309–330, 2012.

[166] J. Z. Li, B. G. Bunney, F. Meng, M. H. Hagenauer, D. M. Walsh, M. P. Vawter, S. J. Evans, P. V. Choudary, P. Cartagena, J. D. Barchas, et al. Circadian patterns of gene expression in the human brain and disruption in major depressive disorder. *Proceedings of the National Academy of Sciences*, 110(24):9950–9955, 2013.

[167] X.-M. Li, F. Delaunay, S. Dulong, B. Claustrat, S. Zampera, Y. Fujii, M. Teboul, J. Beau, and F. Lévi. Cancer inhibition through circadian reprogramming of tumor transcriptome with meal timing. *Cancer research*, 70(8):3351–3360, 2010.

[168] X. M. Li, F. Delaunay, S. Dulong, B. Claustrat, S. Zampera, Y. Fujii, M. Teboul, J. Beau, and F. Lévi. Cancer inhibition through circadian reprogramming of tumor transcriptome with meal timing. *Cancer Research*, 70(8):3351–3360, 2010. [PubMed:20395208] [doi:10.1158/0008-5472.CAN-09-4235].

[169] E. Lieberman-Aiden, N. L. Van Berkum, L. Williams, M. Imakaev, T. Ragoczy, A. Telling, I. Amit, B. R. Lajoie, P. J. Sabo, M. O. Dorschner, et al. Comprehensive mapping of long-range interactions reveals folding principles of the human genome. *science*, 326(5950):289–293, 2009.

[170] J. Lin, C. Handschin, and B. M. Spiegelman. Metabolic control through the pgc-1 family of transcription coactivators. *Cell metabolism*, 1(6):361–370, 2005.

[171] A. C. Liu, D. K. Welsh, C. H. Ko, H. G. Tran, E. E. Zhang, A. A. Priest, E. D. Buhr, O. Singer, K. Meeker, I. M. Verma, et al. Intercellular coupling confers robustness against mutations in the scn circadian clock network. *Cell*, 129(3):605–616, 2007.

[172] G. Liu, A. E. Loraine, R. Shigeta, M. Cline, J. Cheng, V. Valmeekam, S. Sun, D. Kulp, and M. A. Siani-Rose. Netaffx: Affymetrix probesets and annotations. *Nucleic acids research*, 31(1):82–86, 2003.

[173] S. Liu, J. D. Brown, K. J. Stanya, E. Homan, M. Leidl, K. Inouye, P. Bhargava, M. R. Gangl, L. Dai, B. Hatano, et al. A diurnal serum lipid integrates hepatic lipogenesis and peripheral fatty acid use. *Nature*, 502(7472):550, 2013.

[174] Y. Liu, S. Sun, T. Bredy, M. Wood, R. C. Spitale, and P. Baldi. MotifMap-RNA: a genome-wide map of RBP binding sites. *Bioinformatics*, 33(13):2029–2031, jul 2017.

[175] G. Lohmann, D. S. Margulies, A. Horstmann, B. Pleger, J. Lepsien, D. Goldhahn, H. Schloegl, M. Stumvoll, A. Villringer, and R. Turner. Eigenvector centrality mapping for analyzing connectivity patterns in fmri data of the human brain. *PloS one*, 5(4):e10232, 2010.

[176] V. D. Longo and M. P. Mattson. Fasting: molecular mechanisms and clinical applications. *Cell metabolism*, 19(2):181–192, 2014.

[177] V. D. Longo and S. Panda. Fasting, circadian rhythms, and time-restricted feeding in healthy lifespan. *Cell metabolism*, 23(6):1048–1059, 2016.

[178] C. N. Lumeng and A. R. Saltiel. Inflammatory links between obesity and metabolic disease. *The Journal of clinical investigation*, 121(6):2111–2117, 2011.

[179] G. Mansueto, A. Armani, C. Viscomi, L. DOrsi, R. De Cegli, E. V. Polishchuk, C. Lamperti, I. Di Meo, V. Romanello, S. Marchet, et al. Transcription factor eb controls metabolic flexibility during exercise. *Cell metabolism*, 25(1):182–196, 2017.

[180] B. Marcheva, K. M. Ramsey, E. D. Buhr, Y. Kobayashi, H. Su, C. H. Ko, G. Ivanova, C. Omura, S. Mo, M. H. Vitaterna, et al. Disruption of the clock components clock and bmal1 leads to hypoinsulinaemia and diabetes. *Nature*, 466(7306):627, 2010.

[181] S. Masri, K. Kinouchi, and P. Sassone-Corsi. Circadian clocks, epigenetics, and cancer. *Current opinion in oncology*, 27(1):50, 2015.

[182] S. Masri, T. Papagiannakopoulos, K. Kinouchi, Y. Liu, M. Cervantes, P. Baldi, T. Jacks, and P. Sassone-Corsi. Lung Adenocarcinoma Distally Rewires Hepatic Circadian Homeostasis. *Cell*, 165(4):896–909, 2016. [PubMed:27153497] [PubMed Central:PMC5373476] [doi:10.1016/j.cell.2016.04.039].

[183] S. Masri, V. R. Patel, K. L. Eckel-Mahan, S. Peleg, I. Forne, A. G. Ladurner, P. Baldi, A. Imhof, and P. Sassone-Corsi. Circadian acetylome reveals regulation of mitochondrial metabolic pathways. *Proceedings of the National Academy of Sciences*, 110(9):3339–3344, 2013. [PubMed:23341599] [PubMed Central:PMC4908327] [doi:10.1073/pnas.1217632110].

[184] S. Masri, P. Rigor, M. Cervantes, N. Ceglia, C. Sebastian, C. Xiao, M. Roqueta-Rivera, C. Deng, T. F. Osborne, R. Mostoslavsky, et al. Partitioning circadian transcription by sirt6 leads to segregated control of cellular metabolism. *Cell*, 158(3):659–672, 2014.

[185] S. Masri and P. Sassone-Corsi. Plasticity and specificity of the circadian epigenome. *Nature neuroscience*, 13(11):1324, 2010.

[186] K. Matsusue, T. Kusakabe, T. Noguchi, S. Takiguchi, T. Suzuki, S. Yamano, and F. J. Gonzalez. Hepatic steatosis in leptin-deficient mice is promoted by the pparγ target gene fsp27. *Cell metabolism*, 7(4):302–311, 2008.

[187] C. L. McCurry, J. D. Shepherd, D. Tropea, K. H. Wang, M. F. Bear, and M. Sur. Loss of arc renders the visual cortex impervious to the effects of sensory experience or deprivation. *Nature neuroscience*, 13(4):450, 2010.

[188] N. J. McGlincy, A. Valomon, J. E. Chesham, E. S. Maywood, M. H. Hastings, and J. Ule. Regulation of alternative splicing by the circadian clock and food related cues. *Genome biology*, 13(6):R54, 2012.

[189] N. J. McGlincy, A. Valomon, J. E. Chesham, E. S. Maywood, M. H. Hastings, and J. Ule. Regulation of alternative splicing by the circadian clock and food related cues. *Genome biology*, 13(6):R54, 2012.

[190] A. P. Meeson, X. Shi, M. S. Alexander, R. Williams, R. E. Allen, N. Jiang, I. M. Adham, S. C. Goetsch, R. E. Hammer, and D. J. Garry. Sox15 and fhl3 transcriptionally coactivate foxk1 and regulate myogenic progenitor cells. *The EMBO journal*, 26(7):1902–1912, 2007.

[191] A. Mehra, C. L. Baker, J. J. Loros, and J. C. Dunlap. Post-translational modifications in circadian rhythms. *Trends in biochemical sciences*, 34(10):483–490, 2009.

[192] N. Mellios, H. Sugihara, J. Castro, A. Banerjee, C. Le, A. Kumar, B. Crawford, J. Strathmann, D. Tropea, S. S. Levine, et al. mir-132, an experience-dependent microrna, is essential for visual cortex plasticity. *Nature neuroscience*, 14(10):1240, 2011.

[193] J. S. Menet and M. Rosbash. When brain clocks lose track of time: cause or consequence of neuropsychiatric disorders. *Current Opinion in Neurobiology*, 21(6):849–857, dec 2011. [PubMed:21737252] [PubMed Central:PMC3252427] [doi:10.1016/j.conb.2011.06.008].

[194] E. Michishita, R. A. McCord, E. Berber, M. Kioi, H. Padilla-Nash, M. Damian, P. Cheung, R. Kusumoto, T. L. Kawahara, J. C. Barrett, et al. Sirt6 is a histone h3 lysine 9 deacetylase that modulates telomeric chromatin. *Nature*, 452(7186):492, 2008.

[195] G. Milan, V. Romanello, F. Pescatore, A. Armani, J.-H. Paik, L. Frasson, A. Seydel, J. Zhao, R. Abraham, A. L. Goldberg, et al. Regulation of autophagy and the ubiquitin–proteasome system by the foxo transcriptional network during muscle atrophy. *Nature communications*, 6:6670, 2015.

[196] B. H. Miller, E. L. McDearmon, S. Panda, K. R. Hayes, J. Zhang, J. L. Andrews, M. P. Antoch, J. R. Walker, K. A. Esser, J. B. Hogenesch, et al. Circadian and clock-controlled regulation of the mouse transcriptome and cell proliferation. *Proceedings of the National Academy of Sciences*, 104(9):3342–3347, 2007.

[197] B. H. Miller, Z. Zeier, L. Xi, T. A. Lanz, S. Deng, J. Strathmann, D. Willoughby, P. J. Kenny, J. D. Elsworth, M. S. Lawrence, et al. Microrna-132 dysregulation in schizophrenia has implications for both neurodevelopment and adult brain function. *Proceedings of the National Academy of Sciences*, 109(8):3125–3130, 2012.

[198] M. Monsalve, Z. Wu, G. Adelmant, P. Puigserver, M. Fan, and B. M. Spiegelman. Direct coupling of transcription and mrna processing through the thermogenic coactivator pgc-1. *Molecular cell*, 6(2):307–316, 2000.

[199] A. Montagner, A. Polizzi, E. Fouché, S. Ducheix, Y. Lippi, F. Lasserre, V. Barquissau, M. Régnier, C. Lukowicz, F. Benhamed, et al. Liver pparα is crucial for whole-body fatty acid homeostasis and is protective against nafld. *Gut*, pages gutjnl–2015, 2016.

[200] R. Y. Moore and V. B. Eichler. Loss of a circadian adrenal corticosterone rhythm following suprachiasmatic lesions in the rat. *Brain research*, 1972.

[201] J. Morf, G. Rey, K. Schneider, M. Stratmann, J. Fujita, F. Naef, and U. Schibler. Cold-inducible rna-binding protein modulates circadian gene expression posttranscriptionally. *Science*, 338(6105):379–383, 2012.

[202] G. J. Morton, R. W. Gelling, K. D. Niswender, C. D. Morrison, C. J. Rhodes, and M. W. Schwartz. Leptin regulates insulin sensitivity via phosphatidylinositol-3-oh kinase signaling in mediobasal hypothalamic neurons. *Cell metabolism*, 2(6):411–420, 2005.

[203] R. Mostoslavsky, K. F. Chua, D. B. Lombard, W. W. Pang, M. R. Fischer, L. Gellon, P. Liu, G. Mostoslavsky, S. Franco, M. M. Murphy, et al. Genomic instability and aging-like phenotype in the absence of mammalian sirt6. *Cell*, 124(2):315–329, 2006.

[204] M. Murakami, P. Tognini, Y. Liu, K. L. EckelMahan, P. Baldi, and P. SassoneCorsi. Gut microbiota directs PPARγdriven reprogramming of the liver circadian clock by nutritional challenge. *EMBO reports*, 17(9):1292–1303, 2016. [PubMed:27418314] [PubMed Central:PMC5007574] [doi:10.15252/embr.201642463].

[205] Y. Nakahata, M. Kaluzova, B. Grimaldi, S. Sahar, J. Hirayama, D. Chen, L. P. Guarente, and P. Sassone-Corsi. The nad+-dependent deacetylase sirt1 modulates clock-mediated chromatin remodeling and circadian control. *Cell*, 134(2):329–340, 2008.

[206] Y. Nakahata, S. Sahar, G. Astarita, M. Kaluzova, and P. Sassone-Corsi. Circadian control of the nad+ salvage pathway by clock-sirt1. *Science*, 324(5927):654–657, 2009.

[207] A. D. Napper, J. Hixon, T. McDonagh, K. Keavey, J.-F. Pons, J. Barker, W. T. Yau, P. Amouzegh, A. Flegg, E. Hamelin, et al. Discovery of indoles as potent and selective inhibitors of the deacetylase sirt1. *Journal of medicinal chemistry*, 48(25):8045–8054, 2005.

[208] C. B. Newgard, J. An, J. R. Bain, M. J. Muehlbauer, R. D. Stevens, L. F. Lien, A. M. Haqq, S. H. Shah, M. Arlotto, C. A. Slentz, et al. A branched-chain amino acid-related metabolic signature that differentiates obese and lean humans and contributes to insulin resistance. *Cell metabolism*, 9(4):311–326, 2009.

[209] C. M. Niell and M. P. Stryker. Highly selective receptive fields in mouse visual cortex. *Journal of Neuroscience*, 28(30):7520–7536, 2008.

[210] H. Nørrelund, H. Wiggers, M. Halbirk, J. Frystyk, A. Flyvbjerg, H. E. Bøtker, O. Schmitz, J. O. L. Jørgensen, J. S. Christiansen, and N. Møller. Abnormalities of whole body protein turnover, muscle metabolism and levels of metabolic hormones in patients with chronic heart failure. *Journal of internal medicine*, 260(1):11–21, 2006.

[211] K. Oishi, K. Miyazaki, K. Kadota, R. Kikuno, T. Nagase, G.-i. Atsumi, N. Ohkura, T. Azama, M. Mesaki, S. Yukimasa, et al. Genome-wide expression analysis of mouse liver reveals clock-regulated circadian output genes. *Journal of Biological Chemistry*, 278(42):41519–41527, 2003.

[212] M. Oishi, Y. Nagasaki, K. Itaka, N. Nishiyama, and K. Kataoka. Lactosylated poly (ethylene glycol)-sirna conjugate through acid-labile β-thiopropionate linkage to construct ph-sensitive polyion complex micelles achieving enhanced gene silencing in hepatoma cells. *Journal of the American Chemical Society*, 127(6):1624–1625, 2005.

[213] H. Oster, S. Damerow, R. A. Hut, and G. Eichele. Transcriptional profiling in the adrenal gland reveals circadian regulation of hormone biosynthesis genes and nucleosome assembly genes. *Journal of biological rhythms*, 21(5):350–361, 2006.

[214] J. S. ONeill and A. B. Reddy. Circadian clocks in human red blood cells. *Nature*, 469(7331):498, 2011.

[215] J. S. ONeill, G. Van Ooijen, L. E. Dixon, C. Troein, F. Corellou, F.-Y. Bouget, A. B. Reddy, and A. J. Millar. Circadian rhythms persist without transcription in a eukaryote. *Nature*, 469(7331):554, 2011.

[216] I. Pacheco-Leyva, A. C. Matias, D. V. Oliveira, J. M. Santos, R. Nascimento, E. Guerreiro, A. C. Michell, A. M. van De Vrugt, G. Machado-Oliveira, G. Ferreira, et al. Cited2 cooperates with isl1 and promotes cardiac differentiation of mouse embryonic stem cells. *Stem cell reports*, 7(6):1037–1049, 2016.

[217] S. Panda, J. B. Hogenesch, and S. A. Kay. Circadian rhythms from flies to human. *Nature*, 417(6886):329–335, 2002. [PubMed:12015613] [doi:10.1038/417329a].

[218] T. Papagiannakopoulos, M. R. Bauer, S. M. Davidson, M. Heimann, L. Subbaraj, A. Bhutkar, J. Bartlebaugh, M. G. Vander Heiden, and T. Jacks. Circadian rhythm disruption promotes lung tumorigenesis. *Cell metabolism*, 24(2):324–331, 2016.

[219] C. L. Partch, C. B. Green, and J. S. Takahashi. Molecular architecture of the mammalian circadian clock. *Trends in Cell Biology*, 24(2):90–99, 2014. [PubMed:23916625] [PubMed Central:PMC3946763] [doi:10.1016/j.tcb.2013.07.002].

[220] C. L. Partch, C. B. Green, and J. S. Takahashi. Molecular architecture of the mammalian circadian clock. *Trends in cell biology*, 24(2):90–99, 2014.

[221] G. K. Paschos, S. Ibrahim, W.-L. Song, T. Kunieda, G. Grant, T. M. Reyes, C. A. Bradfield, C. H. Vaughan, M. Eiden, M. Masoodi, et al. Obesity in mice with adipocyte-specific deletion of clock component arntl. *Nature medicine*, 18(12):1768, 2012.

[222] S. A. Patel, N. Velingkaar, K. Makwana, A. Chaudhari, and R. Kondratov. Calorie restriction regulates circadian clock gene expression through bmal1 dependent and independent mechanisms. *Scientific reports*, 6:25970, 2016.

[223] S. A. Patel, N. S. Velingkaar, and R. V. Kondratov. Transcriptional control of antioxidant defense by the circadian clock. *Antioxidants & redox signaling*, 20(18):2997–3006, 2014.

[224] V. R. Patel, N. Ceglia, M. Zeller, K. Eckel-Mahan, P. Sassone-Corsi, and P. Baldi. The pervasiveness and plasticity of circadian oscillations: The coupled circadian-oscillators framework. *Bioinformatics*, 31(19):3181–3188, 2015. [PubMed:26049162] [PubMed Central:PMC4592335] [doi:10.1093/bioinformatics/btv353].

[225] V. R. Patel, K. Eckel-Mahan, P. Sassone-Corsi, and P. Baldi. CircadiOmics: Integrating circadian genomics, transcriptomics, proteomics and metabolomics. *Nature Methods*, 9(8):772–773, 2012. [PubMed:22847108] [doi:10.1038/nmeth.2111].

[226] M. A. Pearen, J. G. Ryall, G. S. Lynch, and G. E. Muscat. Expression profiling of skeletal muscle following acute and chronic β 2-adrenergic stimulation: implications for hypertrophy, metabolism and circadian rhythm. *BMC genomics*, 10(1):448, 2009.

[227] C. B. Peek, A. H. Affinati, K. M. Ramsey, H.-Y. Kuo, W. Yu, L. A. Sena, O. Ilkayeva, B. Marcheva, Y. Kobayashi, C. Omura, et al. Circadian clock nad+ cycle drives mitochondrial oxidative metabolism in mice. *Science*, 342(6158):1243417, 2013.

[228] C. B. Peek, D. C. Levine, J. Cedernaes, A. Taguchi, Y. Kobayashi, S. J. Tsai, N. A. Bonar, M. R. McNulty, K. M. Ramsey, and J. Bass. Circadian clock interaction with hif1α mediates oxygenic metabolism and anaerobic glycolysis in skeletal muscle. *Cell metabolism*, 25(1):86–92, 2017.

[229] J. S. Pendergast, K. L. Branecky, W. Yang, K. L. Ellacott, K. D. Niswender, and S. Yamazaki. High-fat diet acutely affects circadian organisation and eating behavior. *European Journal of Neuroscience*, 37(8):1350–1356, 2013.

[230] L. Perreault, B. C. Bergman, D. M. Hunerdosse, and R. H. Eckel. Altered intramuscular lipid metabolism relates to diminished insulin action in men, but not women, in progression to diabetes. *Obesity*, 18(11):2093–2100, 2010.

[231] M. M. Perry, J. E. Baker, D. S. Gibeon, I. M. Adcock, and K. F. Chung. Airway smooth muscle hyperproliferation is regulated by microrna-221 in severe asthma. *American journal of respiratory cell and molecular biology*, 50(1):7–17, 2014.

[232] J. E. Pessin and H. Kwon. Adipokines mediate inflammation and insulin resistance. *Frontiers in endocrinology*, 4:71, 2013.

[233] S. Pichler, W. Gu, D. Hartl, G. Gasparoni, P. Leidinger, A. Keller, E. Meese, M. Mayhaus, H. Hampel, and M. Riemenschneider. The mirnome of alzheimer's disease: consistent downregulation of the mir-132/212 cluster. *Neurobiology of aging*, 50:167–e1, 2017.

[234] A. Pizarro, K. Hayer, N. F. Lahens, and J. B. Hogenesch. CircaDB: A database of mammalian circadian gene expression profiles. *Nucleic Acids Research*, 41(D1):1009–1013, 2013. [PubMed:23180795] [PubMed Central:PMC3531170] [doi:10.1093/nar/gks1161].

[235] V. Porciatti, T. Pizzorusso, and L. Maffei. The visual physiology of the wild type mouse determined with pattern veps. *Vision research*, 39(18):3071–3081, 1999.

[236] I. Rajapakse and M. Groudine. On emerging nuclear order. *The Journal of cell biology*, 192(5):711–721, 2011.

[237] M. R. Ralph, R. G. Foster, F. C. Davis, and M. Menaker. Transplanted suprachiasmatic nucleus determines circadian period. *Science*, 247(4945):975–978, 1990.

[238] B. W. Ramsey, J. Davies, N. G. McElvaney, E. Tullis, S. C. Bell, P. Dřevínek, M. Griese, E. F. McKone, C. E. Wainwright, M. W. Konstan, et al. A cftr potentiator in patients with cystic fibrosis and the g551d mutation. *New England Journal of Medicine*, 365(18):1663–1672, 2011.

[239] K. M. Ramsey, J. Yoshino, C. S. Brace, D. Abrassart, Y. Kobayashi, B. Marcheva, H.-K. Hong, J. L. Chong, E. D. Buhr, C. Lee, et al. Circadian clock feedback cycle through nampt-mediated nad+ biosynthesis. *Science*, 324(5927):651–654, 2009.

[240] C. E. Rasmussen. Gaussian processes in machine learning. In *Advanced lectures on machine learning*, pages 63–71. Springer, 2004.

[241] K. Ravnskjaer, M. F. Hogan, D. Lackey, L. Tora, S. Y. Dent, J. Olefsky, and M. Montminy. Glucagon regulates gluconeogenesis through kat2b-and wdr5-mediated epigenetic effects. *The Journal of clinical investigation*, 123(10):4318–4328, 2013.

[242] J. Remenyi, M. W. van den Bosch, O. Palygin, R. B. Mistry, C. McKenzie, A. Macdonald, G. Hutvagner, J. S. C. Arthur, B. G. Frenguelli, and Y. Pankratov. mir-132/212 knockout mice reveal roles for these mirnas in regulating cortical synaptic transmission and plasticity. *PloS one*, 8(4):e62509, 2013.

[243] J. A. Ripperger and U. Schibler. Rhythmic clock-bmal1 binding to multiple e-box motifs drives circadian dbp transcription and chromatin transitions. *Nature genetics*, 38(3):369, 2006.

[244] J. A. Ripperger and U. Schibler. Rhythmic clock-bmal1 binding to multiple e-box motifs drives circadian dbp transcription and chromatin transitions. *Nature genetics*, 38(3):369, 2006.

[245] M. S. Robles, J. Cox, and M. Mann. In-Vivo Quantitative Proteomics Reveals a Key Contribution of Post-Transcriptional Mechanisms to the Circadian Regulation of Liver Metabolism. *PLoS Genetics*, 10(1), 2014. [PubMed:24391516] [PubMed Central:PMC2840478] [doi:10.1371/journal.pgen.1004047].

[246] M. S. Robles, J. Cox, and M. Mann. In-vivo quantitative proteomics reveals a key contribution of post-transcriptional mechanisms to the circadian regulation of liver metabolism. *PLoS genetics*, 10(1):e1004047, 2014.

[247] J. T. Rodgers, C. Lerin, W. Haas, S. P. Gygi, B. M. Spiegelman, and P. Puigserver. Nutrient control of glucose homeostasis through a complex of pgc-1α and sirt1. *Nature*, 434(7029):113, 2005.

[248] J.-F. Rual, K. Venkatesan, T. Hao, T. Hirozane-Kishikawa, A. Dricot, N. Li, G. F. Berriz, F. D. Gibbons, M. Dreze, N. Ayivi-Guedehoussou, et al. Towards a proteome-scale map of the human protein–protein interaction network. *Nature*, 437(7062):1173, 2005.

[249] R. D. Rudic, P. McNamara, A.-M. Curtis, R. C. Boston, S. Panda, J. B. Hogenesch, and G. A. FitzGerald. Bmal1 and clock, two essential components of the circadian clock, are involved in glucose homeostasis. *PLoS biology*, 2(11):e377, 2004.

[250] L. A. Sadacca, K. A. Lamia, B. Blum, C. Weitz, et al. An intrinsic circadian clock of the pancreas is required for normal insulin release and glucose homeostasis in mice. *Diabetologia*, 54(1):120–124, 2011.

[251] S. Sahar, S. Masubuchi, K. Eckel-Mahan, S. Vollmer, L. Galla, N. Ceglia, S. Masri, T. K. Barth, B. Grimaldi, O. Oluyemi, G. Astarita, W. C. Hallows, D. Piomelli, A. Imhof, P. Baldi, J. M. Denu, and P. Sassone-Corsi. Circadian control of fatty acid elongation by SIRT1 protein-mediated deacetylation of acetyl-coenzyme a synthetase 1. *Journal of Biological Chemistry*, 289(9):6091–6097, 2014. [PubMed:24425865],[PubMed Central:PMC3937675][doi:10.1074/jbc.M113.537191].

[252] S. Sahar and P. Sassone-Corsi. Metabolism and cancer: the circadian clock connection. *Nature Reviews Cancer*, 9(12):886, 2009.

[253] R. Salgado-Delgado, M. Angeles-Castellanos, M. Buijs, and C. Escobar. Internal desynchronization in a model of night-work by forced activity in rats. *Neuroscience*, 154(3):922–931, 2008.

[254] R. C. Salgado-Delgado, N. Saderi, M. del Carmen Basualdo, N. N. Guerrero-Vargas, C. Escobar, and R. M. Buijs. Shift work or food intake during the rest phase promotes metabolic disruption and desynchrony of liver genes in male rats. *PLoS One*, 8(4):e60052, 2013.

[255] R. Sarnaik, B.-S. Wang, and J. Cang. Experience-dependent and independent binocular correspondence of receptive field subregions in mouse visual cortex. *Cerebral cortex*, 24(6):1658–1670, 2013.

[256] M. Sato, M. Murakami, K. Node, R. Matsumura, and M. Akashi. The role of the endocrine system in feeding-induced tissue-specific circadian entrainment. *Cell reports*, 8(2):393–401, 2014.

[257] U. Schibler and P. Sassone-Corsi. A web of circadian pacemakers. *Cell*, 111(7):919–922, 2002.

[258] B. Scholl, J. Burge, and N. J. Priebe. Binocular integration and disparity selectivity in mouse primary visual cortex. *Journal of neurophysiology*, 109(12):3013–3024, 2013.

[259] C. Sebastián, B. M. Zwaans, D. M. Silberman, M. Gymrek, A. Goren, L. Zhong, O. Ram, J. Truelove, A. R. Guimaraes, D. Toiber, et al. The histone deacetylase sirt6 is a tumor suppressor that controls cancer metabolism. *Cell*, 151(6):1185–1199, 2012.

[260] Y.-K. Seo, H. K. Chong, A. M. Infante, S.-S. Im, X. Xie, and T. F. Osborne. Genome-wide analysis of srebp-1 binding in mouse liver chromatin reveals a preference for promoter proximal binding to a new motif. *Proceedings of the National Academy of Sciences*, 106(33):13765–13769, 2009.

[261] Y.-K. Seo, T.-I. Jeon, H. K. Chong, J. Biesinger, X. Xie, and T. F. Osborne. Genome-wide localization of srebp-2 in hepatic chromatin predicts a role in autophagy. *Cell metabolism*, 13(4):367–375, 2011.

[262] C. Settembre and A. Ballabio. Lysosome: regulator of lipid degradation pathways. *Trends in cell biology*, 24(12):743–750, 2014.

[263] C. Settembre, R. De Cegli, G. Mansueto, P. K. Saha, F. Vetrini, O. Visvikis, T. Huynh, A. Carissimo, D. Palmer, T. J. Klisch, et al. Tfeb controls cellular lipid metabolism through a starvation-induced autoregulatory loop. *Nature cell biology*, 15(6):647, 2013.

[264] A. Sharifian, S. Farahani, P. Pasalar, M. Gharavi, and O. Aminian. Shift work as an oxidative stressor. *Journal of circadian rhythms*, 3(1):15, 2005.

[265] S.-q. Shi, T. S. Ansari, O. P. McGuinness, D. H. Wasserman, and C. H. Johnson. Circadian disruption leads to insulin resistance and obesity. *Current Biology*, 23(5):372–381, 2013.

[266] Y. Shigeyoshi, K. Taguchi, S. Yamamoto, S. Takekida, L. Yan, H. Tei, T. Moriya, S. Shibata, J. J. Loros, J. C. Dunlap, et al. Light-induced resetting of a mammalian circadian clock is associated with rapid induction of the mper1 transcript. *Cell*, 91(7):1043–1053, 1997.

[267] T. Shimazu, M. D. Hirschey, J.-Y. Huang, L. T. Ho, and E. Verdin. Acetate metabolism and aging: an emerging connection. *Mechanisms of ageing and development*, 131(7-8):511–516, 2010.

[268] B. C. Skottun, R. L. De Valois, D. H. Grosof, J. A. Movshon, D. G. Albrecht, and A. Bonds. Classifying simple and complex cells on the basis of response modulation. *Vision research*, 31(7-8):1078–1086, 1991.

[269] D. Smedley, S. Haider, S. Durinck, L. Pandini, P. Provero, J. Allen, O. Arnaiz, M. H. Awedh, R. Baldock, G. Barbiera, P. Bardou, T. Beck, A. Blake, M. Bonierbale, A. J. Brookes, G. Bucci, I. Buetti, S. Burge, C. Cabau, J. W. Carlson, C. Chelala, C. Chrysostomou, D. Cittaro, O. Collin, R. Cordova, R. J. Cutts, E. Dassi, A. D. Genova, A. Djari, A. Esposito, H. Estrella, E. Eyras, J. Fernandez-Banet, S. Forbes, R. C. Free, T. Fujisawa, E. Gadaleta, J. M. Garcia-Manteiga, D. Goodstein, K. Gray, J. A. Guerra-Assuno, B. Haggarty, D.-J. Han, B. W. Han, T. Harris, J. Harshbarger, R. K. Hastings, R. D. Hayes, C. Hoede, S. Hu, Z.-L. Hu, L. Hutchins, Z. Kan, H. Kawaji, A. Keliet, A. Kerhornou, S. Kim, R. Kinsella, C. Klopp, L. Kong, D. Lawson, D. Lazarevic, J.-H. Lee, T. Letellier, C.-Y. Li, P. Lio, C.-J. Liu, J. Luo, A. Maass, J. Mariette, T. Maurel, S. Merella, A. M. Mohamed, F. Moreews, I. Nabihoudine, N. Ndegwa, C. Noirot, C. Perez-Llamas, M. Primig, A. Quattrone, H. Quesneville, D. Rambaldi, J. Reecy, M. Riba, S. Rosanoff, A. A. Saddiq, E. Salas, O. Sallou, R. Shepherd, R. Simon, L. Sperling, W. Spooner, D. M. Staines, D. Steinbach, K. Stone, E. Stupka, J. W. Teague, A. Z. DayemUllah, J. Wang, D. Ware, M. Wong-Erasmus, K. Youens-Clark, A. Zadissa, S.-J. Zhang, and A. Kasprzyk. The biomart community portal: an innovative alternative to large, centralized data repositories. *Nucleic Acids Research*, 43(W1):W589–W598, 2015.

[270] J. A. Sobel, I. Krier, T. Andersin, S. Raghav, D. Canella, F. Gilardi, A. S. Kalantzi, G. Rey, B. Weger, F. Gachon, et al. Transcriptional regulatory logic of the diurnal cycle in the mouse liver. *PLoS biology*, 15(4):e2001069, 2017.

[271] B. Spiegelman. Ppar-gamma: adipogenic regulator and thiazolidinedione receptor. *Diabetes*, 47(4):507–514, 1998.

[272] L. M. Steffen, B. Vessby, D. R. Jacobs Jr, J. Steinberger, A. Moran, C.-P. Hong, and A. R. Sinaiko. Serum phospholipid and cholesteryl ester fatty acids and estimated desaturase activities are related to overweight and cardiovascular risk factors in adolescents. *International Journal of Obesity*, 32(8):1297, 2008.

[273] C.-É. Stephany, L. L. Chan, S. N. Parivash, H. M. Dorton, M. Piechowicz, S. Qiu, and A. W. McGee. Plasticity of binocularity and visual acuity are differentially limited by nogo receptor. *Journal of Neuroscience*, 34(35):11631–11640, 2014.

[274] K.-A. Stokkan, S. Yamazaki, H. Tei, Y. Sakaki, and M. Menaker. Entrainment of the circadian clock in the liver by feeding. *Science*, 291(5503):490–493, 2001.

[275] K.-F. Storch, O. Lipan, I. Leykin, N. Viswanathan, F. C. Davis, W. H. Wong, and C. J. Weitz. Extensive and divergent circadian gene expression in liver and heart. *Nature*, 417(6884):78, 2002.

[276] M. S. Strable and J. M. Ntambi. Genetic control of de novo lipogenesis: role in diet-induced obesity. *Critical reviews in biochemistry and molecular biology*, 45(3):199–214, 2010.

[277] M. Stratmann and U. Schibler. Properties, entrainment, and physiological functions of mammalian peripheral oscillators. *Journal of biological rhythms*, 21(6):494–506, 2006.

[278] K. Suhre, C. Meisinger, A. Döring, E. Altmaier, P. Belcredi, C. Gieger, D. Chang, M. V. Milburn, W. E. Gall, K. M. Weinberger, et al. Metabolic footprint of diabetes: a multiplatform metabolomics study in an epidemiological setting. *PloS one*, 5(11):e13953, 2010.

[279] I. Sutskever, J. Martens, G. Dahl, and G. Hinton. On the importance of initialization and momentum in deep learning. In *International conference on machine learning*, pages 1139–1147, 2013.

[280] Y. Suwazono, M. Dochi, K. Sakata, Y. Okubo, M. Oishi, K. Tanaka, E. Kobayashi, T. Kido, and K. Nogawa. A longitudinal study on the effect of shift work on weight gain in male japanese workers. *Obesity*, 16(8):1887–1893, 2008.

[281] D. Szklarczyk, A. Franceschini, S. Wyder, K. Forslund, D. Heller, J. Huerta-Cepas, M. Simonovic, A. Roth, A. Santos, K. P. Tsafou, et al. String v10: protein–protein interaction networks, integrated over the tree of life. *Nucleic acids research*, 43(D1):D447–D452, 2014.

[282] H. Takahashi, J. M. McCaffery, R. A. Irizarry, and J. D. Boeke. Nucleocytosolic acetyl-coenzyme a synthetase is required for histone acetylation and global transcription. *Molecular cell*, 23(2):207–217, 2006.

[283] J. S. Takahashi, H.-K. Hong, C. H. Ko, and E. L. McDearmon. The genetics of mammalian circadian order and disorder: implications for physiology and disease. *Nature Reviews Genetics*, 9(10):764, 2008.

[284] K. Takahashi, K. Tanabe, M. Ohnuki, M. Narita, T. Ichisaka, K. Tomoda, and S. Yamanaka. Induction of pluripotent stem cells from adult human fibroblasts by defined factors. *cell*, 131(5):861–872, 2007.

[285] T. Tamaru, J. Hirayama, Y. Isojima, K. Nagai, S. Norioka, K. Takamatsu, and P. Sassone-Corsi. Ck2α phosphorylates bmal1 to regulate the mammalian clock. *Nature Structural and Molecular Biology*, 16(4):446, 2009.

[286] R. I. Tennen, E. Berber, and K. F. Chua. Functional dissection of sirt6: identification of domains that regulate histone deacetylase activity and chromatin localization. *Mechanisms of ageing and development*, 131(3):185–192, 2010.

[287] H. Terajima, H. Yoshitane, H. Ozaki, Y. Suzuki, S. Shimba, S. Kuroda, W. Iwasaki, and Y. Fukada. Adarb1 catalyzes circadian a-to-i editing and regulates rna rhythm. *Nature genetics*, 49(1):146, 2017.

[288] P. Tognini, M. Murakami, Y. Liu, K. L. Eckel-Mahan, J. C. Newman, E. Verdin, P. Baldi, and P. Sassone-Corsi. Distinct circadian signatures in liver and gut clocks revealed by ketogenic diet. *Cell metabolism*, 26(3):523–538, 2017.

[289] P. Tognini, D. Napoli, and T. Pizzorusso. Dynamic dna methylation in the brain: a new epigenetic mark for experience-dependent plasticity. *Frontiers in cellular neuroscience*, 9:331, 2015.

[290] P. Tognini and T. Pizzorusso. Microrna212/132 family: molecular transducer of neuronal function and plasticity. *The international journal of biochemistry & cell biology*, 44(1):6–10, 2012.

[291] P. Tognini, E. Putignano, A. Coatti, and T. Pizzorusso. Experience-dependent expression of mir-132 regulates ocular dominance plasticity. *Nature neuroscience*, 14(10):1237, 2011.

[292] P. Tontonoz and B. M. Spiegelman. Fat and beyond: the diverse biology of pparγ. *Annu. Rev. Biochem.*, 77:289–312, 2008.

[293] R. Travers, A. Motta, J. Betts, A. Bouloumie, and D. Thompson. The impact of adiposity on adipose tissue-resident lymphocyte activation in humans. *International Journal of Obesity*, 39(5):762, 2015.

[294] D. Tropea, G. Kreiman, A. Lyckman, S. Mukherjee, H. Yu, S. Horng, and M. Sur. Gene expression changes and molecular pathways mediating activity-dependent plasticity in visual cortex. *Nature neuroscience*, 9(5):660, 2006.

[295] F. W. Turek, C. Joshu, A. Kohsaka, E. Lin, G. Ivanova, E. McDearmon, A. Laposky, S. Losee-Olson, A. Easton, D. R. Jensen, et al. Obesity and metabolic syndrome in circadian clock mutant mice. *Science*, 308(5724):1043–1045, 2005.

[296] H. R. Ueda, W. Chen, A. Adachi, H. Wakamatsu, S. Hayashi, T. Takasugi, M. Nagano, K.-i. Nakahama, Y. Suzuki, S. Sugano, et al. A transcription factor response element for gene expression during circadian night. *Nature*, 418(6897):534, 2002.

[297] H. R. Ueda, S. Hayashi, W. Chen, M. Sano, M. Machida, Y. Shigeyoshi, M. Iino, and S. Hashimoto. System-level identification of transcriptional circuits underlying mammalian circadian clocks. *Nature genetics*, 37(2):187, 2005.

[298] M. Umemura, E. Baljinnyam, S. Feske, M. S. De Lorenzo, L.-H. Xie, X. Feng, K. Oda, A. Makino, T. Fujita, U. Yokoyama, et al. Store-operated ca2+ entry (soce) regulates melanoma proliferation and cell migration. *PloS one*, 9(2):e89292, 2014.

[299] V. Vijayan, R. Zuzow, and E. K. O'Shea. Oscillations in supercoiling drive circadian gene expression in cyanobacteria. *Proceedings of the National Academy of Sciences*, 106(52):22564–22568, 2009.

[300] M. H. Vitaterna, D. P. King, A.-M. Chang, J. M. Kornhauser, P. L. Lowrey, J. D. McDonald, W. F. Dove, L. H. Pinto, F. W. Turek, and J. S. Takahashi. Mutagenesis and mapping of a mouse gene, clock, essential for circadian behavior. *Science*, 264(5159):719–725, 1994.

[301] N. Vo, M. E. Klein, O. Varlamova, D. M. Keller, T. Yamamoto, R. H. Goodman, and S. Impey. A camp-response element binding protein-induced microrna regulates neuronal morphogenesis. *Proceedings of the National Academy of Sciences*, 102(45):16426–16431, 2005.

[302] C. Vollmers, S. Gill, L. DiTacchio, S. R. Pulivarthy, H. D. Le, and S. Panda. Time of feeding and the intrinsic circadian clock drive rhythms in hepatic gene expression. *Proceedings of the National Academy of Sciences*, 106(50):21453–21458, 2009.

[303] A. E. Wallberg, S. Yamamura, S. Malik, B. M. Spiegelman, and R. G. Roeder. Coordination of p300-mediated chromatin remodeling and trap/mediator function through coactivator pgc-1α. *Molecular cell*, 12(5):1137–1149, 2003.

[304] B.-S. Wang, L. Feng, M. Liu, X. Liu, and J. Cang. Environmental enrichment rescues binocular matching of orientation preference in mice that have a precocious critical period. *Neuron*, 80(1):198–209, 2013.

[305] B.-S. Wang, R. Sarnaik, and J. Cang. Critical period plasticity matches binocular orientation preference in the visual cortex. *Neuron*, 65(2):246–256, 2010.

[306] Q. Wang, S. Li, L. Jiang, Y. Zhou, Z. Li, M. Shao, W. Li, and Y. Liu. Deficiency in hepatic atp-citrate lyase affects vldl-triglyceride mobilization and liver fatty acid compositions of mice. *Journal of lipid research*, pages jlr–M003335, 2010.

[307] G. A. Wayman, M. Davare, H. Ando, D. Fortin, O. Varlamova, H.-Y. M. Cheng, D. Marks, K. Obrietan, T. R. Soderling, R. H. Goodman, et al. An activity-regulated microrna controls dendritic plasticity by down-regulating p250gap. *Proceedings of the National Academy of Sciences*, 2008.

[308] H. Weintraub. The myod family and myogenesis: redundancy, networks, and thresholds. *Cell*, 75(7):1241–1244, 1993.

[309] H. Weintraub, S. J. Tapscott, R. L. Davis, M. J. Thayer, M. A. Adam, A. B. Lassar, and A. D. Miller. Activation of muscle-specific genes in pigment, nerve, fat, liver, and fibroblast cell lines by forced expression of myod. *Proceedings of the National Academy of Sciences*, 86(14):5434–5438, 1989.

[310] K. E. Wellen, G. Hatzivassiliou, U. M. Sachdeva, T. V. Bui, J. R. Cross, and C. B. Thompson. Atp-citrate lyase links cellular metabolism to histone acetylation. *Science*, 324(5930):1076–1080, 2009.

[311] D. B. West, K. E. Wehberg, K. Kieswetter, and J. P. Granger. Blunted natriuretic response to an acute sodium load in obese hypertensive dogs. *Hypertension*, 19(1 Suppl):I96, 1992.

[312] K. Wibrand, D. Panja, A. Tiron, M. L. Ofte, K.-O. Skaftnesmo, C. S. Lee, J. T. Pena, T. Tuschl, and C. R. Bramham. Differential regulation of mature and precursor microrna expression by nmda and metabotropic glutamate receptor activation during ltp in the adult dentate gyrus in vivo. *European Journal of Neuroscience*, 31(4):636–645, 2010.

[313] H. Wijnen and M. W. Young. Interplay of circadian clocks and metabolic rhythms. *Annu. Rev. Genet.*, 40:409–448, 2006.

[314] S. L. Winter, L. Bosnoyan-Collins, D. Pinnaduwage, and I. L. Andrulis. Expression of the circadian clock genes pert, per2 in sporadic, familial breast tumors. *Neoplasia*, 9(10):797–800, 2007.

[315] X. Xie, P. Rigor, and P. Baldi. MotifMap: A human genome-wide map of candidate regulatory motif sites. *Bioinformatics*, 25(2):167–174, 2009.

[316] Y. Xie, Y. Jin, B. L. Merenick, M. Ding, K. M. Fetalvero, R. J. Wagner, A. Mai, S. Gleim, D. F. Tucker, M. J. Birnbaum, et al. Phosphorylation of gata-6 is required for vascular smooth muscle cell differentiation after mtorc1 inhibition. *Sci. Signal.*, 8(376):ra44–ra44, 2015.

[317] Z. Xie, D. Zhang, D. Chung, Z. Tang, H. Huang, L. Dai, S. Qi, J. Li, G. Colak, Y. Chen, et al. Metabolic regulation of gene expression by histone lysine β-hydroxybutyrylation. *Molecular cell*, 62(2):194–206, 2016.

[318] A. Yadav, M. A. Kataria, V. Saini, and A. Yadav. Role of leptin and adiponectin in insulin resistance. *Clinica Chimica Acta*, 417:80–84, 2013.

[319] K. Yagita, K. Horie, S. Koinuma, W. Nakamura, I. Yamanaka, A. Urasaki, Y. Shigeyoshi, K. Kawakami, S. Shimada, J. Takeda, and Y. Uchiyama. Development of the circadian oscillator during differentiation of mouse embryonic stem cells in vitro. *Proceedings of the National Academy of Sciences*, 107(8):3846–3851, 2010. [PubMed:20133594] [PubMed Central:PMC2840478][doi:10.1073/pnas.0913256107].

[320] S. Yamaguchi, S. Mitsui, L. Yan, K. Yagita, S. Miyake, and H. Okamura. Role of dbp in the circadian oscillatory mechanism. *Molecular and cellular biology*, 20(13):4773–4781, 2000.

[321] L. Yan and R. Silver. Day-length encoding through tonic photic effects in the retinorecipient scn region. *European Journal of Neuroscience*, 28(10):2108–2115, 2008.

[322] R. Yang and Z. Su. Analyzing circadian expression data by harmonic regression based on autoregressive spectral estimation. *Bioinformatics*, 26(12):i168–i174, 2010.

[323] X. Yang, M. Downes, T. Y. Ruth, A. L. Bookout, W. He, M. Straume, D. J. Mangelsdorf, and R. M. Evans. Nuclear receptor expression links the circadian clock to metabolism. *Cell*, 126(4):801–810, 2006.

[324] S.-H. Yoo, S. Yamazaki, P. L. Lowrey, K. Shimomura, C. H. Ko, E. D. Buhr, S. M. Siepka, H.-K. Hong, W. J. Oh, O. J. Yoo, et al. Period2:: Luciferase real-time reporting of circadian dynamics reveals persistent circadian oscillations in mouse peripheral tissues. *Proceedings of the National Academy of Sciences*, 101(15):5339–5346, 2004.

[325] Y. Yoshii, T. Furukawa, H. Yoshii, T. Mori, Y. Kiyono, A. Waki, M. Kobayashi, T. Tsujikawa, T. Kudo, H. Okazawa, et al. Cytosolic acetyl-coa synthetase affected tumor cell survival under hypoxia: the possible function in tumor acetyl-coa/acetate metabolism. *Cancer science*, 100(5):821–827, 2009.

[326] J. Yoshino, K. F. Mills, M. J. Yoon, and S.-i. Imai. Nicotinamide mononucleotide, a key nad+ intermediate, treats the pathophysiology of diet-and age-induced diabetes in mice. *Cell metabolism*, 14(4):528–536, 2011.

[327] E. E. Zhang, A. C. Liu, T. Hirota, L. J. Miraglia, G. Welch, P. Y. Pongsawakul, X. Liu, A. Atwood, J. W. Huss III, J. Janes, et al. A genome-wide rnai screen for modifiers of the circadian clock in human cells. *Cell*, 139(1):199–210, 2009.

[328] E. E. Zhang, Y. Liu, R. Dentin, P. Y. Pongsawakul, A. C. Liu, T. Hirota, D. A. Nusinow, X. Sun, S. Landais, Y. Kodama, et al. Cryptochrome mediates circadian regulation of camp signaling and hepatic gluconeogenesis. *Nature medicine*, 16(10):1152, 2010.

[329] X. Zhang, D. T. Odom, S.-H. Koo, M. D. Conkright, G. Canettieri, J. Best, H. Chen, R. Jenner, E. Herbolsheimer, E. Jacobsen, et al. Genome-wide analysis of camp-response element binding protein occupancy, phosphorylation, and target gene activation in human tissues. *Proceedings of the National Academy of Sciences*, 102(12):4459–4464, 2005.

[330] Y. Zhang, B. Fang, M. Damle, D. Guan, Z. Li, Y. H. Kim, M. Gannon, and M. A. Lazar. Hnf6 and rev-erbα integrate hepatic lipid metabolism by overlapping and distinct transcriptional mechanisms. *Genes & development*, 30(14):1636–1644, 2016.